Technische Universität München
Ingenieurfakultät Bau Geo Umwelt
Lehrstuhl für Bauphysik

Vehicular Climatization Effectiveness

Application of Thermal Perception Models for the Assessment of Direct Passenger Conditioning Concepts in Vehicles

Wolfgang Richard Wöhrle

Vollständiger Abdruck der von der Ingenieurfakultät Bau Geo Umwelt der Technischen Universität München zur Erlangung des akademischen Grades eines

Doktor-Ingenieurs (Dr.-Ing.)

genehmigten Dissertation.

Vorsitzender: Prof. Dr.-Ing. Stefan Winter

Prüfende der Dissertation:

1. Prof. Dr.-Ing. Klaus Peter Sedlbauer
2. Prof. Dr.-Ing. Gunnar Grün
3. Prof. Dr.-Ing. Anton Maas

Diese Dissertation wurde am 22.06.2020 bei der Technischen Universität München eingereicht und durch die Ingenieurfakultät Bau Geo Umwelt am 02.11.2020 angenommen.

Acknowledgements

This dissertation resulted from my work on climatization effectiveness at the BMW Group and from the associated research on thermal comfort I carried out at the Fraunhofer Institute for Building Physics IBP. I had ideal conditions for my work, enabled by a number of people involved, to whom I want to express my gratitude.

First of all, I would like to thank all my colleagues on the Climatization Concepts Team of the BMW HVAC Department for always providing a great working atmosphere on a personal level and for engaging in issues beyond work. I especially thank Hamed Saffarian for horizon broadening philosophical walks, René Zocher for successful stock market hacks and Thomas Rotenburg for family life conversations. In addition, I would like to thank a number of BMW colleagues who have always and without hesitation provided me with technical expertise, test vehicles and equipment. Those who deserve special mention in this respect include Christina Selmeier, Philipp Hofmann, Felix Artmeier, Jürgen Gläßer, Achim Stampflmeier and Andreas Schneider. My special thanks goes to Peter Satzger for the freedom and unrestricted support he has offered me in developing a unique assessment approach against the background of the many challenges associated with climate comfort evaluation in vehicles. I also thank Stefan Wiedemann for his relentless commitment to procedural and administrative challenges and for giving me the flexibility I needed to reconcile family and doctorate.

Furthermore, I want to thank my peers and advisers at the Energy Efficiency and Indoor Climate Department of the Fraunhofer Institute for Building Physics. I particularly would like to thank Dr.-Ing. Sumee Park for her willingness to engage in expansive discussions about thermal comfort research at any time and providing me guidance and advice whenever needed. My gratitude also goes to Prof. Dr.-Ing. Gunnar Grün for his always open door and his advice on effectively supervising students. Furthermore, I thank Michael Visser for his unconditional support of my side projects whenever I suggested them. My special gratitude goes to Prof. Dr.-Ing. Klaus Peter Sedlbauer for his always targeted advice and his uncomplicated approach to the challenges of an industrial doctorate.

Most of all, I would like to thank my wife Lisa, who made it possible during the last three years for me to both realize this dissertation and spend a lot of wonderful time with our children.

Abstract

This dissertation presents a universal approach for assessing the effectiveness of vehicular climatization systems, applicable to central Heating Ventilation and Air-Conditioning (HVAC) as well as to close-to-body Direct Passenger Conditioning (DPC) measures.

The performance of conventional vehicular HVAC systems is assessed on the basis of air temperature measurements in the passenger compartment during vehicle cool-down in summer conditions or during heat-up in winter conditions. Due to the increasing inclusion of local close-to-body climatization measures, such as seat cooling or radiant heating, air temperature is no longer a reliable indicator of the effect on passengers and thus of the actual performance of the system. Rather, a measure is needed that directly relates various heat transport effects on passengers to thermal comfort by means of locally measured climate variables.

For this purpose, the state of the art of evaluation methods for thermal environments is analyzed with regard to the specific requirements of DPC systems. In order to compare the prediction accuracy of selected methods, a new concept is developed that allows the application of multiple thermal perception models with one climate measurement system. In a comprehensive vehicle cool-down study, the predictions of the these models are compared with the actual assessments of human subjects. The results show the highest prediction accuracy with the Park method [44, 41] and confirm a theoretically derived research gap in the measurement based assessment of local thermal comfort under transient and non-uniform climate conditions.

With regard to this research gap, a new methodology to assess local thermal tolerance thresholds is introduced. A literature-based theory on local cold discomfort under simultaneous overall warm discomfort is developed and investigated in a series of human subject studies. Based on the data obtained, stochastic models for the prediction of local thermal tolerance thresholds in relation to measured cooling intensity are developed for the neck, buttocks and back.

As a conclusion of the investigations, a recommendation is made for a holistic assessment methodology for vehicular climatization effectiveness. The quantification of DPC measures' effectiveness with regard to overall thermal comfort improvement is extended by determining local thermal tolerance thresholds to avoid too high local climatization intensity. The methodology adapts the concept of equivalent temperature of international standards and merges it with common practices in the automotive industry to facilitate integration into industrial processes.

Vehicle HVAC | Thermal Comfort | Human Subject Study | Equivalent Temperature

Kurzfassung

Diese Dissertation stellt einen universellen Ansatz zur Beurteilung der Wirksamkeit von Fahrzeugklimatisierungssystemen vor, welcher sowohl für die zentrale Luftklimatisierung, als auch für lokale körpernahe Klimatisierungsmaßnahmen anwendbar ist.

Die Leistungsfähigkeit konventioneller Fahrzeugklimatisierungssysteme wird anhand der Entwicklung der Lufttemperatur im Fahrgastraum während einer Abkühlung unter Sommerbedingungen bzw. einer Aufheizung unter Winterbedingungen beurteilt. Aufgrund der zunehmenden Einbeziehung lokaler, körpernaher Klimatisierungsmaßnahmen, wie Sitzkühlung oder Strahlungsheizung, ist die Lufttemperatur nicht länger ein zuverlässiger Indikator für die Wirkung am Fahrgast und damit für die eigentliche Leistungsfähigkeit des Systems. Vielmehr wird ein Maß benötigt, welches diverse Wärmetransporteffekte am Fahrgast anhand lokal gemessener Klimavariablen in direkten Bezug zu thermischer Behaglichkeit setzt.

Dazu wird der Stand der Forschung zu Bewertungsverfahren der thermischen Umgebung in Hinblick auf die spezifischen Anforderungen dezentraler fahrgastorientierter Klimatisierungskonzepte analysiert. Um die Vorhersagegenauigkeit entsprechender Verfahren zu vergleichen, wird ein neus Konzept entwickelt, welches eine Anwendung mehrerer Behaglichkeitsmodelle mit dem selben Klimamesssystem ermöglicht. In einer umfassenden Fahrzeug-Cool-Down-Studie werden die Prognosen der verschiedenen Behaglichkeitsmodelle mit der tatsächlichen Beurteilung durch Probanden verglichen. Die Ergebnisse zeigen die höchste Prognosegenauigkeit bei der Park-Methode [44, 41] und bestätigen die Relevanz einer Forschungslücke in der messwertbasierten Beurteilung des lokalen thermischen Komforts unter instationären und inhomogenen Klimabedingungen.

In Bezug auf diese Forschungslücke wird eine neue Methodik zur Bewertung lokaler thermischer Toleranzschwellen vorgestellt. Eine literaturbasierte Theorie zu lokalem kaltem Diskomfort bei gleichzeitigem globalem warmem Diskomfort wird entwickelt und in einer Reihe von Probandenstudien empirisch untersucht. Anhand der gewonnenen Daten werden stochastische Modelle zur Prognose lokaler thermischer Toleranzschwellen in Relation zur gemessenen Kühlintensität für Hals, Gesäß und Rücken entwickelt.

Die Ergebnisse der Untersuchungen werden in einer Empfehlung für ein Verfahren zur ganzheitlichen Bewertung der Wirksamkeit von Fahrzeugklimatisierungssystemen zusammengefasst. Die Quantifizierung der Gesamtwirksamkeit dezentraler Klimatisierungsmaßnahmen anhand einer Verbesserung des globalen thermischen Komforts, wird ergänzt um die Bestimmung lokaler thermischer Toleranzschwellen, um zu hohe lokalen Klimatisierungsintensitäten zu vermeiden. Das Verfahren adaptiert das Konzept der Äquivalenttemperatur internationaler Normen und verknüpft es mit in der Automobilindustrie üblichen Standards, um die praktische Anwendbarkeit in industriellen Prozessen zu gewährleisten.

Fahrzeugklimatisierung - Thermische Behaglichkeit - Probandenstudie
Äquivalenttemperatur

Contents

Abstract i

Kurzfassung ii

Nomenclature viii

1 Introduction 1
- 1.1 Motivation . . . 1
- 1.2 Aims and Scientific Procedure . . . 2

2 State of the Art 4
- 2.1 Vehicular Climatization . . . 4
- 2.2 Climatization Performance Assessment . . . 6
- 2.3 Thermal Comfort . . . 7
  - 2.3.1 Climate Conditions . . . 7
  - 2.3.2 Thermophysiology . . . 11
  - 2.3.3 Thermal Perception . . . 13
- 2.4 Thermal Environment Evaluation . . . 13
  - 2.4.1 The Fanger Method . . . 17
  - 2.4.2 The Park Method . . . 20
  - 2.4.3 The Nilsson Method . . . 23
  - 2.4.4 The Fiala Method . . . 25
  - 2.4.5 The Zhang Method . . . 27
- 2.5 Appraisal of the State of the Art . . . 30

3 Methodological Approach 36

4 A New Concept to Evaluate Multiple Thermal Perception Models 39
- 4.1 Theoretical Approach . . . 39
  - 4.1.1 Development of Adaptation Models . . . 39
  - 4.1.2 Norming of different Evaluation Scales . . . 46
  - 4.1.3 Utilization of Prediction Accuracy Measures . . . 50
- 4.2 Methods . . . 51
- 4.3 Results . . . 56
  - 4.3.1 Thermal Perception Model Comparison . . . 57
  - 4.3.2 Park Method Evaluation . . . 58
  - 4.3.3 Local Thermal Comfort Assessment . . . 60
- 4.4 Discussion . . . 62

5 A New Methodology to Assess Local Thermal Tolerance Thresholds 63
- 5.1 Neck Cooling (Methodology Development) . . . 63
  - 5.1.1 Theory . . . 64

5.1.2 Methods . . . 68
5.1.3 Results . . . 72
5.1.4 Thermal Perception Model Comparison . . . 72
5.1.5 Model Development . . . 74
5.1.6 Model Evaluation . . . 79
5.2 Seat Cooling . . . 82
5.2.1 Theory . . . 82
5.2.2 Methods . . . 82
5.2.3 Results . . . 86
5.2.4 Thermal Perception Model Comparison . . . 87
5.2.5 Model Development . . . 89
5.2.6 Model Evaluation . . . 91
5.3 Defining Local Cooling Thresholds . . . 92
5.3.1 Tolerance Thresholds for the Neck . . . 93
5.3.2 Tolerance Thresholds for Seat and Back . . . 95

6 Conclusion and Future Work **97**
6.1 Practical Application . . . 97
6.1.1 Vehicular Climatization Effectiveness Assessment . . . 97
6.1.2 Early-stage DPC Evaluation . . . 99
6.2 Critical Reflection . . . 100
6.2.1 Reflecting on the Evaluation of Multiple Thermal Perception Models 100
6.2.2 Reflecting on the Local Thermal Tolerance Thresholds . . . 101
6.3 Further Investigations . . . 102
6.3.1 Tolerance Thresholds of other Body Areas . . . 102
6.3.2 Thermal Impact from Contact Surfaces . . . 102
6.3.3 Evaporative Impact . . . 102
6.3.4 PD Optimization . . . 103
6.3.5 Equidirectional Local Thermal Discomfort . . . 103
6.3.6 Local Thermal Perception Sensitivity . . . 103
6.3.7 Thermo-Acoustic Comfort . . . 104
6.3.8 DPC Personalization . . . 104
6.3.9 Decentralized Frequency-Optimized Impulse Climatization . . . 105

7 Summary **106**

Bibliography **113**

List of Figures **116**

List of Tables **117**

Appendix **118**

A Sensor Positions of the DressMAN System **118**

B Further Model Evaluations **120**

Nomenclature

Acronyms

ASHRAE	American Society of Heating Refrigerating and Air-conditioning Engineers
BEV	Battery Electric Vehicle
BMW	Bayerische Motoren Werke
CCI	Combined Climate Indicators
CCQ	Climate Control Quality
CET	Contact Equivalent Temperature
CP	Climatization Performance
DeFrOI	Decentralized Frequency-Optimized Impulse
DIN	Deutsches Institut für Normung
DPC	Direct Passenger Conditioning
DressMAN	Dummy Representing Suit for Simulation of huMAN heatloss
DTS	Dynamic Thermal Sensation
ECT	Equivalent Contact Temperature
GOF	Goodness of Fit
HAD	Highly Automated Driving
HVAC	Heating Ventilation and Air-Conditioning
IBP	Institute for Building Physics
IR	Infrared
ISO	International Organization for Standardization
LR	Lewis Ratio
LTC	Local Thermal Comfort
LTP	Local Thermal Perception
LTS	Local Thermal Sensation
MBE	Mean Bias Error
MTV	Mean Thermal Vote
NRMSD	Normalized Root Mean Square Deviation

OEM	Original Equipment Manufacturer
OTC	Overall Thermal Comfort
OTP	Overall Thermal Perception
OTS	Overall Thermal Sensation
PD	Percentage of Dissatisfied
PD_{cold}	Percentage of Dissatisfied people by local cold discomfort
PMV	Predicted Mean Vote
PPD	Predicted Percentage of Dissatisfied
RMSE	Root Mean Square Error
RMSD	Root Mean Square Deviation
SAE	Society of Automotive Engineers
SI	International System of Units *(french: Système international d'unités)*
TEC	Thermoelectric Cooler
TTT_i	Local Thermal Tolerance Threshold

English Symbols

A	area
AH	Absolute Humidity
d	diameter
e	Euler's number
$\dot{E}_{sol}$	solar radiation intensity
f	function
F_{AB}	radiation exchange degree
f_{cl}	clothing area factor
f_v	view factor
h_c	convective heat transfer coefficient
h_{cal}	combined convective and radiative heat transfer coefficient in calibration conditions
h_e	evaporative heat transfer coefficient
h_r	radiative heat transfer coefficient
i	item
M	metabolic rate

M_i	measured value
n	counter
p_s	saturation water vapour pressure
p_a	partial water vapour pressure
$\dot{Q}$	heat flow
$\dot{q}$	area-specific heat flux
$\dot{q}_{TL}$	thermal load
$\dot{q}_c$	conductive heat flux
$\dot{q}_{env}$	area-specific heat exchange with the environment
R	thermal resistance
R_{cl}	thermal resistance of clothing
R_e	clothing evaporative resistance
RH	relative air humidity
s	segment
S_i	predicted value
t	time
T	temperature
T_a	air temperature
T_c	contact temperature
T_{cl}	clothing surface temperature
T_{eq}	equivalent temperature
$T_{eq,contact}$	contact equivalent temperature
$T_{eq,direct}$	directed equivalent temperature
$T_{eq,local}$	local equivalent temperature
$T_{eq,segment}$	segmental equivalent temperature
$T_{eq,whole}$	equivalent temperature for the whole body
T_g	globe temperature
T_{hyp}	hypothalamus temperature
T_{op}	operative temperature
$\bar{T}_r$	mean radiant temperature
T_s	surface temperature

T_{sk}	skin temperature
v_a	air velocity
W	effective mechanical power due to physical activity
w_i	weighting factor
w_w	skin wetting degree

Greek Symbols

α_r	radiative absorption coefficient
Δ	quantity differences
ϵ_r	radiative emission coefficient
Φ	core temperature influence factor
λ	thermal conductivity
Ψ	thermal perception dynamics factor
σ	Stefan-Boltzmann constant
τ	skin temperature derivative influence factor

Chapter 1

Introduction

The automotive industry is currently undergoing major changes. Trends such as electrification and digitalization are drivers for a multitude of vehicular technology developments. This introduction describes the impact of these developments on vehicular climatization systems and the procedure for assessing their effectiveness. It also outlines objectives for the research and the scientific procedure for meeting them in this dissertation.

1.1 Motivation

Vehicular climatization originated in ventilating and heating windscreens to keep them free of fog. Beginning in the mid-20th century, heating and air conditioning systems were available as optional extras in passenger cars. In middle Europe heating devices became standard very quickly, and the same is true for air conditioning in the United States.

Due to the aerodynamic design of vehicles, which became popular at the beginning of the 1980, proportions of glazing and window angles changed. This led to a higher solar heat impact, which caused the combined Heating Ventilation and Air-Conditioning (HVAC) system to become standard in vehicles [22]. Since then, this basic concept of central HVAC has not changed significantly, although seat heating and ventilation gradually appeared as optional extras. Current trends in the automotive industry, however, are leading to a change in the concept of climatization, from central HVAC to decentralized Direct Passenger Conditioning (DPC).

Electrification Conventional HVAC is the most energy intensive auxiliary consumer in passenger cars and can significantly reduce the range of a Battery Electric Vehicle (BEV). The necessary reduction of energy consumption cannot be achieved through energy efficiency improvements alone; rather a whole new climatization approach is needed. Since the purpose of climatization is to provide passengers with thermal comfort, the need for energy intensive conditioning of the entire vehicle cabin is questionable. Consequently central HVAC is successively being complemented by decentralized close-to-body climatization measures. The intention of such systems is to provide maximum thermal comfort to passengers, while reducing energy consumption.

Automation Another driver for DPC is Highly Automated Driving (HAD). At HAD level four[1]passenger seats are expected to be completely free to rotate and tilt. As central HVAC is designed to condition passengers from the front, its effectiveness is no longer

certain. This development has led to a climatization approach, which is often called "Cocooning". It provides an individual micro-climate for each passenger, operated from the seat. The idea behind it, is the direct and targeted conditioning of passengers and the immediate space surrounding them.

Design Besides automation and electrification, a trend towards higher proportions of glazing on the vehicle shell (particularly panoramic roofs) can be observed. This essentially generates two climate relevant effects: First, the inner surface temperature is influenced stronger by the outside climate conditions, because the conductive heat transfer resistance of a glass panel is significantly lower than for a conventional car roof structure. Second, thermal impact from direct solar irradiation on passengers increases, since the radiation transmission coefficient of vehicle glazing is high at visible frequencies, which is the energy intensive portion of the solar spectrum. In sum, high proportions of glazing lead to a more direct affection of passengers from external climate conditions. This direct affection causes thermal asymmetries, as well as higher energy demand for compensation. Ultimately, these effects lead to an increase in the use of local discomfort compensation and passive climate measures to prevent from thermal discomfort.

The above described trends all increase the use of DPC systems and passive measures. Together with the central HVAC unit, they are forming an integral passenger centric climatization system. The state of the art evaluation method for conventional HVAC performance is based on air temperature measurements under defined boundary conditions [8]. Since the aim of HVAC is to condition the air of the vehicle compartment, air temperature is an appropriate indicator for its performance. DPC and passive measures, however, are based on locally differently utilized heat transfer mechanisms for immediate conditioning of passengers, and air temperature does not consider effects of seat conditioning or sunscreens. Thus, for general assessment of vehicular climatization effectiveness a different methodology is needed.

1.2 Aims and Scientific Procedure

Effectiveness is defined as the ratio of a result achieved to an objective intended and must be distinguished from efficiency, which is the ratio of output to input. The effectiveness of vehicular climatization is indicated by the level of thermal comfort generated, wheras the energy-efficiency is reflected in the amount of energy input necessary to generate a certain level of thermal comfort. The aim of this dissertation is to provide a reliable and feasible methodology for assessing the *effectiveness* of vehicular climatization and hence of the ability to provide passengers with thermal comfort. Such effectiveness quantification is also the foundation to assess climatization efficiency, which is, however, not subject of this dissertation. Figure 1.1 depicts the scientific procedure to reach the goal of a universal

[1]The Society of Automotive Engineers (SAE) defines five levels of passenger car automation. Level 4 is defined as follows: "The driving mode-specific performance by an automated driving system of all aspects of the dynamic driving task, even if a human driver does not respond appropriately to a request to intervene." [55].

approach to climatization effectiveness assessment, adapting the "Levels of the Scientific Knowledge Process" from Armin Töpfer's Book on successful research [59].

In an analysis of the state of the art of thermal environment evaluation methods, potential approaches for the assessment of climatization effectiveness are identified and research gaps are illuminated. In a case study of vehicle cool-down situations the prediction quality of the different evaluation approaches is compared and deficiencies in local thermal comfort assessment are revealed. In a series of subject studies, this aspect is investigated in depth and appropriate evaluation models are developed. Based on the results of the conducted research, a recommendation for industrial application and suggestions for future work are made.

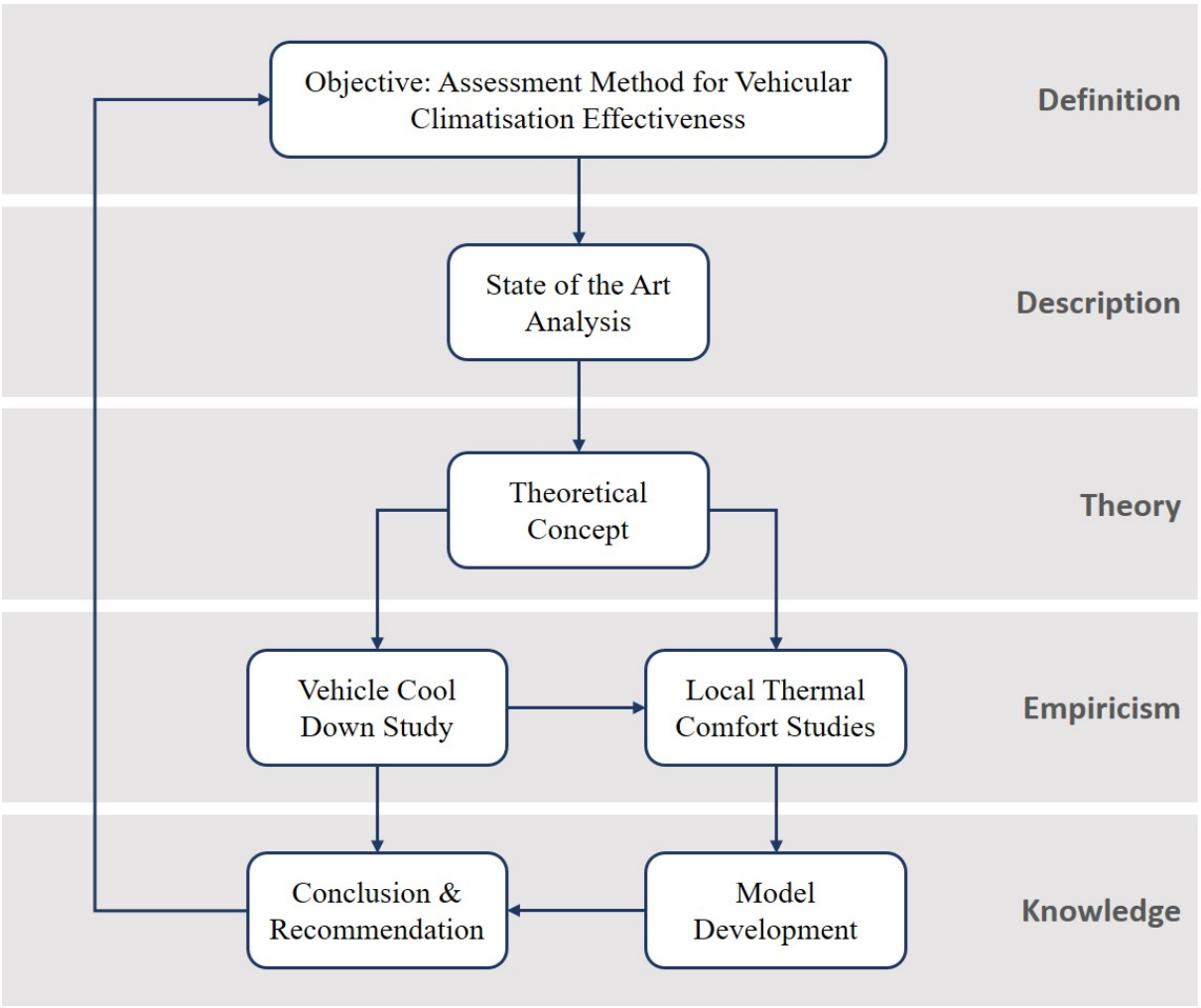

Figure 1.1: Conceptual research approach of the dissertation for achieving the initially formulated goal of an assessment method for vehicular climatization effectiveness.

Chapter 2

State of the Art

This chapter provides an introduction of currently applied climatization assessment methods and relevant findings in thermal comfort research to address deficiencies regarding DPC evaluation.

The first section on vehicular climatization analyses and categorizes DPC technologies and measures in order to derive fundamental characteristics that are relevant for the evaluation of their effectiveness. With regard to these characteristics, an examination of the currently used HVAC assessment method shows good practices and reveals deficiencies with regard to DPC. A review of thermal comfort literature leads to methodological requirements and feasibility criteria to address these deficiencies in climatization assessment. An introduction of relevant evaluation methods for thermal environments introduces thermal perception models that potentially meet these requirements and criteria. An appraisal of the state of the art discusses the strengths and weaknesses of these models and narrows down the research subject of this dissertation.

2.1 Vehicular Climatization

Vehicular climatization basically fulfills three tasks: providing thermal comfort, ensuring a fog-free windscreen and guaranteeing good air quality in the vehicle cabin. Since DPC does not change the principle for defogging, nor for air quality provision, this dissertation is concerned only with the topic of thermal comfort and does not engage with safety or hygiene issues. An overview of relevant standards for evaluation of such properties can be found in [22] and [34].

Basically, climatization measures are devices for targeted manipulation of heat exchange at vehicle passengers. Conventional HVAC realizes this task by adjusting the car cabin air temperature. However, since a number of other parameters are also influencing heat transport, DPC uses a variety of locally different measures. The term *Direct Passenger Conditioning* states the aim of the concept: conditioning the passenger, not the cabin air. DPC technologies, which are currently being tested or have already been introduced in addition to central HVAC are discussed in [22, 34, 57, 61, 62, 63] and can be classified as follows:

Local Air Conditioning uses the same principle as central HVAC but is more targeted to passengers. Air is conditioned[1]either by the central HVAC unit or a local conditioning

device, which could be a Thermoelectric Cooler (TEC)[2], a local electric resistance heater or a local air-water heat exchanger, the fluid of which is chilled centrally. A state of the art example is the convective neck warmer, blowing heated air from the seat top to the passenger's neck in winter conditions.

Contact Surface Tempering heats or cools those surfaces in the vehicle cabin, with which the passenger is in direct contact. Contact surface heating, such as seat heating or steering wheel heating, is usually realized by heating wires just below the respective surface. Cooling surfaces is more complex, since the heat removed must be transported somewhere else for dissipation. Therefore, a transport medium and infrastructure must always be involved. A common application of contact surface tempering is seat conditioning. The principle differs from surface heating in that the surface is perforated and the passenger is hence also cooled directly with air through these perforations. It is therefore, strictly speaking, a combination of contact surface tempering and local air conditioning.

Radiative Technologies are technologically very similar to contact surface tempering, but restricted to non-contact surfaces surrounding passengers. These surfaces are conditioned to influence the radiative heat exchange. The only relevant application of this technology is Infrared (IR) heating, integrated into surfaces of the cabin interior. The main difference to contact surface tempering is that IR surfaces heat to higher temperatures, which raises more complex safety issues.

Passive Measures differ from those discussed above in that they function without active energy use. Instead, the concept behind them is to avoid undesired affection of passengers or the cabin interior from environmental influences, by shielding them. Typical examples include sun screens or IR reflective glazing, which lower the solar heat impact. While sun screens shield the entire solar spectrum, but can only be used if the sight is not impaired or during vehicle downtimes, IR reflection takes place permanently, but only for long wave radiation.

DPC Characteristics When considering all present and possible future DPC applications, an appropriate assessment method must be able to quantify the effects of locally different heat exchange mechanisms on passengers' thermal perception. Apart from that, the concept of effectiveness must be considered in a differenciated way. Vehicular climatization is operated non-stationary. During vehicle downtime, the interior climate adapts to the external climate conditions (passive phase). With activation of the climate control system, the task of climatization is to reach neutral conditions for passengers as fast as possible (conditioning phase), which is a matter of conditioning power or climatization

[2]The thermoelectric effect is the direct conversion of temperature differences to electric voltage and vice versa via a thermocouple. A thermoelectric device creates voltage when there is a different temperature on each side. Conversely, when a voltage is applied to it, heat is transferred from one side to the other, creating a temperature difference. TEC devices are often combined with local fans to pick up the conditioned air and carry it to the passenger.

[2]Here, conditioned air means both, heated and cooled air.

performance respectively. As soon as steady state conditions are attained (steady state phase), thermal comfort is no longer a matter of conditioning power but of appropriate climate control adjustment. Thus, climatization effectiveness comprises both Climatization Performance (CP) and Climate Control Quality (CCQ). DPC measures are characterized by a targeted and responsive conditioning from the very beginning of the conditioning phase, whereas their climatization power can be reduced in steady-states, when overall conditions are close to thermal neutrality. DPC effectiveness is hence reflected especially during vehicle cool-down or heat-up and thus in climatization performance, which is discussed in the following section.

2.2 Climatization Performance Assessment

Assessment methods usually define a standard procedure with measurable criteria that reflect a certain desired property. The resulting measured values are compared with desired targets for these criteria. The target quantity and evaluation procedure for HVAC performance are defined in Germany in DIN 1946-3 [8]. Since this is a guideline rather than a rule, different OEMs[3] have slightly different test procedures. However, they are all designed for central HVAC and differ only in details. An overview of some procedures is provided in [52]. In the following, only the standard test procedure is described.

Table 2.1: Boundary conditions and target values for cool-down and heat-up tests according to DIN 1946-3 [8].

parameter	cooling mode	heating mode
passive conditioning target	$T_{cabin} = T_{env}$ + 60 min solar radiation	$T_{cabin} = T_{env}$
driving speed	$32\frac{km}{h}$ (20 mph)	$32\frac{km}{h}$ (20 mph)
outside air temperature	$40°C$	$-20°C$
solar irradiation	$1'000\frac{W}{m^2}$	-
air humidity	40%	-
mean interior air temperature after 30 min of active HVAC	$< 25°C$	$> 20°C$

The procedure consists of a passive conditioning phase under representative environmental influences and a subsequent active conditioning phase. Performance evaluation is oriented at the time necessary to reach certain target conditions. These conditions are defined in the form of mean air temperatures in the footwell, head area and the cabin as a whole. The corresponding measuring locations and determination of the mean values are clearly defined in the standard. Boundary conditions are based on middle European extreme climates and a low driving velocity. Ventilation nozzles are aligned in such a way, that there is no direct air flow to measuring locations. Table 2.1 provides the boundary conditions and target values for the heating and the cooling mode.

[3]Original Equipment Manufacterer. The term is used synonymously for vehicle manufacturers.

Deficiencies and Good Practice Effectiveness is defined as the ratio of result to goal. The goal of vehicular climatization is not to reach a certain air temperature but to provide thermal comfort. Its effectiveness must be evaluated by quantifying thermal comfort and relating it to ideal thermal comfort. In case of central HVAC performance, air temperature is the only quantity influenced by the system and is hence a sufficient indicator for thermal comfort improvement as well. However, air temperature is not a good indicator for DPC, where passengers are conditioned directly by various heat exchange mechanisms. A different indicator for thermal comfort improvement is needed, one which holds for local thermal impact and its effect on thermal comfort. The phenomenon of thermal comfort is therefore discussed in detail in the following section.

2.3 Thermal Comfort

Thermal Comfort is a complex construct which can be described as *a cognitive interpretation of physiological responses to surrounding climate conditions.*

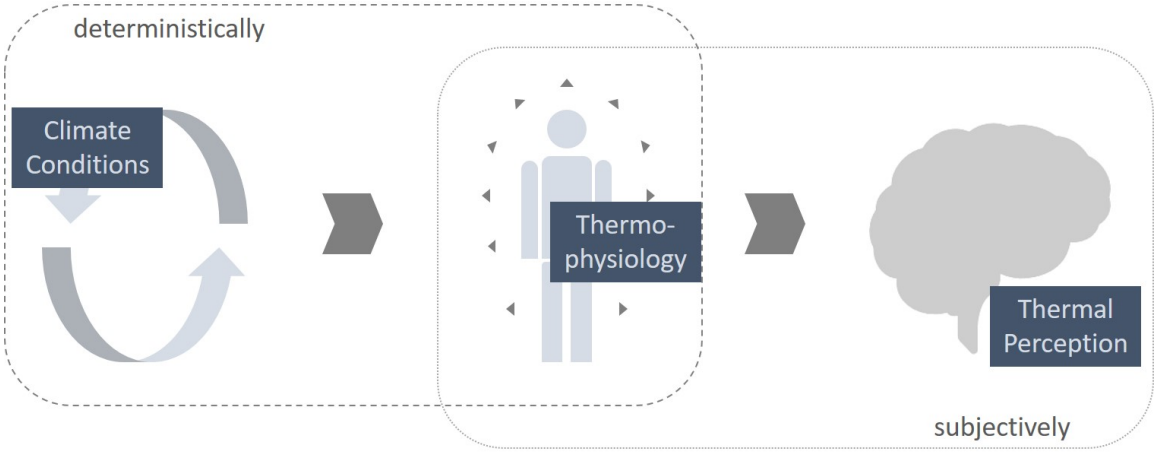

Figure 2.1: Characterization and interrelation of the three dimensions of thermal comfort.

While thermal conditions and physiological reactions can be understood deterministically in physical terms, cognitive interpretations escape causal explainability and can only be described stochastically. Both physiological reactions and cognitive interpretations are highly subjective, whereas thermal conditions have an objective character. In figure 2.1 the three dimensions of thermal comfort are illustrated and they will be discussed in the following sections in detail.

2.3.1 Climate Conditions

Climate conditions can be described based on a variety of physical quantities with respect to different subjects of interest. For climatization effectiveness, the heat exchange between passengers and their surroundings is crucial for identifying relevant physical variables to describe climate conditions. Heat transfer, in general, consists of three mechanisms: conduction, radiation and convection. Besides these heat transfer mechanisms, another effect

must be taken into account, when dealing with human thermal environments: evaporation of sweat on the body surface [47]. Convective and evaporative respiratory heat flow ($\dot{Q}_{res,conv} + \dot{Q}_{res,evap}$) are often differentiated from convection and evaporation at the body surface, for they are calculated differently in practical applications. However, since the physical relations are the same in both cases, respirative heat exchange is not discussed seperately here. Thus, following Parsons' *Human Thermal Environments* [47] and the international standard on heat strain prediction, ISO 7933 [11], heat loss to the environment is comprised of conduction, radiation, convection and evaporation:

$$\dot{Q}_{env} = \dot{Q}_{cond} + \dot{Q}_{rad} + \dot{Q}_{conv} + \dot{Q}_{evap} \tag{2.1}$$

In the following, these heat transport mechanisms and their determinings physical quantities are described. Relevant concepts and techniques for measuring these quantities are introduced in section 2.4.

Conduction One dimensional heat conduction is driven by a temperature gradient (ΔT). In combination with the material specific thermal conductive resistance (R_λ), the conductive heat flow ($\dot{Q}_{cond}$) through a certain area (A) can be calculated as follows [27]:

$$\dot{Q}_{cond} = A \cdot \frac{\Delta T}{R_\lambda} \tag{2.2}$$

Heat Flow through Clothing Conductive heat flow takes place between the skin surface and the outer surface of the clothing. In [17], Fanger adapts the basic principle of equation 2.2 to the calculation of this heat flow through clothing, which depends on the clothings' thermal resistance (R_{cl}) and the gradient between skin temperature (T_{sk}) and clothing surface temperature (T_{cl}). To obtain the total heat transport through clothing for a person, the area-specific heat flux through clothing ($\dot{q}_{cl}$) must be related to the total clothed body surface (A_{cl}). Following [17], the relation can be put as follows:

$$\dot{Q}_{cl} = A_{cl} \cdot \frac{T_{sk} - T_{cl}}{R_{cl}} \tag{2.3}$$

This equation can be combined with the international standard for estimating the thermal insulation and water vapour resistance of clothing, ISO 9920 [14] to evaluate the thermal comfort of sedentary persons. The standard introduces a method for incorporating sitting by varying the original value for the thermal resistance of the clothing with regard to the object being sat on. This method assumes convective, radiative and evaporative heat exchange on the outer surface of the seat or chair and is therefore only appropriate for steady state conditions and with no seat conditioning involved. During a vehicle cool-down, however, passengers are usually sitting on a passively heated seat, which has stored a great amount of thermal energy during down time. If the seat remains unconditioned during cool-down, local heat flux is still governed by the heated seat at the contact surface for several minutes, rather than by the surrounding climate.

Heat Exchange with Contact Surfaces Conduction is hence responsible for heat exchange between passengers and the contacting surfaces of the vehicle interior, such as seat or steering wheel. According to ISO 7933, conductive heat flow can be aligned with convection and radiation for heat strain prediction and therefore provides no calculation method for $\dot{Q}_{cond}$ [11]. This argumentation, however, applies only to moderate climate conditions and cannot be followed for cool-down situations in vehicles, where seats are either very hot or actively cooled.

For integrated seat conditioning, local heat flux depends on the immediate local climate generated at the contact surface. Assuming a quasi-stationary heat exchange between the clothing surface and the object surface, the objects' surface temperature ($T_{s,ob}$) is probably a powerful variable to replace T_{cl} in equation 2.3. However, when doing so, the conductive heat transfer resistance between the person and the object (R_{cond}) must be considered in addition to R_{cl}. The relevant area for total heat flow calculation is here a certain contacting body area (A_i). The total conductive heat flow between the passenger and the contacting object ($\dot{Q}_{cond,c}$) can then be calculated as follows:

$$\dot{Q}_{cond,c} = A_i \cdot \frac{T_{sk} - T_{s,ob}}{R_{cl} + R_{cond}} \tag{2.4}$$

Radiation Radiation is heat transfer by electromagnetic waves. According to the Stefan-Boltzmann law, the radiative heat flow on a surface A, which is exchanging radiation with another surface B, can be obtained with regard to their temperatures $T_{s,A}$ and $T_{s,B}$ as follows [27]:

$$\dot{Q}_{rad,AB} = A_A \cdot F_{AB} \cdot \sigma \cdot (T_{s,B}^4 - T_{s,A}^4) \tag{2.5}$$

where σ is the Stefan-Boltzmann constant, A_A is the area of surface A and F_{AB} is the radiation exchange degree, which depends on the emission coefficients (ϵ) of the two surfaces:

$$F_{AB} = \frac{1}{\frac{1}{\epsilon_A} + \frac{1}{\epsilon_B} - 1} \tag{2.6}$$

This approach is adapted or simplified in several standards for the ergonomics of the thermal environment (see [10, 4, 11, 13]). However, in all cases, the driving variables are the surface temperatures of surrounding objects ($T_{s,ob}$) and the surface temperature of the clothing (T_{cl}). To consider the relative inclination of two surfaces to each other, a view factor (f_v) reduces the respective area with regard to its portional "view" of the other surface, which results in an effective long wave radiative heat flow ($\dot{Q}_{rad,LW}$) between a certain body area and another object of:

$$\dot{Q}_{rad,LW} = f_v \cdot A_i \cdot F_{cl/ob} \cdot \sigma \cdot (T_{s,ob}^4 - T_{cl}^4) \tag{2.7}$$

In addition to the long wave radiative heat exchange, heat flow from direct solar irradiation ($\dot{Q}_{rad,sol}$) must also be considered in a vehicle environment. Since solar radiation intensity ($\dot{E}_{sol}$) can be measured directly, the calculation of $\dot{Q}_{rad,sol}$ can be obtained as follows [27]:

$$\dot{Q}_{rad,sol} = A_{sol} \cdot \alpha_r \cdot \dot{E}_{sol} \tag{2.8}$$

A_{sol} is the irradiated body area and α_r the radiative absorption coefficient of the person's skin and clothing (which is usually equal to ϵ). In sum, the radiative heat flow comprise solar irradiation and long wave radiation exchange:

$$\dot{Q}_{rad} = \dot{Q}_{rad,LW} + \dot{Q}_{rad,sol} \tag{2.9}$$

Convection Convection is heat transfer by mass transport. Air at the immediate boundary air layer of the passenger's body surface is picked up and replaced by conditioned air. The passenger's skin or clothing is cooled by this conditioned air, which is thus reheated and the process of air exchange begins again. Convective heat transfer depends on the gradient between the passengers' body surface temperature (either T_{sk} or T_{cl}), the air temperature (T_a) and the convective heat transfer coefficient (h_c) [47]:

$$\dot{Q}_{conv} = A_i \cdot h_c \cdot (T_{cl} - T_a) \tag{2.10}$$

where h_c can be determined by different calculation methods, which usually depend on the fluid dynamic conditions at the boundary layer and thus of air velocity (v_a) and clothing or skin properties. The exact relationships and calculation methods can be found in [47].

Evaporation denotes the transformation of latent to sensible heat by vapourization of sweat on the skin or clothing surface. Since conditioned air is usually not saturated with water vapour, a partial pressure gradient between the surface and the surrounding air occurs, which leads to a phase transition of liquid sweat to gaseous vapour. This process draws transformation enthalpy from the boundary air layer and decreases the air temperature. This temperature decrease in the boundary air layer increases the temperature gradient to the skin surface and thus causes a significant increase of convective heat transfer.

Following ISO 7933, the evaporative heat loss depends on the degree of which sweat is covering the skin surface (w_w), the saturation water vapour pressure at skin temperature ($p_{sk,s}$), the partial water vapour pressure of the surrounding air (p_a) and the evaporation resistance of the clothing and the boundary air layer (R_e) [11]:

$$\dot{Q}_{evap} = A_i \cdot w_w \cdot \frac{p_{sk,s} - p_a}{R_e} \tag{2.11}$$

Ultimately, when considering all heat exchange mechanisms and the underlying physical quantities and ignoring physiological and clothing aspects, relevant climate variables for thermal comfort evaluation are:

- Surface temperature of contacting (conduction) and non contacting (radiation) objects ($T_{s,ob}$)
- Solar irradiation intensity ($\dot{E}_{sol}$)
- Air temperature (T_a)
- Air velocity (v_a)
- Partial water vapour pressure of the air (p_a)

These variables must be considered locally for different body parts and with respect to the corresponding impact area. However, climate variables describe only the immediate thermal environment of a person but not the effect *on* the person. As the interface between climate impact and thermophysiology, clothing properties have also significant influence on the heat exchange of passengers with their surroundings and are hence essential to describe the actual thermal load on the human body. The resulting heat exchange with the environment effects certain body tissue temperatures and respective physiological responses, which are introduced the following section.

2.3.2 Thermophysiology

Humans are homeothermal mammals. In order to maintain an ideal body core temperature, the above described heat loss to the environment must match the heat generated by exothermic metabolic processes. If dissipation differs from metabolic heat generation, the body core temperature changes, which causes damage when exceeding certain limits. Thus, to enable the body to adapt to a wide range of climates, it relies on thermoregulation mechanisms [16, 47], balancing heat exchange with the environment and heat generation within the body.

Thermoregulation consists of three mechanisms: sweating, shivering and vasomotor activity. Sweating increases heat dissipation by additional evaporation in hot climate conditions. Shivering raises metabolic heat production by spontaneous muscle contractions in cold environments. Vasomotoric activity regulates local skin perfusion and therefore heat distribution to the extremities. In warm environments, vasodilitation ensures maximum blood flow to the extremities by widening blood vessels. This causes optimal utilization of the entire body surface for heat dissipation. In cool environments, vasoconstriction causes deliberate cooling of the extremities by narrowing blood vessels and therefore restricting perfusion. Heat circulation is then concentrated on the body core. While sweating and shivering occur only under extreme conditions, vasomotoric activity regulates heat dissipation in close-to-neutral conditions [49] as well.

Both thermoregulation and thermal perception depend on the activity of thermoreceptors, which can be considered thermal sensors of the human body. Relevant thermoreceptors are located in the skin and the hypothalamus. Their activity rate and the corresponding thermal sensation are related to the temperature of the tissue (skin/brain) and its temporal derivatives [25].

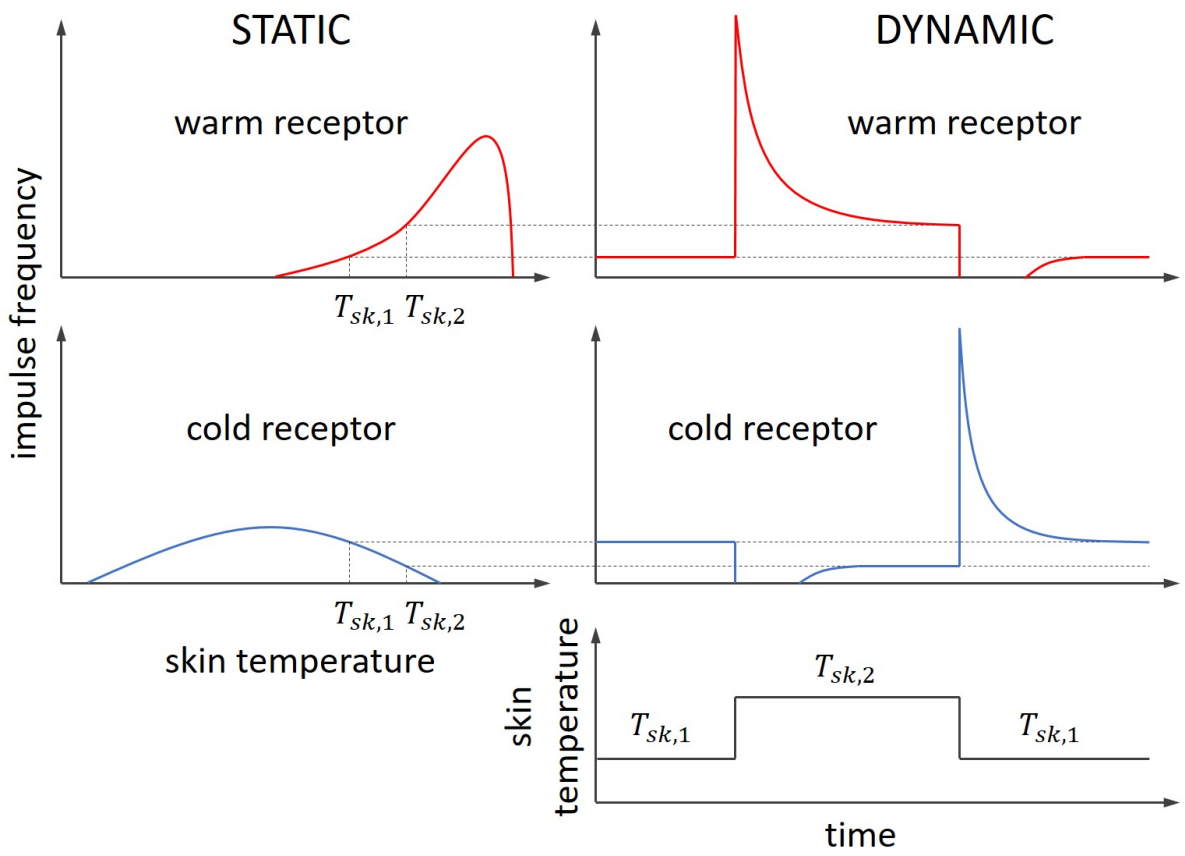

Figure 2.2: Illustration of the static and dynamic properties of thermoreceptors in the human skin (redrawn from [25]).

Figure 2.2 illustrates the properties of cutaneous thermal receptors. The left side of the graphic shows their static behaviour: A lower skin temperature $T_{sk,1}$ causes a lower impulse frequency of the warm receptor and a higher impulse frequency of the cold receptor, compared to a higher skin temperature $T_{sk,2}$ resulting in the opposite effects. The right side of the graphic illustrates the dynamic properties of the receptors when a sudden change of skin temperature occurs, presented by the skin temperature profile over time in the bottom right diagram: Initially the impulse frequencies are equal to the corresponding static ones, since skin temperature is constant. Upon a sudden jump from $T_{sk,1}$ to $T_{sk,2}$, the warm receptor overshoots while the cold receptor shuts down completely. By maintaining $T_{sk,2}$, the fire rates of both receptors approach their steady state impulse frequencies for this temperature. Following a sudden drop from $T_{sk,2}$ to $T_{sk,1}$, the opposite behaviour can be observed: activity of the warm receptor stops and the cold receptor overshoots. Apparently, the impulse frequency due to skin temperature change can be much higher than for the same skin temperatures when static, depending on the temporal change rate [25].

The level of thermoreceptors' activity is responsible for the perception of the immediate thermal environment, which is discussed in the following section.

2.3.3 Thermal Perception

Thermal perception distinguishes between sensation and comfort [65]. Thermal sensation is characterized by objective and rational expressions, e.g. "It is cold", whereas thermal comfort is highly subjective and is usually expressed emotionally, e.g. "I am freezing". This is not a hypothetical distinction, but an important fact to include in the evaluation of thermal environments. Depending on the current thermophysiological state, one and the same thermal sensation can be perceived as pleasant or unpleasant. This phenomenon is called alliesthesia[4] and is referred to as "Thermal Pleasure" in thermal comfort research [46]. For example, a person who has spent the whole day skiing on the slopes may experience seat heating on the journey back home as very pleasant, whereas someone who has spent the day in an overheated office at 30°C may perceive a warm seat as uncomfortable, even though in both cases the seat has the same temperature. Thus, the same local thermal stimulus can cause different thermal perceptions, depending on the overall thermophysiological state [35].

This leads to another distinction that must be made between overall thermal perception and local thermal perception. Obviously a person can experience cold discomfort over most of the body and at the same time thermal pleasure at the warmed body area. Therefore, overall and local perception must be considered both together and separately. A detailed discussion of the subject can be found in [65].

Benzinger et al. found that overall warm discomfort occurs as soon as tympanic temperature (indicating brain temperature) exceeds 37°C. Overall cold discomfort occurs when mean skin temperature falls below 34°C [5]. Fiala [19] defined the thresholds for thermal discomfort very similarly, following Hardy [23]. For Local Thermal Comfort (LTC), however, no such clear definition exists, in particular because of the above described dependency of LTC on the overall thermal state.

2.4 Thermal Environment Evaluation

Section 2.3 introduced the characteristics of and interrelations between the three dimensions of thermal comfort: climate conditions, thermophysiology and thermal perception. The task of thermal comfort research is to objectively describe these dimensions and interrelations to evaluate thermal environments with regard to their human occupants. In this section respective evaluation methods are introduced and the thermal perception models used for the investigations in this dissertation are described in detail.

Climate Measurement The impact of the climate conditions on vehicle passengers must be quantified to assess the effectiveness of climatization. However, as described in section 2.3.1, the climate impact can only be understood in interaction with the passenger, which would mean measuring physiological variables (such as skin temperature or sweat

[4] A psychophysiological phenomenon that describes the dependent relationship between the internal state of an organism and the perceived pleasure or displeasure of stimuli.

rates) and relating them to climate variables (such as air temperature or air humidity). Since physiological properties are highly subjective, a statistically representative number of human subjects would be needed for each assessment procedure, which is certainly not feasible. Researchers therefore usually define standard values for physiological and clothing properties, which allow quantifying the thermal impact from climate conditions objectively. For such quantification, one possibility would be to directly measure the individual physical variables separately and then to calculate the expected heat exchange. Since this approach is complex and expensive, researchers developed Combined Climate Indicators (CCI), describing the effects of different climate influences on passengers by one quantity. A review of such CCI for vehicular applications can be found in [53] and a description of instruments to measure different climate quantities is given in [10] and [16]. Relevant CCI that are incorporated in the evaluation methods described in this section are introduced in the following:

Mean Radiant Temperature ($\bar{T_r}$) is *"the uniform temperature of an imaginary enclosed space in which the radiation-induced heat transfer away from the human body is just as great as that in the real, inhomogeneous enclosed space" [10].* $\bar{T_r}$ can be calculated from air temperature, air velocity and the so-called globe temperature, which can be measured by a black-globe thermometer. The instrument consists of a black globe in the center of which is placed a temperature sensor measuring the air temperature inside the globe (globe temperature (T_g)), which in turn is influenced by convection and radiation on its outer surface. If air temperature and air velocity are additionally measured outside the globe, the influence of convection and radiation on the inner temperature of the globe can be quantified mathematically with respect to the globe's geometry and surface properties. The mean radiant temperature can then be calculated via an adaptation of the Stefan-Boltzmann law. A detailed description of the calculation for natural and forced convection can be found in Appendix B of ISO 7726:2001 [10]. Besides the globe-temperature, the air temperature and the air velocity, $\bar{T_r}$ depends on the emission coefficient of the black-globe (ϵ_g) and the globe diameter (d_g):

$$\text{Natural Convection:} \quad \bar{T_r} = \left[(T_g + 273)^4 + \frac{0.25 \cdot 10^8}{\epsilon_g} \left(\frac{|T_g - T_a|}{d_g} \right)^{\frac{1}{4}} \cdot (T_g - T_a) \right]^{\frac{1}{4}} - 273 \tag{2.12}$$

$$\text{Forced Convection:} \quad \bar{T_r} = \left[(T_g + 273)^4 + \frac{1.1 \cdot 10^8 \cdot v_a^{0.6}}{\epsilon_g \cdot d_g^{0.4}} \cdot (T_g - T_a) \right]^{\frac{1}{4}} - 273 \tag{2.13}$$

Operative Temperature (T_{op}) is defined as *"the uniform temperature of an enclosure in which a person would exchange the same amount of heat by radiation and convection as in the existing non-uniform environment" [10].* T_{op} can be calculated from the air temperature, the mean radiant temperature and the corresponding heat transer coefficients for

convection (h_c) and radiation (h_r) and can thus be obtained from the same measurements as $\bar{T}_r$ [10]:

$$T_{op} = \frac{h_c \cdot T_a + h_r \cdot \bar{T}_r}{h_c + h_r} \tag{2.14}$$

Equivalent Temperature (T_{eq}) Since the measurements necessary for T_{op} are only applicable in steady-state climate conditions the concept can not be applied to transient conditions as they occur in vehicles. ISO 14505-2 therefore defines equivalent temperature very similar to the definition of T_{op}, however based on a different mathematical relation and thus on a different measuring technique (see section 3.1 of ISO 14505-2:2006 [9]):

"The equivalent temperature is the temperature of a uniform space with a mean radiant temperature equal to the air temperature and an air velocity of zero, in which the heat loss of a person by convection and radiation is equal to the heat loss under the conditions actually assessed" [9].

T_{eq} is obtained from the actual heat loss in the assessed environment (Q_{env}), the surface temperature of the person (T_s) and the combined heat tranfer coefficient for convection and radiation in the uniform environment (h_{cal}):

$$T_{eq} = T_s - \frac{Q_{env}}{h_{cal}} \tag{2.15}$$

In practical applications T_{eq} is measured using heated sensors for which ISO 14505-2 provides additional definitions.

The climate impact on passengers needs to be measured locally to evaluate DPC. For this purpose, only measurements with human dummies (manikins) are feasible. These manikins can be divided into sensor-wearing (see [20] and [58]) and thermal manikins (see [39]). Another distinction can be made with regard to the measuring principle. Some manikins directly measure physical quantities, such as air temperature and air velocity, and interpret the measurements mathematically afterwards (see [58]); others use CCI to quantify the effect of several climate properties together (see [20]). Reviews of manikins for climate impact measurement can be found in [1] and [29]. The most relevant CCI quantity with regard to manikins is equivalent temperature in its various forms, that are explained in [1, 9, 40] and will be discussed in more detail in the following sections.

Clothing Properties Clothing ensembles vary from person to person and also depend on the season. Evaluation methods for thermal environments therefore usually assume standard clothing ensembles (see [9, 11, 13]) and the associated standardized properties, as defined in the international standard ISO 9920 [14]. The thermal insulation properties of clothing ensembles are usually specified in *clo*, which refers to a thermal resistance and can be converted into the corresponding SI[5]unit R_{cl} [14]:

$$R_{cl} : 1clo = 0.155\frac{m^2K}{W} \tag{2.16}$$

Thermophysiology Physiological responses to climate conditions, such as thermoregulation or thermoreceptor activity, can be simulated by thermophysiological models. The historical development of such models goes back to Fanger's one-node model [18], which simulates human heat exchange with the environment for steady state and uniform conditions. In 1971, Gagge introduced a two-node model, which separated the body shell from the body core [21], enabling the simulation of thermoregulation mechanisms. In the same year Stolwijk published a multi-node model with six body segments, which takes into account non-uniform climate conditions and is able to simulate local tissue temperatures and detailed heat distributions inside the human body [56]. In 1998 Fiala introduced a multi-segment model, which makes a detailed and especially transient simulation of local and overall thermophysiological processes possible [19]. Comprehensive reviews of thermophysiological models can be found in [6] and [32]. However, the basic concept is the same for all thermophysiological models: predicting thermophysiological processes and properties in a deterministic simulation model.

Thermal Perception Causal relations between physiological conditions and the corresponding cognitive interpretations cannot exhaustively be explained. It is therefore not possible to mathematically model human feelings or emotions. Rather, stochastic models are built, correlating thermal perceptions with physiological or environmental variables without claiming to produce full causal explanations. The description of such stochastic relations is achieved by means of human subjects' evaluations under defined climate conditions and subsequent stochastic modelling. These models are designed to objectively describe the expectable physiological or emotional reaction to an exposure to certain climate conditions. Some of these methods correlate human thermal perception directly with climate variables and some relate to the intermediate physiological reactions. The models can be classified with regard to the three dimensions of thermal comfort again. The resulting principle of thermal environment evaluation models is illustrated in figure 2.3 and the model concepts are listed below:

(A) Climate variables based thermophysiological models
(B) Physiological variables based thermal perception models
(C) Climate variables based thermal perception models

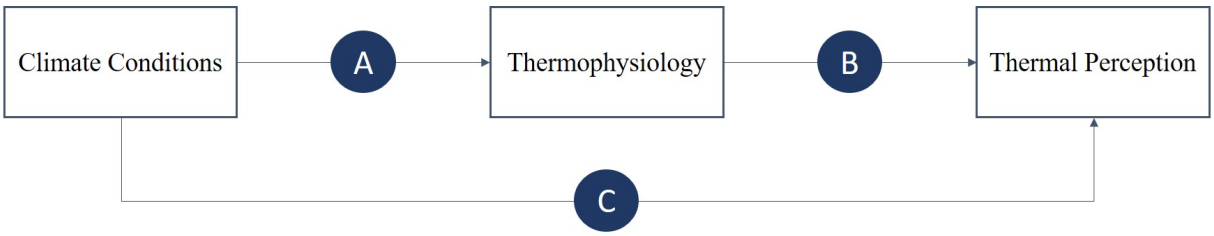

Figure 2.3: Principle of thermal environment evaluation models.

[5]International System of Units *(french: Système international d'unités)* (SI)

Since the mid 1990's, a variety of evaluation methods for vehicle thermal comfort have been introduced. Reviews and historical overviews can be found in [1, 2, 7, 28]. However, only a few have the potential to serve as an approach to climatization performance assessment. The evaluation methods employed in this work were chosen on the basis of at least one of the following criteria:

- Previous relevance in automotive industrial applications
- Potential for meeting DPC performance assessment requirements

The next section describes the state of the art of the selected methods, based on the three dimensions of thermal comfort.

2.4.1 The Fanger Method

Fanger's work on thermal comfort [17, 18] is a milestone in thermal environment evaluation research. It introduced a thermal comfort prediction model based on measurable physical variables in 1970. Since then the method has been widely used and has been incorporated into the international standard DIN EN ISO 7730 [13]. Although the method can only be used to evaluate uniform and steady state climate conditions, it introduced the concept of mathematical description of heat exchange between humans and their surroundings and hence laid the foundation for many further evaluation methods to come.

Climate Measurement The method integrates the concept of overall thermal load, which is determined by heat exchange mechanisms between people and their environment. Therefore, several climate quantities serve as input variables for the model and must be measured directly:

$\bar{T}_r$	Mean Radiant Temperature
T_a	Air Temperature
RH	Relative Humidity
v_a	Relative Air Velocity

Air temperature can be measured directly by any temperature sensor, such as a mercury thermometer, a thermocouple or a resistance probe. Relative air humidity is also measured directly or obtained from air temperature and absolute humidity by various types of hygrometers. Air velocity can be measured using an impeller anemometer, if air velocity is expected to be high and the direction of the air movement is of interest. If direction does not matter and air velocity is low, a hot-wire anemometer can be used. $\bar{T}_r$ can be obtained from the globe temperature measured by a black-globe thermometer.

Physiological Interpretation The Fanger method does not involve a detailed thermophysiological model but interpretes climate impact on the basis of a hypothetical heat exchange assuming static thermophysiological properties. This objective Thermal Load ($\dot{q}_{TL}$) on the human body bis calculated using the basic heat exchange equation 2.17.

$$\dot{q}_{TL} = \dot{q}_{TL,C,res} + \dot{q}_{TL,E,res} + \dot{q}_{TL,E,s} + \dot{q}_{TL,D,s} + \dot{q}_{TL,R,s} + \dot{q}_{TL,C,s} \tag{2.17}$$

$\dot{q}_{TL,C,res}$ is the respiratory convective heat loss in the lungs and is calculated using:

$$\dot{q}_{TL,C,res} = 0.0014M(34 - T_a) \tag{2.18}$$

with M being the metabolic rate, depending on the activity level. $\dot{q}_{TL,E,res}$ is the respiratory evaporative heat loss in the lungs and is calculated using:

$$\dot{q}_{TL,E,res} = 1.7 \cdot 10^{-5} M(5867 - p_a) \tag{2.19}$$

with the partial water vapour pressure of the surrounding air:

$$p_a = 610.5 e^{\frac{17.269 \cdot T_a}{237.3 + T_a}} \cdot RH$$

$\dot{q}_{TL,E,s}$ is the evaporative heat loss on the skin surface due to sweat vapourization and is calculated using:

$$\dot{q}_{TL,E,s} = 0.42[(M - W) - 58.15] \tag{2.20}$$

with W being the effective mechanical power due to physical activity, which is zero for vehicle passengers. $\dot{q}_{TL,D,s}$ is the heat loss due to water vapour diffusion through the skin and is calculated using:

$$\dot{q}_{TL,D,s} = 3.05 \cdot 10^{-3}[5733 - 6.99(M - W) - p_a] \tag{2.21}$$

$\dot{q}_{TL,R,s}$ is the radiative heat exchange at the body surface and is calculated using:

$$\dot{q}_{TL,R,s} = 3.96 \cdot 10^{-8} f_{cl}[(T_{cl} + 273)^4 - (\bar{T_r} + 273)^4] \tag{2.22}$$

$\dot{q}_{TL,C,s}$ is the convective heat exchange on the body surface and is calculated using:

$$\dot{q}_{TL,C,s} = f_{cl} h_c (T_{cl} - T_a) \tag{2.23}$$

T_{cl} is the clothing surface temperature, which is calculated iteratively from convective and radiative heat exchange:

$$T_{cl} = 35.7 - 0.028(M - W) - R_{cl}\left(\dot{q}_{TL,R,s} + \dot{q}_{TL,C,s}\right) \tag{2.24}$$

with f_{cl} being the clothing area factor, which is calculated by incorporating the thermal resistance of the clothing ensemble (R_{cl}):

$$f_{cl} = \begin{cases} 1.00 + 1.290R_{cl} & \text{for} \quad R_{cl} \leq 0.078\frac{m^2K}{W} \\ 1.05 + 0.645R_{cl} & \text{for} \quad R_{cl} > 0.078\frac{m^2K}{W} \end{cases}$$

and with h_c being the convective heat transfer coefficient:

$$h_c = \begin{cases} 2.38 \cdot |T_{cl} - T_a|^{0.25} & \text{for} \quad 2.38 \cdot |T_{cl} - T_a|^{0.25} > 12.1 \cdot \sqrt{v_a} \\ 12.1 \cdot \sqrt{v_a} & \text{for} \quad 2.38 \cdot |T_{cl} - T_a|^{0.25} < 12.1 \cdot \sqrt{v_a} \end{cases}$$

Thermal Perception Fanger's thermal perception model differentiates between thermal sensation and thermal comfort. Thermal sensation is represented by the so-called Predicted Mean Vote (PMV), represented by the ASHRAE[6] thermal sensation scale (see table 2.2) and is calculated using an exponential relationship of M and $\dot{q}_{TL}$:

$$PMV = \dot{q}_{TL}(0.303e^{-0.036M} + 0.028) \tag{2.25}$$

PMV	Interpretation
+3	hot
+2	warm
+1	slightly warm
0	neutral
−1	slightly cool
−2	cool
−3	cold

Table 2.2: Thermal sensation scale in the Fanger PMV model [13].

Thermal comfort is represented by the Predicted Percentage of Dissatisfied (PPD). This thermal discomfort quantification is again an exponential function of PMV:

$$PPD = 100 - 95e^{(-0.03353PMV^4 - 0.2179PMV^2)} \tag{2.26}$$

[6]American Society of Heating Refrigerating and Air-conditioning Engineers

The entire assessment procedure of the Fanger method is illustrated in figure 2.4. The symbols fo r the three dimensions of thermal comfort represent the presence of models for each dimension (climate measurement, thermophysiology and thermal perception). The filled squares illustrate the models' ability to evaluate thermal conditions only for the entire body but not for local effects. The mathematical symbols in the boxes represent the input and output variables of each submodel. The graphic should be read as follows: The Fanger method provides for the assessment of overall thermal sensation (PMV) and overall thermal comfort (PPD) in relation to overall thermal load ($\dot{q}_{TL}$), which can be obtained by centrally measuring $\bar{T}_r$, T_a, RH and v_a. For each of the three dimensions of thermal comfort, the method provides a description model or technique. The Fanger method is valid for steady state and uniform climate conditions, only.

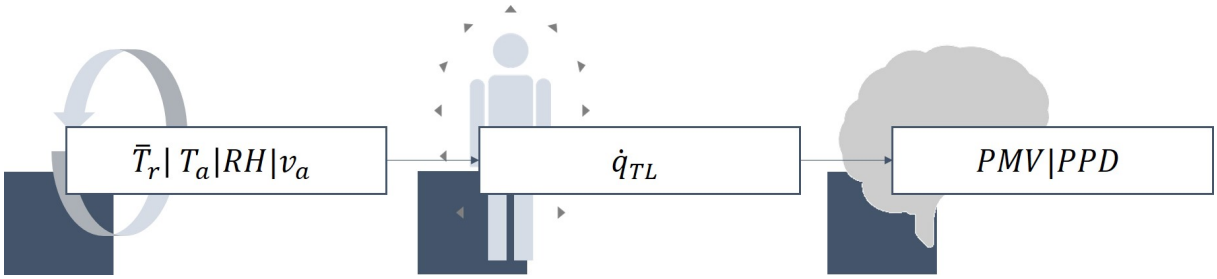

Figure 2.4: Evaluation principle of the Fanger method.

2.4.2 The Park Method

The evaluation method of Park et al. [41, 44] is especially designed to assess the performance of vehicular climatization systems in terms of thermal comfort. The authors combine Fanger's approach of thermal load calculation [13, 17] with a local climate impact measurement system and the climatization performance procedure for vehicle HVAC.

As described in section 2.2, the current evaluation method of [8] uses the duration until a certain air temperature is reached (*Time to Temperature*) to assess climatization performance. The target temperature can be considered an indicator of the (near) thermal neutrality of passengers. Accordingly, the quicker this condition is reached, the higher the overall climatization system is rated. Park et al. approach evaluating performance by generalizing this method and redefining the evaluation quantity as *Time to Comfort*, with comfort being understood to mean thermal neutrality. For DPC systems, such thermal neutrality is expected to be reached at non-uniform climate conditions and must be defined using a different quantity than air temperature.

For a thermophysiological interpretation, the local climate measurement is transformed into an overall thermal load on the passenger's body. Thermal perception is represented by Overall Thermal Sensation (OTS) in relation to that thermal load.

Climate Measurement For climate measurement, a combined sensor system, called DressMAN[7], is used (see original introduction in [37] and the currently used state of the art system in [20]). DressMAN consists of from 16 to 60 sensors, distributed over the entire body of a person or manikin. The latest version (Autumn 2018 to Summer 2019) allows measuring Local Directed Equivalent Temperature ($T_{eq,direct}$) at each air adjacent position. $T_{eq,direct}$ quantifies the local climate impact from convection and radiation on passengers and is measured using a heated sensor. DIN EN ISO 14505-2 [9] defines $T_{eq,direct}$ with the mathematical relationship of equation 2.27 and the following verbal expression:

"Directed equivalent temperature is the uniform temperature of an imaginary enclosed space with the same temperature of air and surrounding surfaces and with an air velocity of zero, in which a small flat heated surface dissipates the same dry heat by radiation and convection as in the actual non-uniform environment."[9]:

$$T_{eq,direct} = T_{s,sensor} - \frac{\dot{q}_{env,sensor}}{h_{cal,sensor}} \tag{2.27}$$

where the combined heat transfer coefficient for radiation and convection at the sensor ($h_{cal,sensor}$) is derived from calibration conditions (uniform environment). $T_{s,sensor}$ is the surface temperature of the sensor and $\dot{q}_{env,sensor}$ the area-specific heat flux at the sensor surface. On contact surface areas the contact temperature (T_c) and heat flux ($\dot{q}_{env,c}$) are measured between an average sized man and the contacting object. The DressMAN system also includes central measurements of relative air humidity (RH) and air temperature (T_a) to calculate absolute air humidity.

Physiological Interpretation Similar to the Fanger approach, the Park method does not involve a detailed simulation of thermophysiological processes. An extension of the $T_{eq,direct}$ definition of equation 2.27 by local heat resistance of clothing and trapped air ($R_{t,local}$) enables the calculation of Dry Local Thermal Load at Air-adjacent body areas ($\dot{q}_{TL,dr,A,i}$), by assuming an ideal (constant) skin temperature ($T_{sk,ideal}$) and integrating the actually measured $T_{eq,direct}$ using:

$$\dot{q}_{TL,dr,A,i} = \frac{T_{sk,ideal} - T_{eq,direct}}{R_{t,local}} \tag{2.28}$$

Since $T_{eq,direct}$ is by definition not applicable to the thermal impact of contact surfaces, a different approach is needed here. Currently, no sensor is available to objectively acquire the contact thermal load, so Park et al. decided to use directly measured T_c at the contact between an average sized man and the seat. By assuming a constant skin temperature for

[7]Dummy Representing Suit for Simulation of huMAN heatloss

this man, a hypothetical heat flux between the skin and the contact surface is interpreted as the Dry Thermal Load at contacting body areas ($\dot{q}_{TL,dr,K,i}$) assuming the idealized constant local skin temperature:

$$\dot{q}_{TL,dr,K,i} = \frac{T_{sk,ideal} - T_c}{R_{t,local}} \tag{2.29}$$

The area-specific thermal load is integrated over a defined local impact area for each sensor ($A_{i,i}$) and summed up over the entire number of sensors (n) to determine the Dry Overall Thermal Load ($\dot{q}_{TL,dr}$). This $\dot{q}_{TL,dr}$ can be understood as the mean (uniform) thermal impact on the passenger's body from the surrounding (non-uniform) climate conditions. A detailed simulation of thermophysiological processes is not part of the method; however, the method accounts for the local thermophysiological impact of a certain thermal load on different body parts. This impact is expected to depend mainly on body part specific thermophysiological properties like body fat percentage, local metabolic heat generation and blood perfusion [30]. The head, for example, has a relatively high metabolic rate, compared to the other body parts, at low activity rates. Therefore, the same immediate thermal surrounding will result in a higher skin temperature at the head, compared to the hand. This means, area-specific thermal load is derived differently for individual body parts. Park et al. consider this local thermophysiological impact using local weighting factors (w_i) on $\dot{q}_{TL,dr,i}$:

$$\dot{q}_{TL,dr} = \sum_{i=1}^{n} \left(\dot{q}_{TL,dr,i} \cdot \frac{w_i \cdot A_{i,i}}{\sum_{i=1}^{n} (w_i \cdot A_{i,i})} \right) \tag{2.30}$$

Thermal Perception In human subject studies for heat-up and cool-down conditions, the physical quantity $\dot{q}_{TL,dr}$ was related to subjects' thermal perception ratings on an ASHRAE scale, just as Fanger (see table 2.2). The resulting logistic prediction model returns OTS for thermal perception evaluation, where thermal neutrality is defined as $OTS = 0$.

$$OTS = \frac{6}{e^{(a \cdot \dot{q}_{TL,dr} + b)}} - 3 \tag{2.31}$$

In heat-up or winter conditions, the coefficients a and b are scalars. For cool-down conditions in summer, b varies in a linear relation to absolute humidity (AH):

$$b_{winter} = const. \qquad b_{summer} = c \cdot AH + d$$

In short, the Park method enables assessment of overall thermal perception in relation to overall dry thermal load and absolute humidity, based on partly centrally and partly

locally measured climate variables (indicated by the tiled squares in 2.5). The method is comprised of a technique for local climate measurement, a model for local and overall dry thermal load quantification and a model for overall thermal sensation prediction. The Park method is valid for transient and non-uniform climate conditions as they occur in vehicles.

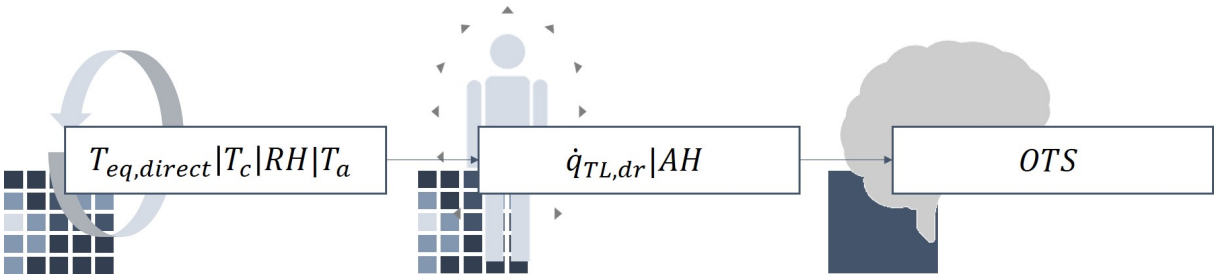

Figure 2.5: Evaluation principle of the Park method.

2.4.3 The Nilsson Method

An evaluation method for steady state thermal environments in vehicles was introduced by Nilsson [39] and is implemented in DIN EN ISO 14505-2 [9]. The method suggests *Comfort Zones* which are defined for both the whole body and individual body segments, such as scalp, chest or lower back.

Climate Measurement Measurements are realized by a segmentally heated thermal manikin, returning measured Segmental Equivalent Temperature ($T_{eq,segment}$) [9]:

$$T_{eq,segment} = T_{s,segment} - \frac{\dot{q}_{env,segment}}{h_{cal,segment}} \tag{2.32}$$

Using area weighted summation, Equivalent Temperature for the Wohle Body ($T_{eq,whole}$) is calculated from $T_{eq,segment}$ using equation 2.33.

$$T_{eq,whole} = \sum_{s=1}^{n} \left(T_{eq,segment} \cdot \frac{A_{segment}}{A_{whole}} \right) \tag{2.33}$$

While Park et al. [44, 41] interprete the $T_{eq,direct}$ measurement mathematically with respect to clothing thermal resistance, Nilsson measured $T_{eq,segment}$ using different clothing ensembles on the thermal manikin. This allows for direct correlation of equivalent temperature for the whole body ($T_{eq,whole}$) with thermal perception without converting it to thermal load, yet comes with the drawback of being restricted to a certain clothing ensemble.

Physiological Interpretation The Nilsson method basically follows the same argumentation as the Park method, yet in this case, it is already incorporated in the measuring technique. $T_{eq,whole}$ and segmental equivalent temperature ($T_{eq,segment}$) are understood as the perceived temperature of passengers and directly correlated with thermal perception.

Thermal Perception The method relates measured $T_{eq,whole}$ and $T_{eq,segment}$ to Mean Thermal Vote (MTV), using a mixed thermal sensation and comfort scale (see table 2.3).

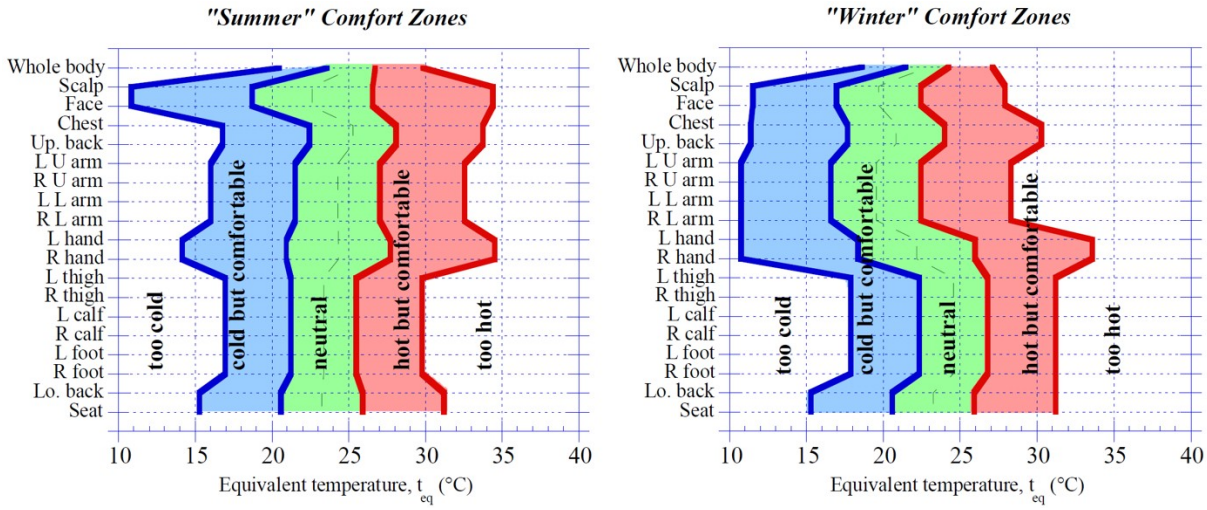

Figure 2.6: Comfort Zones of the Nilsson model relating to $T_{eq,segment}$ and $T_{eq,whole}$ (from [39]).

MTV	Interpretation
5	too hot
4	hot but comfortable
3	neutral
2	cold but comfortable
1	too cold

Table 2.3: Mixed thermal sensation and comfort scale of the Nilsson model [39].

The comfort zones reflect the range of T_{eq} in which at least 80% of people are predicted to give the corresponding vote. Thermal neutrality is defined as MTV = 3. Nilsson defined comfort zones for winter and summer applications differently, depending on clothing ensembles. In figure 2.6 these comfort zones are visualized.

In brief, the Nilsson method enables evaluating local and overall thermal comfort in relation to body segment related climate measurements. The method comprises a technique for body segment wise and overall equivalent temperature measurement and a model for segmental and overall thermal comfort prediction (see figure 2.7). The method is valid for steady state and non-uniform climate conditions.

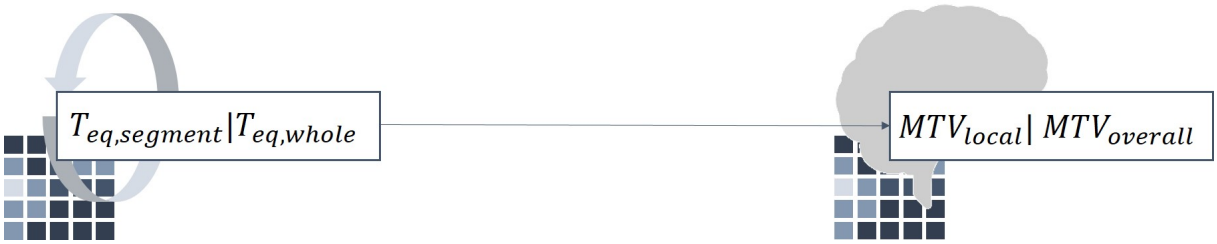

Figure 2.7: Evaluation principle of the Nilsson method.

2.4.4 The Fiala Method

The thermal perception models introduced thus far use either climate variables or a rudimentary physiological interpretation as input variables. Fiala's thermal perception model, however, uses actual physiological input variables utilizing an additional thermophysiological model to simulate them [19].

Climate Measurement Physiological models are typically designed for use in simulation programs and are integrated into virtual environments. These models are not intended for use in combination with climate measurements. However, since the model is designed to represent realistic heat exchange between persons and their environment, the input variables are physical quantities, which can also be obtained by measurements. Fiala's method examines heat exchange with the environment by incorporating convection, radiation and evaporation. The following physical quantities can thus serve as climate input variables:

- Mean Radiant Temperature ($\bar{T}_r$)
- Area-specific solar irradiation intensity ($\dot{E}_{sol}$)
- Local air temperature (T_a)
- Local air velocity (v_a)
- Relative air humidity (RH)

Physiological Interpretation Fiala's thermophysiological model is designed to simulate the thermal impact on people in various thermal environments. The model consists of two complementary submodels: The *Active System* computes thermophysiological properties (shivering, sweating, vasomotoric activity). The*Passive System* simulates heat transfer within the tissue (heat conduction, metabolism, blood circulation) and heat exchange with the environment (convection, radiation, clothing insulation, evaporation and respiratory heat loss). The physiological model enables dynamic computation of thermophysiological processes and properties.

Thermal Perception In addition to his thermophysiological model, Fiala developed a thermal perception model to derive Dynamic Thermal Sensation (DTS) from the simu-

lated tissue temperatures. He has drawn the corresponding relations from a number of other publications on thermal comfort investigations and synthesized them in the following equations:

$$DTS = 3 \cdot tanh(f_{sk} + \Phi + \Psi) \tag{2.34}$$

The coefficient f_{sk} represents the deviation from thermal neutrality:

$$f_{sk} = 1.026 \cdot \Delta T_{sk,m} \qquad \text{for} \qquad \Delta T_{sk,m} > 0 \tag{2.35}$$
$$f_{sk} = 0.298 \cdot \Delta T_{sk,m} \qquad \text{for} \qquad \Delta T_{sk,m} < 0 \tag{2.36}$$

The term Φ represents the influence of core temperature on thermal sensation and depends on hypothalamus temperature (T_{hyp}) and mean skin temperature ($T_{sk,m}$):

$$\Phi = 6.662 exp\left(\frac{-0.565}{\Delta T_{hyp}}\right) exp\left(\frac{-7.634}{5 - \Delta T_{sk,m}}\right) \tag{2.37}$$

$$\Phi = 0 \qquad \text{for} \qquad \Delta T_{hyp} \leq 0K \text{and} \Delta T_{sk,m} \geq 5K \tag{2.38}$$

Since Fiala's DTS index is intended to be used in a dynamic thermophysiological simulation, the coefficient Ψ represents the dynamic behavior of thermal perception in relation to a temporal skin temperature change of the current simulation time step (Δt):

$$\Psi = \frac{\tau_- + \tau_+}{1 + \Phi} \tag{2.39}$$

$$\tau_- = 0.0114 \frac{dTsk,m}{dt} \qquad \text{for} \qquad \frac{dTsk,m}{dt} < 0 \tag{2.40}$$

$$\tau_+ = 0.137 \left(\frac{dT_{sk,m}}{dt}\right)_{max} \cdot e^{-0.681 \Delta t} \qquad \text{for} \qquad \frac{dT_{sk,m}}{dt} > 0 \tag{2.41}$$

In sum, the Fiala method allows the evaluation of overall thermal perception in relation to local and overall physiological variables, obtained by thermophysiological simulation with regard to local climate variables. The procedure is illustrated in figure 2.8. The method comprises a model for detailed simulation of local and overall thermophysiological

properties and processes and a model for overall thermal sensation prediction. A technique for measuring the necessary local climate input variables for the physiological model is not part of the method. The Fiala method is valid for transient and non-uniform climate conditions.

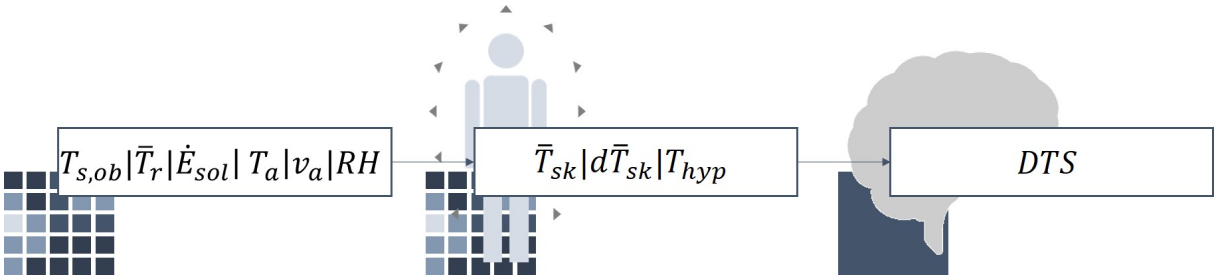

Figure 2.8: Evaluation principle of the Fiala method.

2.4.5 The Zhang Method

The Zhang model [65, 66, 67, 68, 69] was specially developed to evaluate transient and non-uniform thermal environments. However, it is not a comprehensive thermal environment evaluation method, but only a thermal perception model, using physiological input variables. Consequently, the model must be connected to a thermophysiological model, which again requires simulated climate conditions. Thus, neither climate measurement nor physiological interpretations are considered here and only the thermal perception model and its submodels are described. The original model was introduced in Zhang's dissertation in 2003 [65] and later slightly changed with regard to the model's coefficients [66, 67, 68, 69]. For my own investigations in the following chapters I merged the Zhang model with Fiala's thermophysiological model [19] and hence decided to use a simulation implementation of both. The corresponding simulation tool [50] only implemented the first version of Zhang's model, which the following descriptions refer to.

Thermal Perception The Zhang model consists of four submodels, which each builds on the other (see figure 2.9). The basic model is the Local Thermal Sensation (LTS) model, which is based on a modified logistic function and consists of one part for static sensation (LTS_{st}) and one for dynamic sensation (LTS_{dy}):

$$LTS = LTS_{st} + LTS_{dy} \tag{2.42}$$

The static sensation equation 2.43 calculates the static portion of local thermal sensation from mean skin temperature ($T_{sk,mean}$) and local skin temperature ($T_{sk,i}$). The setpoint ($T_{sk,set}$) is the skin temperature, at which a certain body part is perceived as thermally neutral.

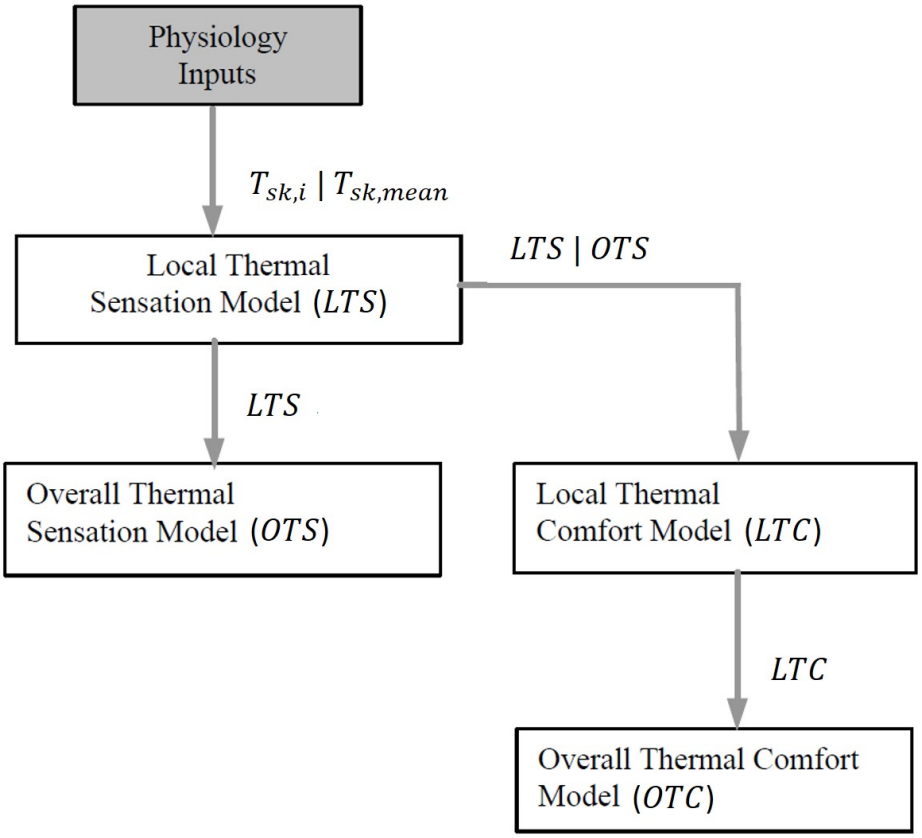

Figure 2.9: Illustration of Zhang's thermal perception model with connection of sub models and physiological input (adapted from [65]).

$$LTS_{st} = 4\left(\frac{2}{1+e^{-C1\left(T_{sk,i}-T_{sk,i,set}\right)-K1\left[\left(T_{sk,i}-T_{sk,mean}\right)-\left(T_{sk,i,set}-T_{sk,mean,set}\right)\right]}}-1\right) \tag{2.43}$$

The dynamic portion of local thermal sensation is calculated from the temporal derivatives of the body core temperature $\left(\frac{dT_{core}}{dt}\right)$ and of the local skin temperature $\left(\frac{dT_{sk}}{dt}\right)$ using equation 2.44.

$$LTS_{dy} = C2_i\frac{dT_{sk,i}}{dt} + C3_i\frac{dT_{core}}{dt} \tag{2.44}$$

The resulting LTS serves again as input for the successor models. Overall Thermal Sensation (OTS) is obtained by employing a weighted average of all local sensations (LTS_i) using equation 2.45, where the weighting factor w_i refers to the corresponding body part i.

$$OTS = \frac{\sum_{i=1}^{n}(LTS_i \cdot w_i)}{\sum_{i=1}^{n} w_i} \tag{2.45}$$

Both LTS and OTS are based on a 9-step scale [4] for thermal sensation, extending the original ASHRAE scale by the extreme ratings "very hot" and "very cold" (see table 2.4), where thermal neutrality is defined as OTS = 0.

Table 2.4: Thermal sensation scale of the Zhang model [65].

Thermal Sensation	Interpretation
4	very hot
3	hot
2	warm
1	slightly warm
0	neutral
−1	slightly cool
−2	cool
−3	cold
−4	very cold

Table 2.5: Thermal comfort scale of the Zhang model [65].

Thermal Comfort	Interpretation
4	very comfortable
3	
2	
1	just comfortable
0	
−1	just uncomfortable
−2	
−3	
−4	very uncomfortable

The Zhang model strictly differenciates between sensation and comfort. Local Thermal Comfort (LTC) is derived using a separate comfort scale (see table 2.5) and the quantification is obtained by a complex mathematical expression, Zhang calls a "logistic-adapted linear model" of LTS, which shifts slope and magnitude with respect to the overall thermal state, represented by OTS [65] (see equation 2.46).

$$\begin{aligned} LTC = &\left[\frac{\frac{-4-\left(C6+C71\left|OTS^-\right|+C72\left|OTS^+\right|\right)}{\left|(-4+C31|OTS^-|+C8)\right|^n} - \frac{-4-\left(C6+C71\left|OTS^-\right|+C72\left|OTS^+\right|\right)}{\left|(4+C31|OTS^-|+C32|OTS^+|+C8)\right|^n}}{e^{15(LTS+C31|OTS^-|+C32|OTS^+|+C8)}+1} \right. \\ &\left. + \frac{-4-(C6+C71\,|OTS^-|+C72\,|OTS^+|)}{|(4+C31\,|OTS^-|+C32\,|OTS^+|+C8)|^n} \right] \\ &\left(LTS+C31\left|OTS^-\right|+C32\left|OTS^+\right|+C8\right)^n \\ &+C6+C71\left|OTS^-\right|+C72\left|OTS^+\right| \end{aligned} \tag{2.46}$$

Overall Thermal Comfort (OTC) is dominated by local discomfort. Unlike OTS, OTC cannot be obtained from a weighted sum of all OTC_i. Rather, it is a rule-based model, with the two following rules:

Rule 1: OTC is the average of the two minimum LTC votes, unless rule 2 applies
Rule 2: If the following criteria are met, then OTC is the average of the two minimum votes and the maximum vote:

- The second lowest LTC vote is greater than -2.5
- The subject has some control over the thermal environment or the thermal conditions are transient

The Zhang method allows the assessment of local and overall thermal sensation and comfort in relation to local and overall physiological variables. The procedure is illustrated in figure 2.10. The method is comprised of a comprehensive model complex for LTS, LTC, OTS and OTC in transient and non-uniform climate conditions. The Zhang method does not provide a simulation of thermophysiological properties and processes nor climate measurements.

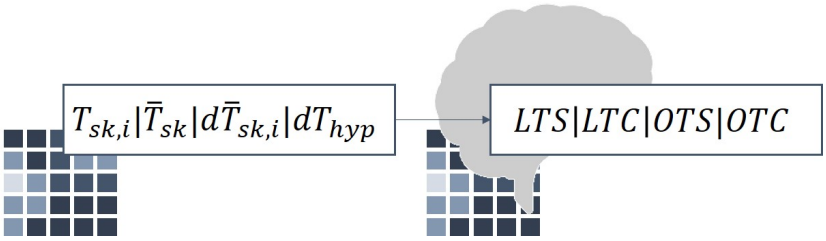

Figure 2.10: Evaluation principle of the Zhang method.

2.5 Appraisal of the State of the Art

The examination of the state of the art commenced with current DPC technologies and their specifications. A subsequent analysis of the current HVAC assessment procedure revealed deficiencies with regard to these specifications and led to relevant knowledge in the field of thermal comfort. Accordingly, potentially applicable thermal environment evaluation methods were introduced. In this section the applicability of these methods to DPC performance assessment is discussed and corresponding research gaps are uncovered.

As described in section 2.1, climatization performance must be evaluated with regard to the specific climate conditions during a vehicle conditioning phase. From a physical point of view, a distinction between winter, or the heating mode, and sommer, or the cooling mode, is reasonable, with respect to climatization effectiveness assessment. In summer, evaporative heat loss is relevant in addition to convection, radiation and conduction. The consideration of evaporation is especially to be respected in extreme conditions as they

occur during cool-down situations, because of increased sweating. This also makes the cooling mode the more relevant case for identifying appropriate measuring and evaluation methods for the cooling *and* the heating mode. Therefore only the cooling mode is examined in the following investigations. However, the argumentation equally applies to the heat-up performance assessment.

The climate conditions and the expectable charcteristics of thermal perception during a vehicle cool-down are quite specific. A passenger car parked in the sun for several hours is comparable to a greenhouse. Interior air temperatures can reach 80°C and inner surface temperatures 100°C [22]. Even when coming from thermal neutrality, such conditions are likely to evoke warm discomfort in passengers very quickly after entering the car. Upon activation of the climatization system, local cooling at different body areas causes non-uniformly induced relief from this discomfort and therefore thermal pleasure. Ultimately, local cooling improves overall thermal comfort.

Since the goal of vehicular climatization during the conditioning phase is to reach thermal neutrality as quickly as possible, the procedure of [8], introduced in section 2.2, is considered good practice, except for the invalid target quantity. An appropriate evaluation quantity for DPC performance would be Overall Thermal Perception (OTP), meaning either OTS or OTC, both of which include ratings for thermal neutrality. However, *how* thermal neutrality is reached during cool down is also important for passengers' overall satisfaction with the climatization. Unlike central HVAC, DPC directly conditions body parts of passengers, which raises the question about the right cooling intensity. No local cold discomfort should be induced, yet, the full potential of overall cooling performance is sought. Local cooling causes thermal pleasure only to a certain degree. With increasing cooling intensity, a shift in passengers' local perception from pleasant to unpleasant can arise. This local cold discomfort may override the pleasantly perceived effect of lowering overall warm discomfort and is here referred to as Local Thermal Tolerance Threshold of a certain body part i ($\mathrm{TTT_i}$). Consequently, a comprehensive evaluation method must allow for quantification of local thermal discomfort as well. To quantify both OTP and LTC, a corresponding measurement system is paramount, allowing for measuring diverse climate impact on local body areas and the cumulative effect on the whole body.

In conclusion, a thermal environment evaluation method for the application in DPC effectiveness assessment must meet the following **Methodological Requirements**:

- Local Measurement of Diverse Climate Impact
- Quantification of overall thermal perception in transient and non-uniform climate conditions
- Quantification of local thermal discomfort in transient and non-uniform climate conditions

Since the evaluation procedure of advanced thermal environment evaluation methods is much more complex than the air temperature measurement currently used, additional criteria with regard to practical applications are necessary. Since the method is to be used in industrial R&D processes, the entire evaluation procedure must be highly transparent, to enable test engineers to quickly comprehend it. Transparency would allow them to very quickly trace an implausible model behaviour to its origins and therefore lower the

probability of systematic errors. With regard to a low susceptibility to errors, simplicity of the thermal perception models is also to be preferred. Since each regression model is subject to a certain statistical error, a great number of submodels and higher complexity of mathematical relations will lead to a higher overall stochastic uncertainty in the application of the method. Thus, the following **Feasibility Criteria** are defined:

- Transparency of the procedure
- Simplicity of thermal perception models

In the following, the thermal environment evaluation methods introduced in section 2.4 are analyzed with reference to these methodological requirements and feasibility criteria, to illustrate their potential for the assessment of DPC effectiveness and to identifiy relevant gaps in the research. Figure 2.11 provides an overview of the properties of the different methods and an appraisal of their applicability to DPC assessment follows below.

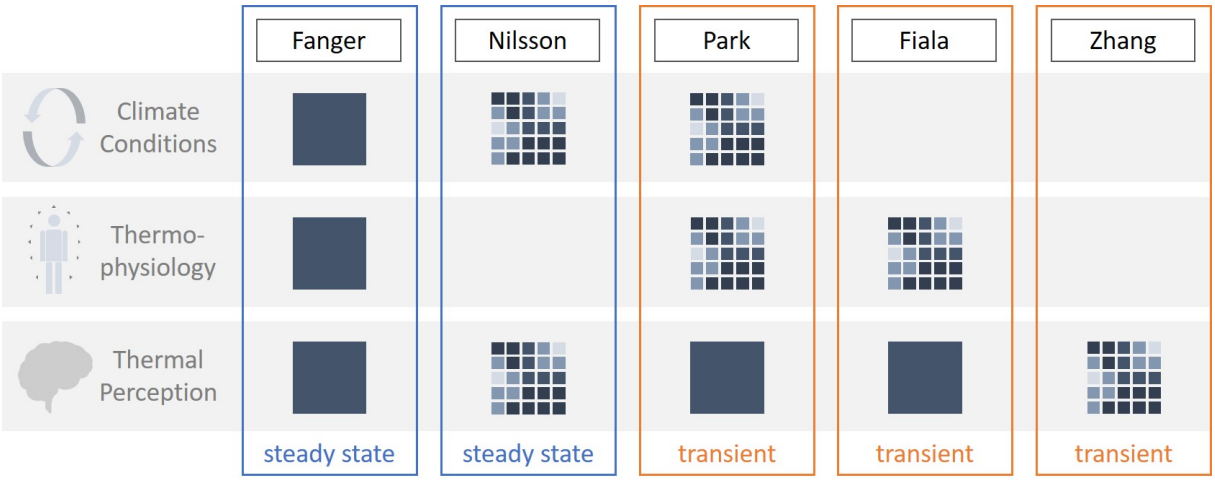

Figure 2.11: Comparison of properties of the thermal environment evaluation methods investigated in the context of the three dimensions of thermal comfort. The solid squares indicate evaluation for the whole body, whereas the tiled squares indicate local evaluation.

The Fanger Method provides for overall thermal impact quantification from convection, radiation and evaporation in relation to central climate measurements. Conductive heat exchange is not considered. The relevant sensor systems available to measure the required climate variables are not suitable for local measurements. Thermal perception relates to overall thermal load in steady-state and uniform climate conditions and has not been validated for transient and non-uniform conditions. However, as can be seen in the Park method, the concept of thermal load can be applied to such conditions as well. With regard to the available sensor technology, though, no evaporative heat load can be considered. But since relative humidity is not expected to vary very much locally, evaporative heat load might be obtained from central humidity measurements. Evaluation of local thermal discomfort is not covered by Fanger's thermal perception model and therefore cannot be conducted, even with inclusion of local climate measurement. Considering the feasibility criteria, the Fanger method provides a promising approach. It contains relatively simple mathematical models, and the concept of thermal load is

easy to understand and comprehensible. Thus, an investigation of the methods validity in transient and non-uniform conditions might be constructive.

The Park Method provides for local and overall thermal impact quantification from convection, radiation and conduction in relation to local climate measurements. Evaporative effects are considered stochastically with regard to central air humidity measurement. Local evaporative impact might therefore not be taken into sufficent consideration. Conductive effects can currently be evaluated only by involving a human occupant in the measuring procedure, which might lead to errors with regard to individual thermophysiological properties and poor reproducibility. Apart from that, the concept of involving a human occupant in an actual industrial assessment process appears not feasible. However, the Fraunhofer Institute for Building Physics IBP is working on the development of both a sensor to measure contact thermal impact and a solution to account for local evaporative thermal impact (personal correspondence in February 2020). The Park method provides for overall thermal perception assessment in transient and non-uniform climate conditions. Moreover, it is especially designed to evaluate the performance of DPC systems. The Park method does not, however, include local thermal discomfort evaluation. Regarding feasibility, the same arguments as for the Fanger method apply and the criteria seem to be fully met. Since the method is already validated for vehicle cool-down and heat-up and is built on local climate measurements, searching for an extension of the method to include local discomfort models appears worthwile.

The Nilsson Method provides for local and overall thermal impact quantification from convection and radiation in relation to local climate measurements. Neither conductive nor evaporative impact are considered. Overall thermal perception can be assessed in non-uniform but steady-state climate conditions. The segmental comfort zones of the Nilsson model seem to allow for local cold discomfort assessment. However, the local thermal comfort zones were derived from relatively low thermal asymmetries. During vehicle cool-down, however, thermal asymmetries on passengers can be extreme. Especially in case of DPC, local cooling can cause equivalent temperatures of 10°C, while other body parts are affected by direct solar radiation, resulting in 80°C. Moreover the *Cold but Comfortable* zone was derived from winter conditions, where the overall thermal state is cold rather than warm. Its validity for transient and highly asymmetrical conditions is questionable. Apart from that, a body segment in real vehicle climate conditions may not be influenced uniformly, but extremely asymmetrically. A directly ventilated forearm, for instance, may be influenced only on one side by cold air, whereas the other side may be exposed to warm air and radiation from the nearby hot door panel. The segmental heat loss therefore does not necessarily reflect *area-specific* thermal load. Cooling intensity might hence be perceived as too high *locally*, rather than with regard to an entire body segment. Despite these critical reflections, the comfort zones might apply to extreme thermal asymmetries as well and investigating the Nilsson models' validity in such conditions could be profitable.

The Fiala Method does not provide for climate measurements. For an application with climate sensors, the different climate variables must be captured at each of the body

segments of the thermophysiological model. The method allows for the assessment of overall thermal sensation in non-uniform and transient climate conditions. Local thermal perception cannot be evaluated, although local thermal heat exchange and thermophysiological properties are simulated, which provides suitable preconditions for an extension of the method by local thermal comfort assessment or a merging with the Zhang method. With regard to the feasibility criteria, the thermal perception model is relatively comprehensible. However, the thermophysiological processes and the accopanying tissue temperatures are very complex and thus hard to trace. Apart from that, the model requires the setting of many boundary conditions, such as clothing ensemble or radiation related material properties. Since reliable values for such boundary conditions are hard to find, the temptation to just use any value may be high, thus increasing the probability of systematic errors in the application process. Thermophysiological models are typically implemented in a thermal simulation environment for industrial applications. Since these simulation programs usually do not provide for connections with measurement systems, applying them to climate assessment is work intensive and probably involves different corporate departments. Nevertheless, the thermophysiological model provides for direct application of climate variables, which theoretically allows for its application to measured quantities. An investigation of the reliability of such an approach might be beneficial for measurement-based thermal comfort assessment.

The Zhang Method does neither provide for climate measurements, nor for thermophysiological simulations. It is therefore not considered to be a complete thermal environment evaluation method, but only a thermal perception model. However, it is the only method, which allows for the assessment of local thermal discomfort in transient and non-uniform climate conditions as defined in the methodological requirements above. The thermal perception model needs to be merged with a thermophysiological model, which in turn must be somehow linked to local climate measurements. But even if an appropriate climate measurement technique could be applied, the same weaknesses as for the Fiala method apply here but to an even greater extent. In addition to the uncertainty of boundary conditions and the intransparency of the physiological model, the complexity of the thermal perception model is to be considered here. Since many sub-models are coupled, individual errors accumulate and the ultimate reliability of thermal perception prediction may be reduced. However, if research effort is put into the application of a thermophysiological model with local climate measurements, an investigation of the reliability of Zhang's thermal perception models in such an approach could be beneficial.

Research Gaps The Fanger method is not valid for non-uniform, nor for transient climate conditions and does not allow for local thermal perception evaluation. Nilsson does provide evaluation for both overall and local thermal perceptions, and is also not valid for transient conditions. The only method that allows for evaluation of overall and local thermal perceptions in transient and non-uniform climate conditions is the Zhang model, which needs extensions for climate measurements and physiological interpretations. Such an approach may not meet the defined feasibility criteria. The Park method is considered the most promising approach, since it was developed in transient conditions of vehicular DPC cool-down and heat-up and includes climate impact of contact surfaces over

the entire assessment procedure. Apart from that, the DressMAN system used in the Park method allows local measurement of convective, radiative and conductive impact and incorporates the evaporative impact at least centrally. Thus, it largely meets the measurement requirements. The main deficiency of the Park method is the lack of LTC quantification. Since local comfort is crucial for the effectiveness of local climatization measures, it is considered to be highly important for a comprehensive DPC assessment method. The most relevant research gap with regard to climatization effectiveness assessment is therefore the *measurement based evaluation of local thermal comfort in transient and non-uniform climate conditions*. However, the Park method provides good prerequisites for the development of local thermal comfort models in relation to DressMAN measurements, since climate impact is captured locally.

In the following chapter a methodological approach to address the above discussed assumptions is introduced.

Chapter 3

Methodological Approach

This chapter takes up the appraisal of the state of the art in section 2.5 and presents a methodological approach to the investigations of its main assumptions.

The theoretical exploration of thermal comfort and its characteristics during DPC vehicle cool-down led to methodological requirements and feasibility criteria, which a DPC performance assessment method has to meet. The introduced methods for thermal environment evaluation were analyzed in line with these requirements and criteria and the Park method was determined to be the most promising approach. However, a research gap was uncovered, regarding measurement-based evaluation of local thermal comfort in transient and non-uniform climate conditions. To address this research gap the development of local thermal comfort models in relation to the DressMAN measurements was considered appropriate. Ultimately, the assumptions of the Appraisal of the State of the Art can be expressed in the following three working hypotheses:

1. *The Park method is more reliable in measurement-based predictions of overall thermal perception compared to other relevant thermal environment evaluation methods.*
2. *The predictions of the Park method are only reliable as long as no local cold discomfort occurs.*
3. *Local cold discomfort at high overall heat load can be quantified in relation to local climate measurements of the DressMAN system.*

In the following the methodological approach for investigating these hypotheses is described:

Hypothesis 1 *The Park method is more reliable in measurement-based predictions of overall thermal perception compared to other relevant thermal environment evaluation methods.*

The reliability of thermal perception predictions can only be investigated in comparison to human subjects' assessment. To represent the specifics of climatization effectiveness assessment, a vehicle cool-down case study appears effective. A laboratory experiment is preferred over field studies, since boundary conditions are very particular for a cool down situation and therefore difficult to reproduce. In order to compare the predictions of multiple methods, the question arises of how to obtain their different input variables with reasonable effort. To address this question, a new concept is developed to evaluate multiple thermal perception models using one sensor system. The climate input variables of all methods are physically related to each other and thus mathematically convertible.

Consequently, the DressMAN system output can be applied to all evaluation methods used here, by employing appropriate adaptation models. Thus, a moderate DPC vehicle cool-down scenario is designed, which is experienced by human subjects and measured by the DressMAN system. The DressMAN output is converted to the input variables of the various evaluation methods using such adaptation models. The output of the various models refers to their different thermal perception scales, which are hence standardized to one common norm scale to enable comparisons. Using this norm scale the predictions of all models are compared with the mean vote of the human subjects to examine their prediction accuracy and test the above hypothesis.

Hypothesis 2 *The predictions of the Park method are only reliable as long as no local cold discomfort occurs.*

Hypothesis 2 is tested by comparing the prediction accuracy of the Park model with the assessments of human subjects in two different DPC cool-down scenarios: A moderate one, without causing local cold discomfort, and one with strong conditioning asymmetry, causing local cold discomfort. Since one of the necessary scenarios is already covered by the investigations of hypothesis one, a similar procedure with different boundary conditions is used for the second scenario. The deviations between subjects' mean vote and the Park model's predictions are then compared in both scenarios to test the above hypothesis.

Hypothesis 3 *Local cold discomfort at high overall heat load can be quantified in relation to local climate measurements of the DressMAN system.*

To investigate this hypothesis a new methodology is developed for assessing Local Thermal Tolerance Thresholds (TTT_i). The subject is addressed by a literature-based theory on local cold discomfort under simultaneous overall warm discomfort. Based on that theory quantifiable research hypotheses are developed and tested in a series of human subject studies on local cooling in hot environments. Local climate measurement is conducted using the DressMAN system. By applying the above described adaptation models, local thermal discomfort predictions of the Zhang model and the Nilsson model are compared with the subjects' responses, to evaluate the quality of their predictions in cases of extreme thermal asymmetry. The acquired data is then used to develop new stochastic models for local cold discomfort predictions. Finally, from these models, local cooling intensity thresholds are derived.

Research Design The scientific approach for the whole investigation is illustrated in figure 3.1. The original research of this dissertation is highlighted in green. The investigations on the prediction quality of the different thermal perception models (working hypotheses 1 and 2) are described in chapter 4 and the development of prediction models for local cold discomfort (hypothesis 3) in chapter 5.

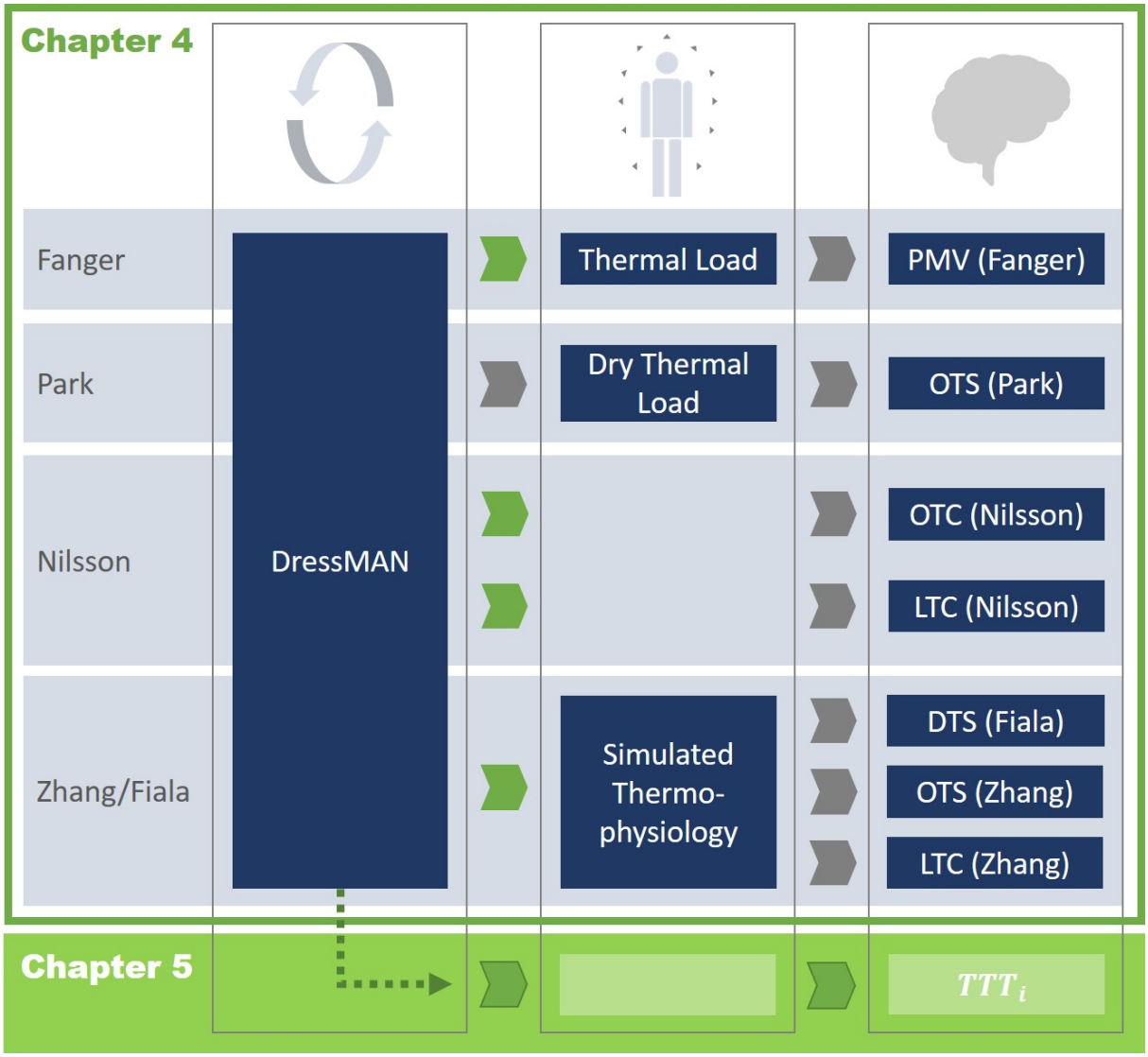

Figure 3.1: Visualization of the applied research design. The green frame represents the new concept to evaluate multiple thermal perception models, with the green arrows indicating the adaptation models for input conversion. The grey arrows stand for the original models of the different evaluation methods. The filled green box below represents the new methodology to assess TTT_i with regard to the three dimensions of thermal comfort.

Chapter 4

A New Concept to Evaluate Multiple Thermal Perception Models

This chapter introduces a new concept for applying different thermal perception models to one common climate measurement system. It also describes the procedures and the results of comparing the prediction quality of selected thermal perception models with evaluations of human subjects during a vehicle cool-down to investigate the models' ability of assessing climatization effectiveness. The results of this comparison are used to test hypothesis 1 and 2 regarding the prediction accuracy of the Park method.

4.1 Theoretical Approach

Quantification models for OTP are found in each of the thermal environment evaluation methods introduced in section 2.4. Since those methods have different input variables, adaptation to common physical quantities is needed to employ all thermal perception models with the same sensor system. Besides convertibility to the individual input variables of the models, these quantities must be also chosen with respect to the ability of measuring local climate impact. These requirements are met by the DressMAN system, whose measurements are converted and used for all thermal perception models investigated. To compare the output of the various models, their thermal perception scales are normalized to one standard scale.

4.1.1 Development of Adaptation Models

This section describes the conversion of DressMAN output variables to the input requirements of the different thermal perception models. This conversion is achieved by developing adaptation models, which incorporate physical relations of the different variables. Since the Park method already uses the DressMAN system, no adaptation is needed here.

Adapting the Fanger Method The Fanger method can be employed by incorporating ideas from the Park method, which presents the concept of area-specific dry thermal load, as introduced in equation 2.30 of section 2.4.2. Dry thermal load at air adjacent body segments consists of convection and radiation (see equation 2.28), which are also part of Fanger's overall heat load equation 2.17 of section 2.4.1. The concept of dry thermal load

can thus be used for substituting $\dot{q}_{TL,R,s}$ and $\dot{q}_{TL,C,s}$ in the overall (air adjacent) thermal load equation:

$$\dot{q}_{TL} = \dot{q}_{TL,C,res} + \dot{q}_{TL,E,res} + \dot{q}_{TL,E,s} + \dot{q}_{TL,D,s} + \dot{q}_{TL,dr,A} \tag{4.1}$$

However, this equation neglects the thermal impact from contact surfaces. Since this contact thermal impact is relatively high in vehicles, equation 4.1 can be extended by $\dot{q}_{TL,dr,K}$, which results in substituting $\dot{q}_{TL,R,s}$ and $\dot{q}_{TL,C,s}$ with overall dry thermal load $\dot{q}_{TL,dr}$:

$$\dot{q}_{TL} = \dot{q}_{TL,C,res} + \dot{q}_{TL,E,res} + \dot{q}_{TL,E,s} + \dot{q}_{TL,D,s} + \dot{q}_{TL,dr} \tag{4.2}$$

Another option for adaptation is to use Fanger's original equations for convection and radiation, but replace air temperature and mean radiant temperature with the mean directed equivalent temperature ($T_{eq,direct,mean}$). The adaptation of the radiative portion would thus result in:

$$\dot{q}_{TL,R,s} = 3.96 \cdot 10^{-8} f_{cl} l \left[(T_{cl} + 273)^4 - (T_{eq,direct,mean} + 273)^4 \right] \tag{4.3}$$

and the adaptation of the convective portion would result in:

$$\dot{q}_{TL,C,s} = f_{cl} h_c (T_{cl} - T_{eq,direct,mean}) \tag{4.4}$$

In this variant the thermal impact from contact surfaces is also not considered. However, equation 2.17 can be extended by contact thermal load (equation 2.29 of section 2.4.2) respectively:

$$\dot{q}_{TL} = \dot{q}_{TL,C,res} + \dot{q}_{TL,E,res} + \dot{q}_{TL,E,s} + \dot{q}_{TL,D,s} + \dot{q}_{TL,R,s} + \dot{q}_{TL,C,s} + \dot{q}_{TL,dr,K} \tag{4.5}$$

In the original Fanger method, contact thermal load is not integrated, so the method must correctly be applied with $\dot{q}_{TL,dr,K}$ excluded, which results in two more variants to calculate overall thermal load. For any of these variants, only $T_{eq,direct}$, T_c and RH need to be measured, all of which are covered by the DressMAN system. I compared the different calculation variants and the differences in PMV prediction are not significant in terms of prediction accuracy (compared to the other methods). Accordingly, I decided to use equation 4.2 for the further investigation, for the following reasons:

1. The convective heat transfer calculation is very sensitive to the convective heat transfer coefficient (h_c). The calculation of this coefficient in the Fanger method is based on climate conditions in buildings and might cause errors in vehicular environment applications. Such errors can be avoided by directly measuring convective heat loss, as the DressMAN system is operating.

2. Thermal impact from contacting surfaces is low in building environments, which is why the Fanger method (designed for climate evaluation in buildings) does not include it. The logic of thermal load, however, is to translate diverse climate conditions into thermal impact on the human body. Since the thermal impact from contact surfaces is high in vehicles, conductive heat exchange with the vehicle interior must be considered separately.

Adapting the Nilsson Method The Park model and the Nilsson model both depend on equivalent temperature measurements. In fact, $T_{eq,segment}$ and $T_{eq,whole}$ can be derived from $T_{eq,direct}$ measurements. Even the measurements of the DressMAN system for contact thermal impact can be converted to the same quantity, as will be shown in the following proposal:

A Proposal of a Concept for a Contact Equivalent Temperature (CET)
Objective monitoring of contact surface thermal impact is crucial for DPC evaluation. To apply the Nilsson model, segmental equivalent temperature must be derived also for contacting body segments. A concept for an Equivalent Contact Temperature (ECT) was introduced by Schmidt et al. in 2018 [51]. Although the idea of considering evaporative effects presented there seems beneficial, the concept is considered immature and impractical for use in an assessment situation. It is not consistent with the definitions of equivalent temperature in ISO 14505-2, and there is no proposal for a corresponding sensor design. Here, I introduce a different approach, by simply interpreting the definition in ISO 14505-2 [9] to also be true for contact measurements. According to this definition, a sensor element dissipates the same amount of heat in a uniform thermal environment (with a specific air and surface temperature), as in the actual non-uniform environment. The *"actual non-uniform environment"* is here understood to include sensor contact with surrounding surfaces. A definition of Contact Equivalent Temperature (CET), which would be consistent with the general definition of [9], might read:

Contact equivalent temperature is the uniform temperature of an imaginary enclosed space with the same temperature of air and surrounding surfaces and with an air velocity of zero, in which a heated surface dissipates the same dry heat by radiation and convection as in contact with a solid object in the actual non-uniform environment.

Figure 4.1 illustrates the principle and equation 4.6 defines it mathematically.

$$T_{eq,contact} = T_s - \frac{\dot{q}_{env}}{h_{cal}} \tag{4.6}$$

A comparison of the above definition of CET with the definition of local directed equivalent temperature in ISO 14505-2 [9] (see equation 2.27 in section 2.4.2) reveals the mathematical relations are exactly the same and the verbal definitions of the two concepts are very similar. In fact, when following this definition, a special Contact Equivalent Temperature Sensor would not even be necessary. However, the $T_{eq,direct}$ sensors in their current design (optimized to air-adjacent measurements) would probably not reliably represent the thermal impact of contacting surfaces on the human body. Since no appropriate sensor

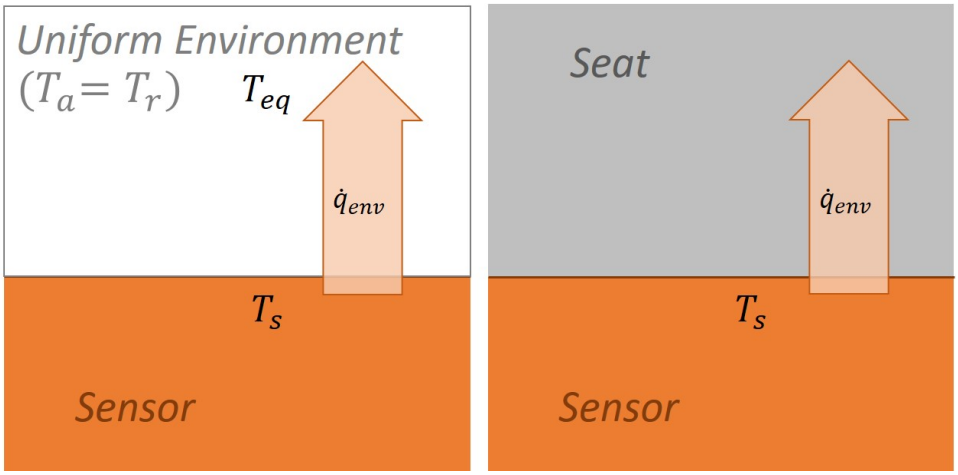

Figure 4.1: Illustration of the principle of Contact Equivalent Temperature (CET). Left: The calibration environment with uniform thermal conditions. Right: The corresponding hypothetical measurement situation of the investigated environment, if an adequate sensor were available.

for $T_{eq,contact}$ is available yet, I suggest an adaptation of the current DressMAN concept to calculate $T_{eq,contact}$ from contact temperature and heat flux measurements at human subjects (see illustration in Figure 4.2). This approach is also consistent with the general definition of equivalent temperature, which relates to the actual heat loss of a *person* [9], as introduced in section 2.3.3.

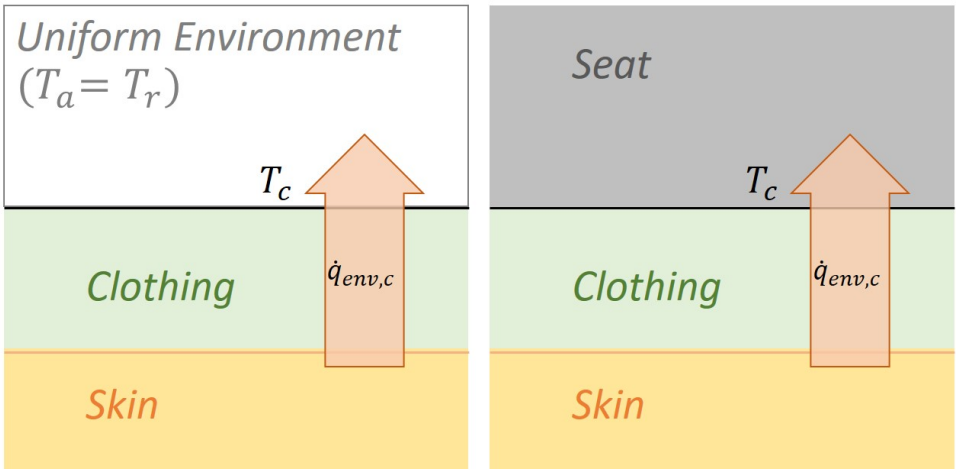

Figure 4.2: Illustration of the adaptation of Contact Equivalent Temperature (CET) to human subject measurements. Left: The hypothetical calibration environment. Right: The actual situation with contact temperature measurement at human subjects.

Under the idealized assumption that the combined heat transfer coefficient for radiation and convection at a person's clothing surface ($h_{cal,clothing}$) is the same as for a heated sensor element ($h_{cal,sensor}$), a hypothetical uniform environment can be assumed and CET can be calculated from the measured heat flux ($\dot{q}_{env,c}$) and contact temperature (T_c) using equation 4.7.

$$T_{eq,contact} = T_c - \frac{\dot{q}_{env,c}}{h_{cal}} \tag{4.7}$$

However, when applying this method, it must be clear that a systematic error is accepted, in the awareness that the actual heat transfer at a sensor element in a uniform environment may be different. Any results from such experiments must be calibrated to an objective $T_{eq,contact}$, as soon as an appropriate sensor is available.

Local Equivalent Temperature

ISO 14505-2 defines another variant of equivalent temperature, called Local Equivalent Temperature ($T_{eq,local}$) [9]. This definition considers a certain impact area for which either one measured $T_{eq,direct}$ or several differently oriented measurements build a combined local dry thermal load. Since the DressMAN system does not provide for several measurements at one impact area, each measured $T_{eq,direct}$ is exclusively related to a certain impact area. However, the idea of local equivalent temperature can also be adapted for CET and thus provide a common quantity for air-adjacent and contacting measurements:

$$T_{eq,local} = \begin{cases} T_{eq,direct}(A_{i,a,i}) & \text{for air-adjacent impact areas} \\ T_{eq,contact}(A_{i,c,i}) & \text{for contacting impact areas} \end{cases} \tag{4.8}$$

Segmental Equivalent Temperature

To obtain the Segmental Equivalent Temperature (introduced in section 2.4.3) from local equivalent temperature, the T_{eq} measurements are weighted according to the percentage of the entire segment area covered by the sensor's corresponding impact area. With regard to this area weighting, the segmental equivalent temperature is calculated from the impact of several differently placed sensors of a certain body segment s:

$$T_{eq,segment} = \sum_{i(s)=1}^{n(s)} \left(T_{eq,local,i(s)} \cdot \frac{A_{i,i(s)}}{\sum_{i(s)=1}^{n(s)} A_{i,i(s)}} \right) \tag{4.9}$$

Even though in its original form the Nilsson model is not applicable to contact surface climate impact, the described adaptation models allow the effect to be taken into account in both the local and the overall evaluation. Equivalent temperature for the whole body is then calculated using equation 2.33 introduced in section 2.4.3.

Adapting the Zhang and Fiala Method Zhang's thermal perception model can be merged with Fiala's thermophysiological model, which in turn can be applied to the DressMAN system. The commercial software THESEUS FE® [50] implemented Fiala's thermophysiological model and the thermal perception models of both Zhang and Fiala. The software is designed to model and simulate the thermal behavior of vehicle compartments and the corresponding thermal effects on passengers. Apart from that, it also facilitates direct definition of the immediate local climatic boundary conditions at the thermophysiological model, which can theoretically be obtained from climate measurements, as proposed in section 2.4.4. The original model, introduced in Fiala's dissertation [19] does not include heat exchange with contacting objects. However, in response to my personal request the software provider of THESEUS FE® implemented a transformed version of the model and introduced an approach encompassing local conductive heat flux [48]. This conductive heat flux again can be obtained from the DressMAN system.

The immediate boundary conditions are to be defined by the following quantities: Local heat flux for contact surfaces ($\dot{q}_c$), Air Temperature (T_a), Air Velocity (v_a), Mean Radiant Temperature ($\bar{T}_r$) and Relative Humidity (RH) for air-adjacent body areas. These quantities can be specified as course over time in the form of tables. Following the definition of ISO 14505-2, measured equivalent temperature can be interpreted as the same temperature of air and surrounding surfaces in a uniform environment as in the actually assessed environment. Therefore, the boundary conditions can be defined according to calibration conditions of equivalent temperature and the input variables can be adapted accordingly. Consequently, when considering air movement from natural convection and the combined heat transfer coefficient of calibration conditions, measured $T_{eq,direct}$ results in the following boundary condition at a certain impact area:

$$\begin{aligned} \dot{q}_c &= \dot{q}_c \\ T_a &= T_{eq,direct} \\ T_r &= T_{eq,direct} \\ v_a &= 0.05\frac{m}{s} \\ h_{cal} &= 10\frac{W}{m^2K} \end{aligned} \tag{4.10}$$

Application of Assessment Methods The above introduced adaptation models are applied to the DressMAN measurements and connected to the submodels of the corresponding thermal environment evaluation methods (see figure 4.3). The original research of this dissertation is highlighted in green and comprises the submodels M_{Fa0}, M_{N0} and M_{Fi0} and the comparison of the different models' predictions, indicated by the green frame. The grey boxes present the submodels, introduced in section 2.4 for deriving the mediator or target quantities (white filled boxes) of the different evaluation methods. In the following, the different models are listed with their color marking and described with regard to their function in the evaluation procedure.

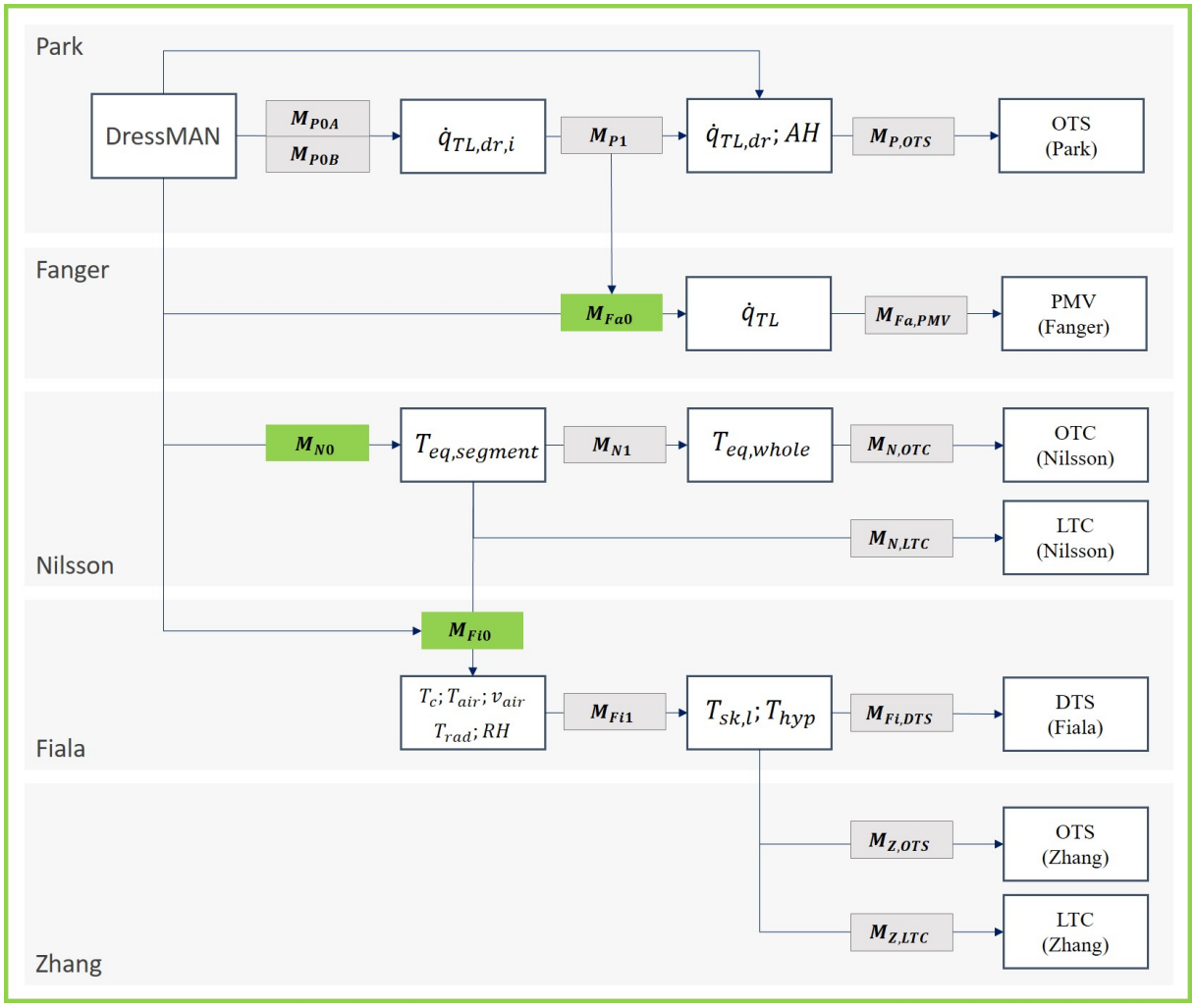

Figure 4.3: Illustration of the concept for applying multiple thermal perception models to the DressMAN system by incorporating adaptation models and linking them with existing submodels of thermal environment evaluation methods.

Park Approach

M_{P0A} Submodel for deriving air adjacent Local Thermal Load ($\dot{q}_{TL,dr,A}$) from measured Directed Equivalent Temperature ($T_{eq,direct}$) (equation 2.28 in section 2.4.2).

M_{P0B} Submodel for deriving Contact Local Thermal Load ($\dot{q}_{TL,dr,K}$) from measured Contact Temperature (T_c) (equation 2.29 in section 2.4.2).

M_{P1} Submodel for deriving Dry Overall Thermal Load ($\dot{q}_{TL,dr}$) from Dry Local Thermal Load ($\dot{q}_{TL,dr,i}$) and the Impact Area ($A_{i,i}$) (equation 2.30 in section 2.4.2).

$M_{P,OTS}$ Model for deriving Overall Thermal Sensation (OTS) from Dry Overall Thermal Load ($\dot{q}_{TL,dr}$) and Absolute Humidity (AH) (equation 2.31 in section 2.4.2).

Fanger Approach

M_{Fa0} Adapted model for thermal load calculation from DressMAN measurements (see equation 4.2).

$M_{Fa,PMV}$ Submodel for deriving Predicted Mean Vote (PMV) from Overall Thermal Load ($\dot{q}_{TL}$) (equation 2.25 in section 2.4.1).

Nilsson Approach

M_{N0} Model for deriving Segmental Equivalent Temperature ($T_{eq,segment}$) from Local Equivalent Temperature ($T_{eq,local}$) (equation 4.9).

M_{N1} Model for deriving Equivalent Temperature for the whole body ($T_{eq,whole}$) from Segmental Equivalent Temperature ($T_{eq,segment}$) (equation 2.33 in section 2.4.3).

$M_{N,OTC}$ Model for deriving Overall Thermal Comfort (OTC) from Equivalent Temperature for the whole body ($T_{eq,whole}$) (*Comfort Zones* in section 2.4.3).

$M_{N,LTC}$ Model for deriving Local Thermal Comfort (LTC) from Segmental Equivalent Temperature ($T_{eq,segment}$) (*Comfort Zones* in section 2.4.3).

Fiala Approach

M_{Fi0} Model for deriving appropriate input variables for THESEUS FE® from Segmental Equivalent Temperature ($T_{eq,segment}$) (equations 4.10).

M_{Fi1} Fiala's thermophysiological model for deriving dynamic tissue temperatures from specified climatic boundary conditions (section 2.4.4).

$M_{Fi,DTS}$ Fiala's thermal perception model for deriving Dynamic Thermal Sensation (DTS) from dynamic tissue temperatures (equation 2.34 in section 2.4.4).

Zhang Approach

$M_{Z,OTS}$ Zhangs model for deriving Overall Thermal Sensation (OTS) from dynamic tissue temperatures (equation 2.45 in section 2.4.5).

$M_{Z,LTC}$ Zhangs model for deriving Local Thermal Comfort (LTC) from dynamic tissue temperatures (equation 2.46 in section 2.4.5).

4.1.2 Norming of different Evaluation Scales

To compare the output of the applied thermal comfort models, their in places different thermal perception scales need to be normalized to one standard scale.

Essentially two approaches exist to do so:

1. Considering the highest possible rating of each scale as also the highest value in the norm scale and evenly allocating the distances between the remaining assessment levels, which resembles a plastic stretching of the scale.
2. Considering the evaluation ratings of the different scales as equal and the distances between them transferable, which results in equal steps from thermal neutrality for each scale and resembles a static translation.

In the following the scale norming for OTP and LTC is discussed with regard to these approaches.

Overall Thermal Perception In total, the evaluation methods use three different scales for OTP. However, the Zhang scale is an extended ASHRAE scale, expanded to cover extreme climate conditions, not considered by the original ASHRAE scale [65]. Since Fanger, Fiala and Park are using the original ASHRAE scale, the verbal rating is the same as in Zhang's assessment up to 'hot' (+3) and down to 'cold' (-3). The Nilsson method uses a limited MTV scale, which is a mixed sensation and comfort scale. The two scales are shown in tables 4.1 and 4.2.

Table 4.1: (Extended) ASHRAE scale.

evaluation	value
very hot	4
hot	3
warm	2
slightly warm	1
neutral	0
slightly cool	-1
cool	-2
cold	-3
very cold	-4

Table 4.2: (Limited) MTV scale.

evaluation	value
too hot	5
hot but comfortable	4
neutral	3
cold but comfortable	2
too cold	1

Schweiker et. al investigated common assumptions about thermal sensation and comfort scales [54]. Among other examinations they compared subjects' responses to a continuous scale with those to the categorial ASHRAE scale. Despite concluding that the scales are not equidistant, the authors found that the ranges of operative temperatures for the two scale types were similar. Accordingly, at least in moderate climate conditions, thermal perception ratings might be transferable between different scales.

The international standard ISO 10551 introduces methods for developing subjective scales for surveying subjects about their perception of the physical environment [12]. The standard recommends separating thermal sensation questions from comfort questions. The reason for this separation, discussed in section 2.3.3, is that a sudden cool sensation can be perceived as pleasant in a hot environment and unpleasant in a cold environment. Thus, thermal sensation scales, such as the ASHRAE scale, and thermal comfort scales, such as

Nilsson's MTV scale, are not directly comparable in an evaluation procedure. However, in the special case of vehicle cool-down, the overall performance of the climatization system can be evaluated by the deviation from thermal neutrality, which is represented in both scales. Since the overall thermal conditions in a cool-down situation are initially far from thermal neutrality, a decrease in overall thermal sensation is expected to be proportional to an improvement of overall thermal comfort; however, not necessarily an equidistant one and only as long as thermal asymmetries are low.

For overall thermal comfort assessment, Fanger considers the thermal sensation range between 'slightly cool' and 'slightly warm' as comfortable and any rating beyond these limits as uncomfortable [18]. Putting this interpretation in the terminology of Nilsson's MTV scale, 'slightly cool' can be considered equal to 'cold but comfortable' and 'slightly warm' equal to 'hot but comfortable'. This also speaks for equality of the rating scales in the range of one evaluation unit from thermal neutrality with regard to overall thermal perception. Since the MTV scale comprises only one more evaluation category in both directions, representing thermal discomfort, no further differenciation is possible using the Nilsson model. Hence, an assessment of $MTV = 5$ may compare to any (unknown) value higher than +1 on the extended ASHRAE scale.

Based on the above argumentation, I decided to use the second approach[1] of norming the different scales to one standard scale. Table 4.3 visualizes the applied norming method and equations 4.11 and 4.12 present the mathematical relations for a norm scale from -1 to +1 for the ASHRAE scale and MTV scale.

According to this norming approach, an output of the Park model of +3, for instance, would result in a norm value of +0.75. The methods using the original ASHRAE scale will thus never reach +1 or -1 and the Nilsson output will never exceed +0.5 or fall below -0.5. However, the actual result should be interpreted in such a way that an output of +0.5 can be any unknown value between +0.5 and +1, which is consistent with the limited scale. The Nilsson model is simply not able to quantify deviations from thermal neutrality, which are further than 'too hot', whereas the Zhang model is able to evaluate very extreme climate conditions. This difference is due to the fact, that the Nilsson model was designed for thermal comfort assessment near thermal neutrality, while the Zhang model was designed to quantify thermal discomfort in more extreme climate conditions.

$$\text{ASHRAE Norming:} \qquad OTP_{Norm}(ASHRAE) = \frac{OTS_{ASHRAE}}{4} \tag{4.11}$$

$$\text{MTV Norming:} \qquad OTP_{Norm}(MTV) = \frac{OTC_{MTV} - 3}{4} \tag{4.12}$$

Local Thermal Perception LTC can only be assessed using the Nilsson and the Zhang models. The two models use very different assessment approaches and model outputs.

[1]For comparison, I also applied the other approach of scale norming to the data and found that qualitative conclusions apply independently and the prediction quality of all methods is better with approach 2.

Table 4.3: Illustration of the norming principle for the different Thermal Perception Scales.

Norm	Zhang	Fiala	Fanger	Park	Nilsson
1	4				
	3	3	3	3	
	2	2	2	2	5
	1	1	1	1	4
0	0	0	0	0	3
	-1	-1	-1	-1	2
	-2	-2	-2	-2	1
	-3	-3	-3	-3	
-1	-4				

While the Nilsson model ranks a body segment according to comfort zones in relation to the segmental equivalent temperature, the Zhang model gives two separate values for local thermal sensation and local thermal comfort with respect to local skin temperature. A mere thermal sensation scale is not sufficient in this case, since the intention is to determine thresholds, where sensation only increases, but comfort shifts from pleasant to unpleasant. For this purpose, I consider the MTV scale suitable, since the shift from 'cold but comfortable' to 'too cold' represents this threshold quite well. The 5-point scale is also better applicable without confusion in subject studies for comparison. Therefore, the Zhang output is transformed into the 5-point MTV scale. Table 4.4 visualizes the transformation and equation 4.13 gives the corresponding mathematical relationship.

Table 4.4: LTC norming concept.

LTS_{Zhang}	LTC_{Zhang}	$LTC_{Nilsson}$
	-4	5
	-3	
	-2	
	-1	
+	0	4
	1	
	2	
	3	
	4	3
	3	
	2	
	1	
-	0	2
	-1	
	-2	
	-3	
	-4	1

$$LTC_{ZN} = \begin{cases} 4 - \frac{LTC_{Zhang}}{4} & \text{for} \quad LTS_{Zhang} \geq 0 \\ 2 + \frac{LTC_{Zhang}}{4} & \text{for} \quad LTS_{Zhang} < 0 \end{cases} \tag{4.13}$$

Since the MTV scale differenciates between warm and cold thermal comfort, the Zhang output is first considered in terms of thermal sensation. If LTS is positive, the value on the MTV scale will be somewhere between 3 and 5. If it is negative, the value will be between 1 and 3. With this method, absolute local thermal neutrality cannot be achieved. However, the approach is employed to quantify local discomfort and for this purpose it is well suited. Cold sensation, accompanied by discomfort, results in the MTV rating 'too cold', which would be interpreted as too intense local cooling. The grading of this local cold discomfort is represented by the relative deviation of the LTC value from 0.

4.1.3 Utilization of Prediction Accuracy Measures

To be able to compare the prediction quality of different model outputs, an evaluation criterion is necessary. For this purpose, the deviations between the predicted values (S_i) and the actually measured values (M_i) appear useful. These deviations are called residuals when the calculations are performed on the data sample that was used for the estimations and are called prediction errors when computed out-of-sample [31]:

$$e_i = S_i - M_i \tag{4.14}$$

These prediction errors (e_i) can be calculated for each measured value and visualized in a time series diagram for qualitative evaluation of the deviations over time. However, the output of one model may differ substantially at the beginning of the time series, but less later, while another model behaves in exactly the opposite way. Thus, a criterion for the deviation of a forecast over the entire time series is needed. A common approach to demonstrate the tendency of a model to over- or underestimate is the Mean Bias Error (MBE), which is the mean value of all residuals in a time series:

$$MBE = \frac{1}{n}\sum_{i}^{n}(S_i - M_i) \tag{4.15}$$

While the polarity of the MBE is an important indicator for tendency interpretation, the magnitude of the value is not particularly informative. Since positive and negative residuals cancel each other, the MBE does not allow for quantification of the overall prediction deviation. For such a purpose, the Root Mean Square Deviation (RMSD) can be used, which is computed as the square root of the mean of the squares of the prediction errors [31]:

$$RMSD = \sqrt{\frac{1}{n}\sum_{i}^{n}(S_i - M_i)^2} \tag{4.16}$$

In some cases, using a percentage deviation with regard to the scale applied might be more descriptive. For this, RMSD is related to the total scale range (s_r), which is the range between the maximum scale value (s_{max}) and the minimum scale value (s_{min}). This relative deviation measure is called the Normalized Root Mean Square Deviation (NRMSD):

$$NRMSD = \frac{RMSD}{s_{max} - s_{min}} = \frac{RMSD}{s_r} \tag{4.17}$$

The prediction accuracy must be distinguished from the Goodness of Fit (GOF). In this respect, RMSD is to be differentiated from the Root Mean Square Error (RMSE), although the terms are used sometimes synonymously in the literature (see [31] and [36]). RMSE here refers to the data involved in the development of a regression model and is a measure for the quality of the regression function with regard to the data sample. RMSE is computed, very similar to RMSD, as follows [36]:

$$RMSE = \sqrt{\frac{1}{n-m}\sum_{i}^{n}(S_i - M_i)^2} \tag{4.18}$$

where $n-m$ is the number of degrees of freedom or the number of freely adjustable values involved in a regression. Empirically, the number of degrees of freedom is calculated from the number of observations (n) minus the number of regression coefficients (m). In a bivariate model, for example, usually two coefficients are estimated and therefore the number of degrees of freedom is '$n-2$' [60]. Since the purpose here is to compare the predictions of different thermal perception models with validation data, the RMSD is the appropriate measure to use.

4.2 Methods

The two central working hypotheses from the Methodological Approach of chapter 3 are investigated here. The first hypothesis claims higher prediction quality of the Park model over the other models in DPC performance assessment, which is tested by comparing the prediction accuracy of all the models in a vehicle cool-down situation with moderate DPC. The second hypothesis argues that the Park prediction is only valid, as long as no local cold discomfort occurs. This hypothesis is tested by comparing the prediction accuracy of the Park model in the moderate scenario with its prediction accuracy in a cool-down situation with strong thermal asymmetries. Thus, for the whole investigation, two cool down scenarios are designed:

- LOW: A moderate climatization scenario with low thermal asymmetry and no local cold discomfort
- STRONG: A climatization scenario with strong thermal asymmetry that deliberately evokes local cold discomfort

Experimental Design Since the current HVAC performance assessment procedure of DIN 1946-3 (section 2.2) can basically be retained for DPC, using the same boundary conditions in the experiment would be reasonable. However, although such conditions are likely to also occur in reality, for health reasons they cannot be employed in human subject studies. Thus, for the investigation I selected less extreme but still very similar boundary conditions.

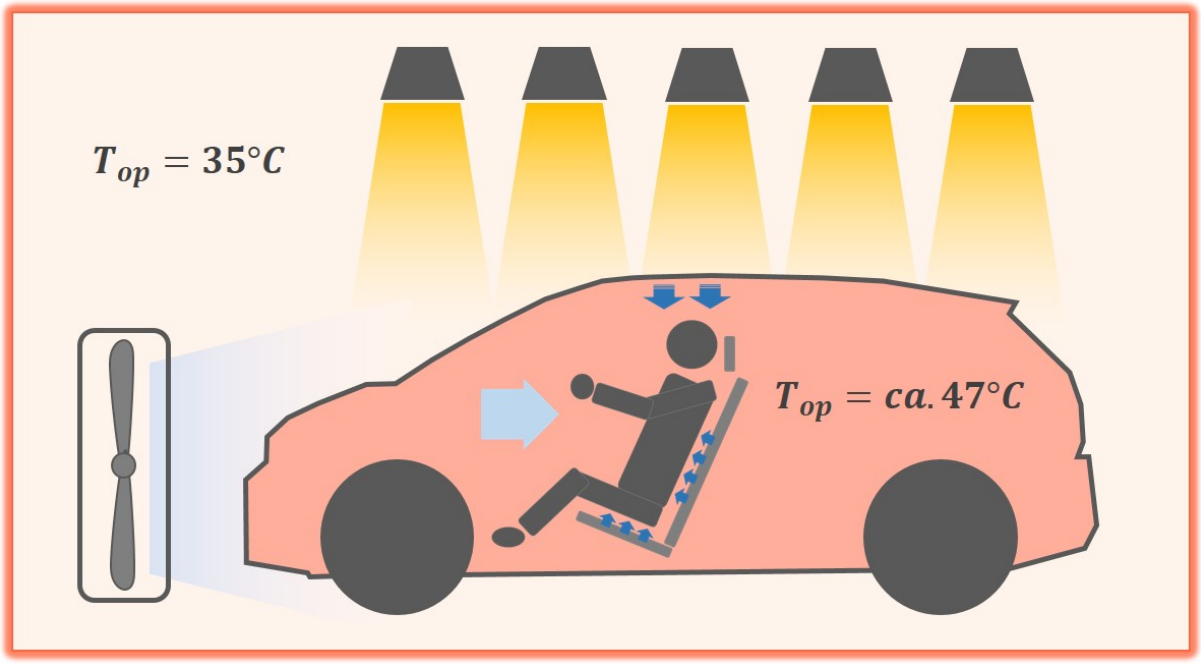

Figure 4.4: Illustration of the test setup for vehicle cool-down with DPC, consisting of central air conditioning, seat cooling and convective head cooling.

The tests were conducted, using a modified BMW i3 in a climate chamber at the Fraunhofer Institute for Building Physics IBP in Holzkirchen, Germany, in August and September 2019. The chamber was conditioned to an operative temperature of 35°C. Spotlights attached to the chamber roof and focused on the vehicle artificially generated a solar-like radiation spectrum of about $500\frac{W}{m^2}$ intensity at the vehicle roof top, causing the passenger compartment to heat up to approximately 47°C operative temperature (greenhouse effect). A blower in front of the vehicle dissipated the heat of the vehicle radiator, to ensure proper functioning of the central air conditioning system. The driver's position was conditioned using a combination of moderate central air conditioning, seat cooling and a customized local air conditioning device for the head area (see test setup in figure 4.4).

The two climatization scenarios were designed by conducting pre-tests with local cooling intensity variations and the corresponding thermal perception responses of three test subjects. The intention was to obtain nearly equal overall thermal loads for the human subjects in both scenarios, but different local thermal asymmetries. The LOW scenario was chosen to moderately improve overall thermal comfort without causing local cold discomfort. For the STRONG scenario, local cold discomfort was generated employing high cooling intensity in the head area. Since overall thermal perception reaches neutrality

very quickly in such conditions, no additional cooling measure was activated. Figure 4.5 illustrates the different climate conditions in the two scenarios and figure 4.6 presents selected local cooling intensities. The LOW scenario on the left side comprises moderate central air conditioning, seat cooling and convective head cooling. The STRONG scenario employs convective head cooling only, at a very high intensity.

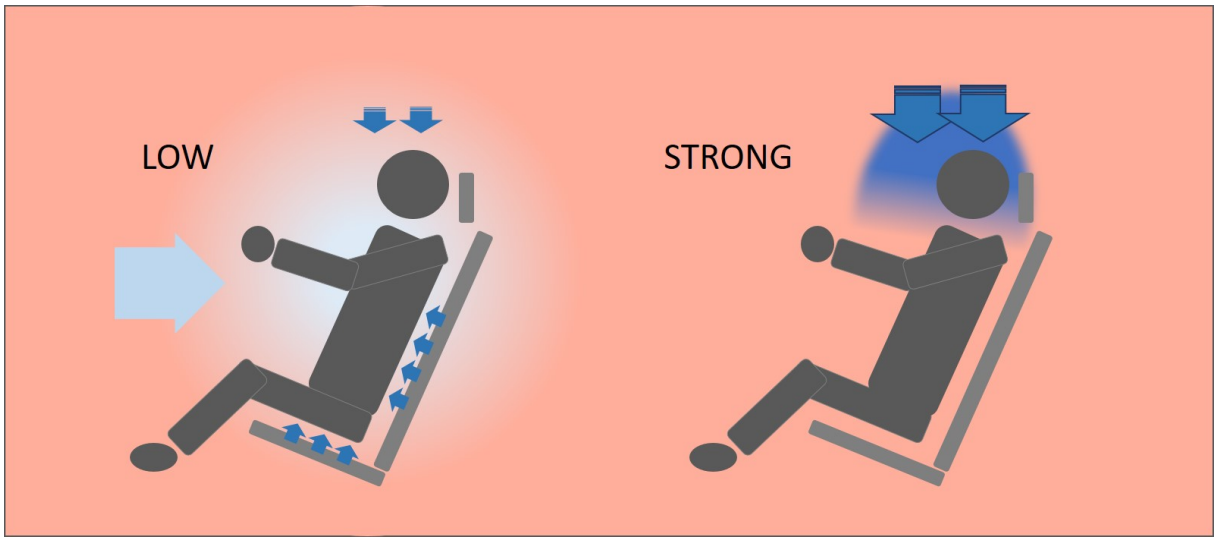

Figure 4.5: Illustration of cooling asymmetries in the two vehicle cool-down scenarios.

body segment	**LOW** *equivalent temperature [°C]*	**STRONG** *equivalent temperature [°C]*
Head	26.9	20.1
Chest	28.4	25.9
Back	33.9	34.7
Seat	31.5	35.5
Lower Legs	23.3	27.9

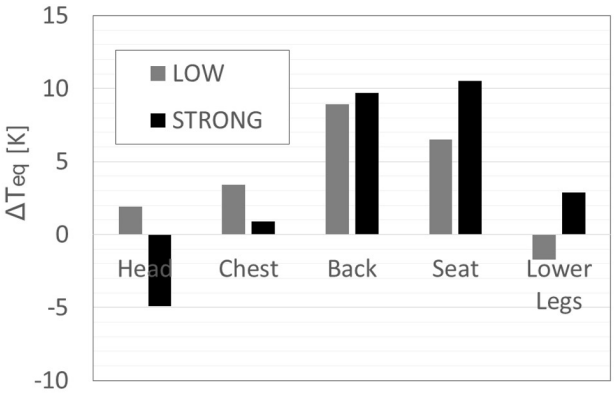

Figure 4.6: Thermal asymmetries in the two vehicle cool-down scenarios, represented by local equivalent temperature at quasi-stationary conditions after the complete cool-down duration (table left) and its difference from neutral conditions, characterized by an equivalent temperature of 25°C (diagram right).

Experimental Procedure Figure 4.7 illustrates the chronological procedure in both cool-down scenarios. After spending 75 minutes in neutral conditions, subjects filled out a questionnaire and went into the climate chamber. They spent 9 minutes in the warm conditions of the chamber, outside the vehicle and another 5 minutes inside the vehicle under heavy heat load. Then the DPC system was activated and subjects were questioned about local and overall thermal perception.

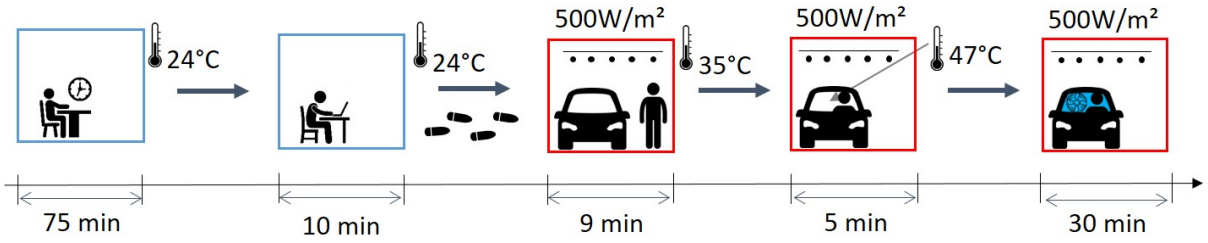

Figure 4.7: Experimental procedure of the vehicle cool-down study.

Figure 4.8 shows photographs of the procedure with a human subject. The same procedure was conducted in both scenarios with the DressMAN system, measuring the exact same climate impact as experienced by the human subjects.

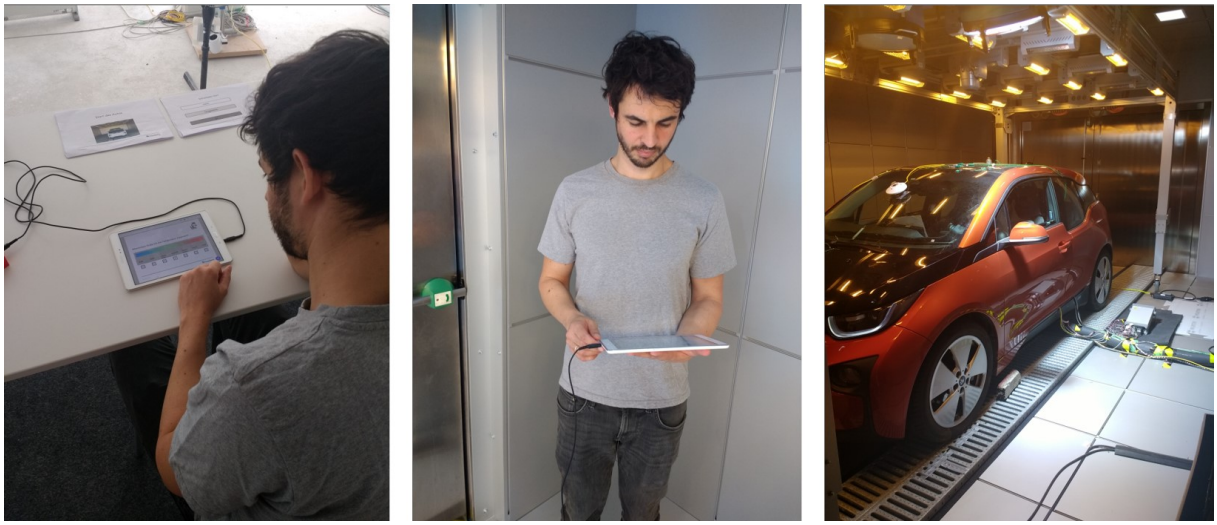

Figure 4.8: Photographs of a person undergoing the experimental procedure of the vehicle cool-down study.

Measurements To measure the climate impact the *DressMAN 3.1* system was used. $T_{eq,direct}$ was measured at 28 positions. The thermal impact of the seat was measured using *FluxTeq PHFS01* sensors between the seat surface and the human subjects. The sensors measure both temperature and heat flux, which are averaged over all subjects. Measurement positions of the *DressMAN 3.1* system are shown in appendix A. Figure 4.9 shows pictures of the system in the experimental environment of the vehicle cool-down study. Due to a technical problem, the relative humidity measurements were not recorded. However, since both scenarios have high air exchange rates with cooled and thus dried air, the air humidity evolvement is expected to be very similar in the two scenarios. Therefore, a substitute data set from another DPC cool-down study was used for the humidity in both scenarios.

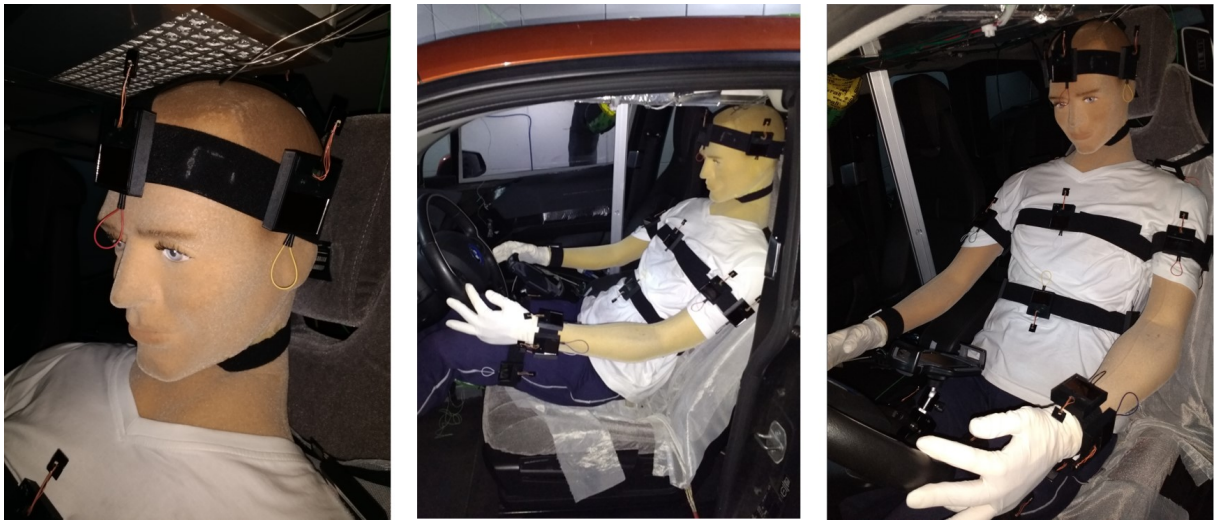

Figure 4.9: Pictures of the DressMAN 3.1 system in the experiment vehicle.

Subjects and Questionnaire A total of 18 German subjects, 6 male, 12 female participated in the experiment. The smaller number of male subjects was due to the head cooling setup allowing only for people no taller than 1.75 m to participate. The subjects had a normal range of BMI and were between 19 and 69 years old. For climatization performance assessment, a definition of standard clothing is expedient. Since the Nilsson model relates to a certain clothing ensemble with a clo value of 0.6 [9], a similar ensemble was used for subjects in the study, comprising light closed shoes, light trousers and a T-shirt. Overall and local thermal perception at different body areas was captured during the heat load and the cool-down phase in the vehicle in 15 second steps. Subjects completed the questionnaire on a tablet, referring to the MTV scale for LTC and to the ASHRAE scale for OTS (see tables 4.5 and 4.6). However, the rating values for OTS were chosen in a range of 1 to 7 and the MTV rating terms were changed to 'warm' instead of 'hot', since the phrasing 'too hot' might be understood as 'painful' for local thermal perception assessment, at least for German subjects.

Table 4.5: Thermal sensation scale used in the vehicle cool-down study.

OTS	value	norm
		1
hot	7	
warm	6	
slightly warm	5	
neutral	4	0
slightly cool	3	
cool	2	
cold	1	
		-1

Table 4.6: Thermal comfort scale used in the vehicle cool-down study.

LTC	value
too warm	5
warm but comfortable	4
neutral	3
cold but comfortable	2
too cold	1

Since the scaling of 1 to 7 is different to the original ASHRAE scale, which ranges from -3 to +3, the scale norming looks a little different here. However, the principle is the same as defined in equation 4.11 of section 4.1.2:

$$\text{Survey Norming:} \qquad OTS_{N,ASHRAE} = \frac{OTS_{ASHRAE} - 4}{4} \tag{4.19}$$

4.3 Results

This section presents the results of the vehicle cool-down study with regard to the hypotheses presented in chapter 3. Thermal perception votes are averaged over all subjects at each time step and compared to the thermal perception models' predictions. The statistical indicators for the accuracy of the predictions, introduced in section 4.1.3, are then used to quantify the quality of each prediction.

As described previously, the aim of the two scenarios was to evoke local cold discomfort in only one case, while obtaining similar overall thermal load in both cases. Since equivalent temperature T_{eq} is a measure of dry thermal load $\dot{q}_{TL,dry}$, local and overall T_{eq} measurements are indicators for the success of this effort. Figure 4.10 shows equivalent temperature progressions over cooling duration time for selected body segments and the overall conditions. Overall equivalent temperature is quite similar in both scenarios, while segmental equivalent temperatures vary significantly more in the STRONG scenario than in the LOW scenario.

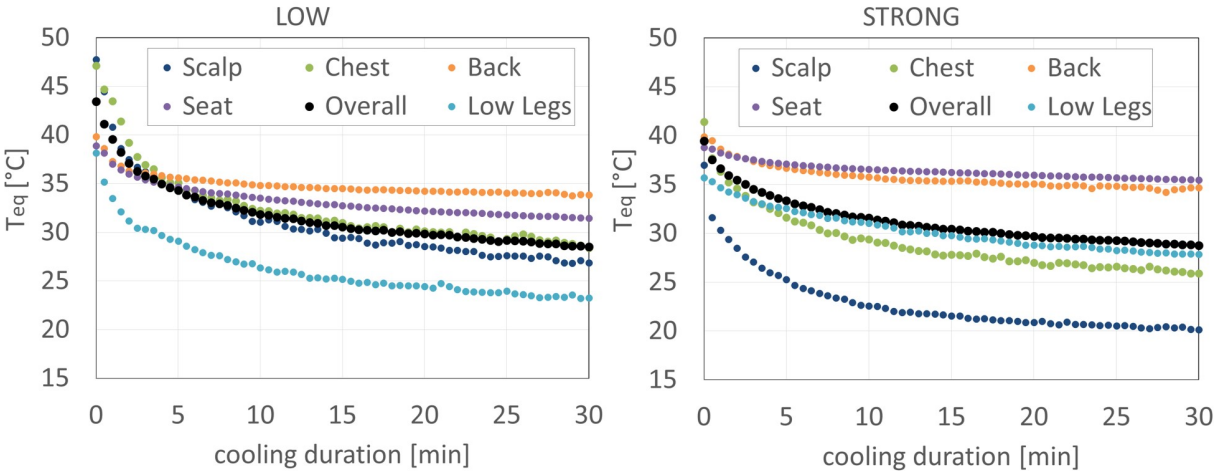

Figure 4.10: Course of segmental and overall equivalent temperature over cooling duration time.

Figure 4.11 shows the subjects' ratings of the corresponding body segments with regard to the MTV scale. While in the LOW scenario all segments remain between 3 and 4, the STRONG scenario shows ratings below 2 for the scalp, representing "too cold" and hence local cold discomfort.

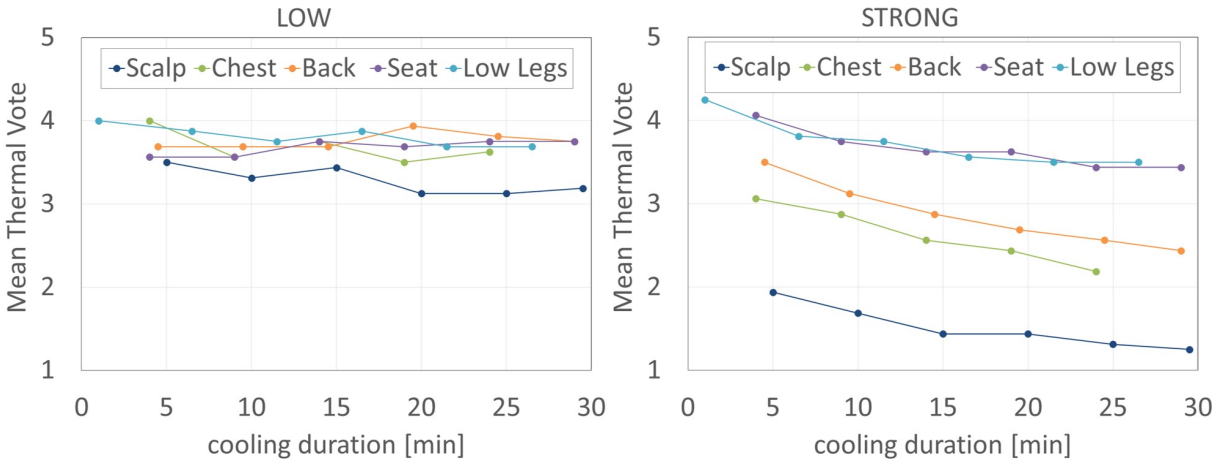

Figure 4.11: Course of segmental thermal comfort over cooling duration time with regard to the MTV scale.

4.3.1 Thermal Perception Model Comparison

In this section, the data from the LOW scenario is interpreted with respect to hypothesis one: *The Park method is more reliable in measurement-based predictions of overall thermal perception compared to other relevant thermal environment evaluation methods.*

The left side of figure 4.12 shows the course of overall thermal perception over cooling duration time for both subjects' mean vote and the predictions of the different models. During the first 5 minutes, a slight undershoot in the course of subjects' mean vote can be observed, which may be explained by high skin temperature change rates at the beginning of the cool-down. Such an undershoot is also predicted by the models of Fiala and Zhang. Since both models take skin temperature derivatives into account, this model output is plausible. However, the effect is apparently overestimated in their OTP quantification. The thermal-load-based models of Fanger and Park both ignore such an effect and follow a continuous course, which is too high for the Fanger prediction. A similar behaviour is observed in the Nilsson predictions. However, since the Nilsson model does not assess the thermal environment analogously, but in five categories, its thermal perception prediction follows a discrete course. As described in the scale norming theory in section 4.1.2, a prediction from the Nilsson model of 0.5 can be any unknown value between 0.5 and 1.

On the right side of figure 4.12, the relative deviations of the models' predictions in relation to subjects' mean vote is presented. The predictions of Park and Fiala follow the subjects' mean vote course most closely. Both predictions show their maximum deviation at the beginning of the cool-down, where Park overestimates (12%), while Fiala underestimates (9%). Both deviations decrease over time to approximately 5%. Towards the end of the cooling phase all predictions approach the actual assessment of the human subjects and the deviations tend towards zero, indicating an improvement of the prediction quality of all models with increasing proximity to thermal neutrality.

Figure 4.13 illustrates the cumulated deviations over cooling duration time. The MBEs of the different models' predictions reveals their tendency to overestimate or underestimate.

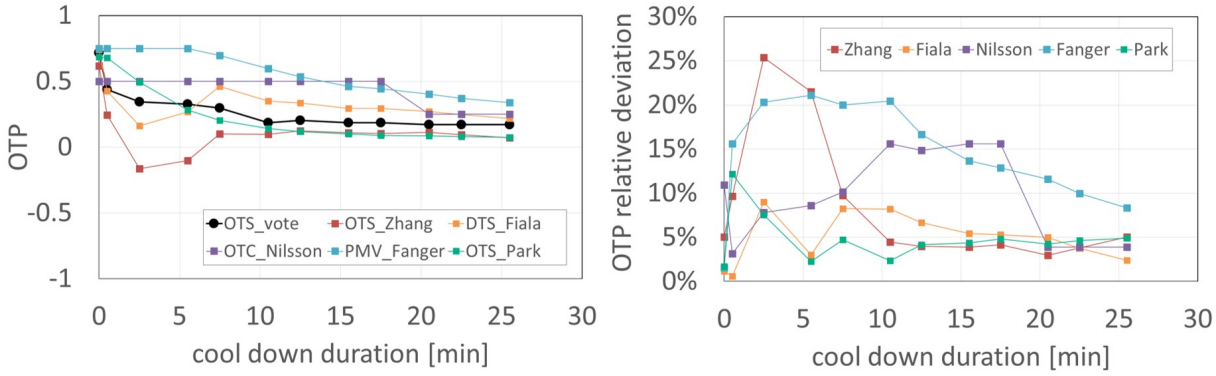

Figure 4.12: Normalized OTP courses (left) and their relative deviations (right) from subjects mean vote over cooling duration time in the LOW scenario.

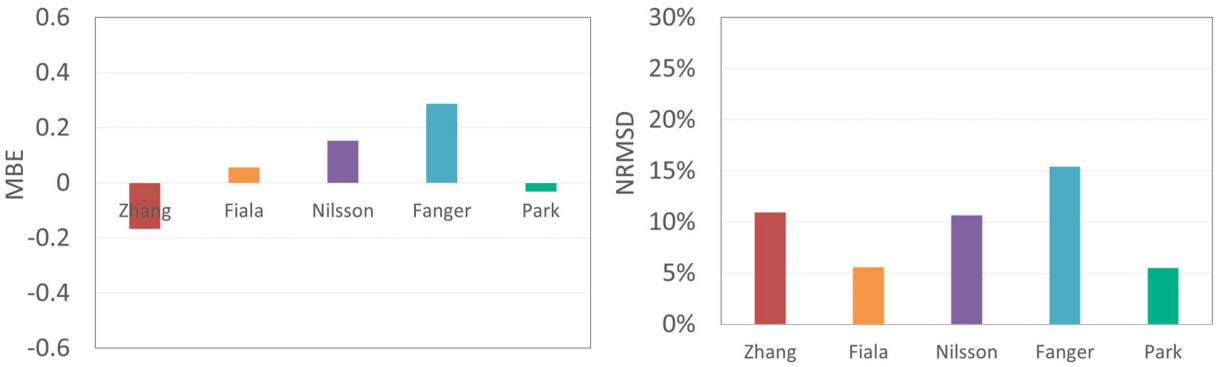

Figure 4.13: MBE and NRMSD of thermal perception predictions in the LOW scenario.

The negative MBE of Park and Zhang denote their tendency to assess thermal conditions as cooler than the actual subjects' mean vote. The other models tend to assess the climate conditions to be perceived warmer than they were actually rated. Since both Fiala and Park have a NRMSD of 6%, which is the lowest deviation of all predictions, they seem to predict thermal perception more accurately than the other models.

4.3.2 Park Method Evaluation

In this section, the data for both scenarios is interpreted with respect to hypothesis two: *The predictions of the Park method are only reliable as long as no local cold discomfort occurs.*

Figure 4.14 shows the course of subjects' mean thermal vote in comparison to the Park models' predictions for both scenarios. The high deviation between model prediction and subjects' mean vote in the STRONG scenario is evident and reflected in a significantly higher NRMSD than in the LOW scenario. The subjects' perceptions are apparently not only influenced by overall thermal load. Head cooling also appears to have strong influence on the overall thermal perception. Although the course of overall thermal load is nearly the same in the two scenarios, subjects' mean vote passes thermal neutrality already after 5 minutes in the STRONG scenario, while in the LOW scenario thermal

neutrality is not even reached after the entire cool-down duration. With respect to these results, hypothesis two can be determined to be true. No general standard exists for tolerable deviations of a model's predictions. However, the investigation shows, that the same overall thermal load can lead to very different deviations in different thermal asymmetries. These deviations are high when local discomfort occurs, which speaks for the necessity of LTC quantification for a holistic DPC assessment method.

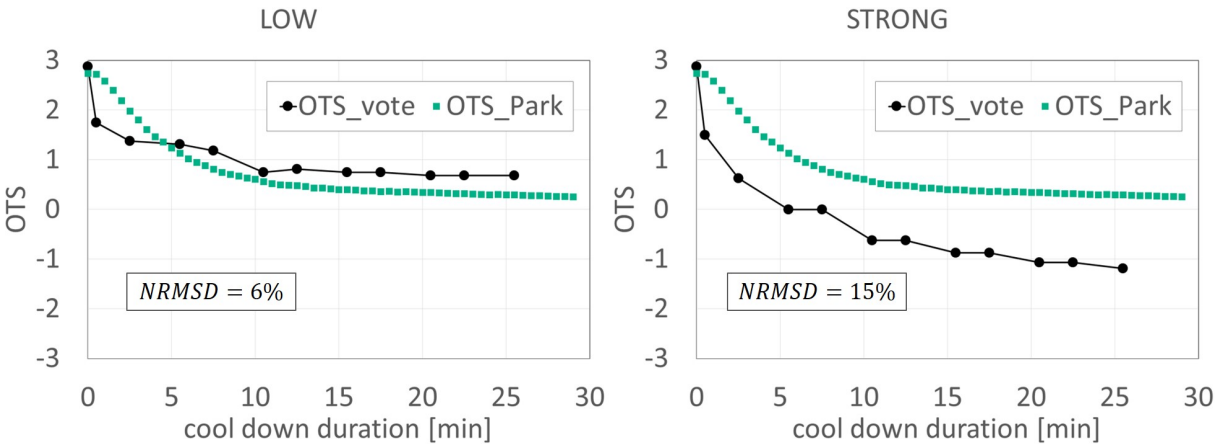

Figure 4.14: OTS comparison of subjects' mean vote with the Park model predictions in both cool-down scenarios, with regard to the original ASHRAE thermal sensation scale.

The Park OTS trajectories are very similar in the two scenarios. This can be explained in consideration of two effects: First, as explained in the Methods section 4.2, the two scenarios were designed to produce a nearly equal overall thermal load on the human subjects. The very similar progressions of overall equivalent temperature in the two scenarios (see figure 4.10) validates the success of this endeavour. A second reason for the similar Park OTS trajectories may be found in the high sensitivity of the Park model to air humidity. As described above, air humidity was not measured, but adopted from another DPC cool-down experiment. Since the same humidity data was used for both scenarios, the Park predictions show a similar behaviour over time.

Comparison of the Prediction Accuracy of other Models Since the Park model's prediction accuracy is significantly lower in the STRONG scenario, a fair presumption would be that one of the other models' predictions fits better here and may therefore be a better choice for both scenarios. Figure 4.15 shows the OTP predictions over cooling duration time and the resulting NRMSD for all models in the STRONG scenario. Apparently, the NRMSD of all models' predictions are higher than in the LOW scenario.

None of the models is able to deal with high thermal asymmetry and predict the steep evolvement of subjects' thermal perception in the STRONG scenario. A mere five minutes after the start of the cool-down, thermal neutrality is reached. With reference to figure 4.11, from this time step on, mean local thermal perception in the head area is "too cold"; hence, local cooling is too intense, which should not happen in a well designed climate control. Cool-down performance can only be assessed when no discomfort due to cooling intensity occurs. In a real vehicle's power design, cooling intensity would be lowered

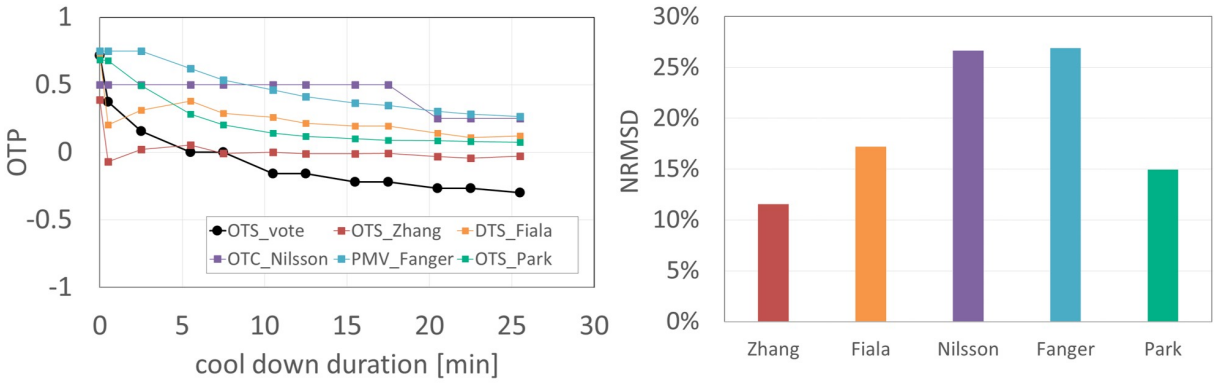

Figure 4.15: OTP courses over cooling duration time and their corresponding NRMSD in the STRONG scenario.

until no local cold discomfort occurs. To evaluate such local cooling intensity thresholds objectively, quantification of local cold discomfort is necessary and such discomfort can be assessed using the Nilsson model (designed for steady-state conditions) and the Zhang model (designed for application in simulations). In the following section, I investigate to what extent these models deliver reliable results with regard to the DressMAN measurements in a vehicle cool-down.

4.3.3 Local Thermal Comfort Assessment

For the potential utilization as an assessment method for Local Thermal Tolerance Thresholds (TTT_i), the LTC predictions of the Zhang and the Nilsson models are compared to subjects' local thermal perceptions at different body segments according to the MTV scale. Figure 4.16 shows the NRMSD of the models for each body segment in both cool-down scenarios. Both models appear to have a significant error in each scenario. In the LOW scenario, the average NRMSD over all body segments is 20% for the Nilsson model and 22% for the Zhang model. The STRONG scenario leads to 31% for the Nilsson model and 17% for the Zhang model.

Figure 4.17 depicts the MBE of the models' predictions for all body segments in each of the cool-down scenarios. It reveals the Nilsson model's tendency to evaluate local thermal perception too warm, while the Zhang model tends to evaluate it too cold.

In the STRONG scenario, subjects' mean vote shows local cold discomfort in the head area. Figure 4.18 compares this vote with the models' predictions. Apparently, neither the Nilsson model nor the Zhang model are able to predict this discomfort. While subjects' MTV continues to be "too cold" after 5 minutes, the Zhang prediction is between "cold but comfortable" and "neutral" while the Nilsson prediction is "neutral" for the scalp and "warm but comfortable" for the face. The Zhang predictions seem to be quite close to subjects mean vote, however, the relevant evaluation property of too intense local cooling recognition is not achieved.

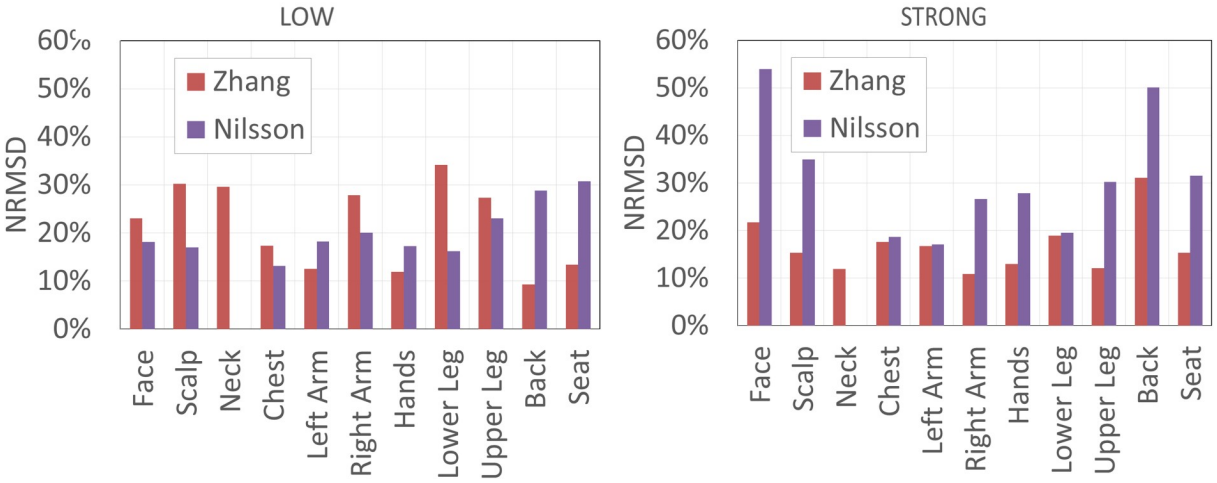

Figure 4.16: NRMSD of the Nilsson and Zhang LTC predictions for each body segment.

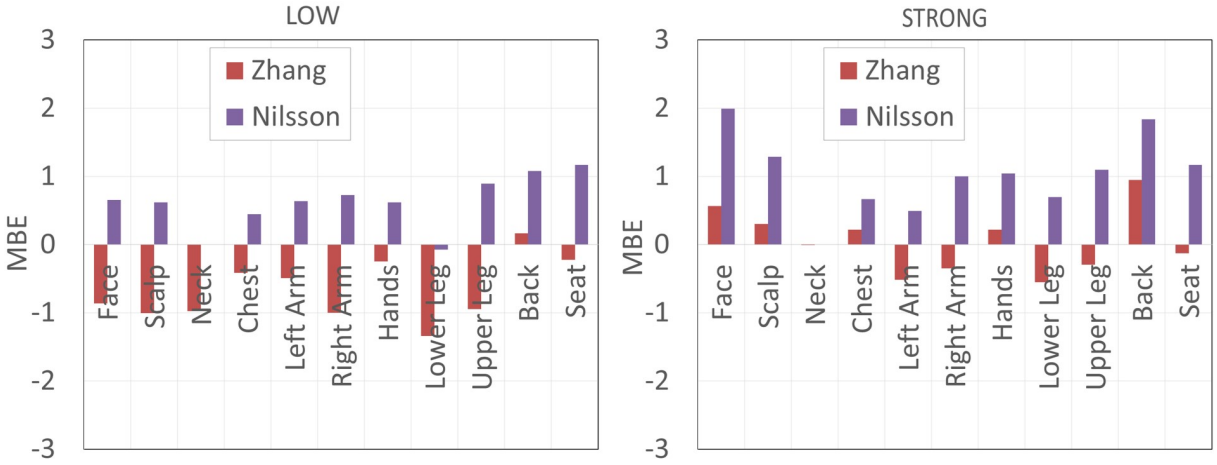

Figure 4.17: MBE of the Nilsson and Zhang LTC predictions for each body segment in deviation steps regarding the MTV scale.

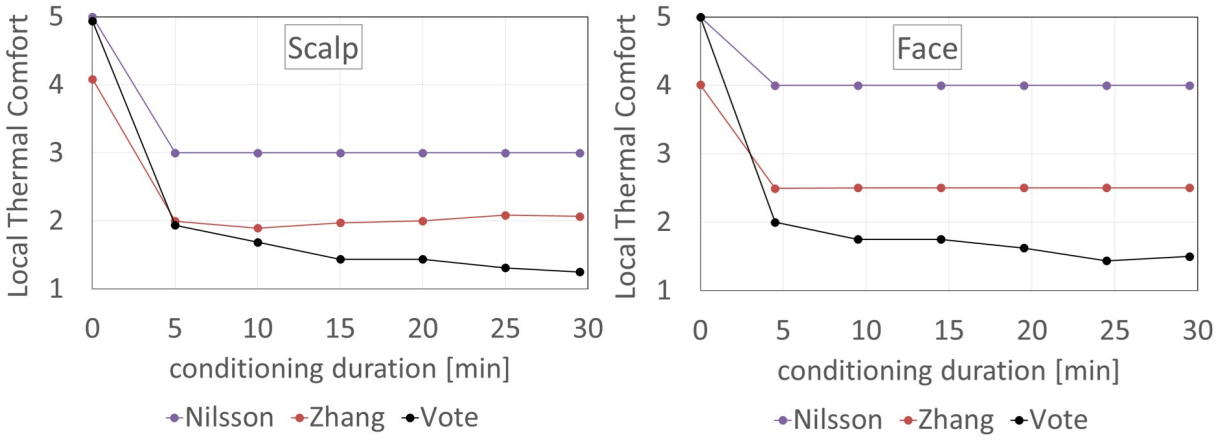

Figure 4.18: Progression of the Nilsson and Zhang LTC predictions and subjects' actual mean vote in the STRONG scenario for the head area with regard to the MTV scale.

4.4 Discussion

The results of the vehicle cool-down study confirm the hypotheses made in the Methodological Approach (chapter 3) for the applied adaptation models and scale norming method. The Park model and the Fiala model offer the most reliable predictions of overall thermal perception in relation to the DressMAN mesurements. Since the Park model fits the feasibility criteria of section 2.5 better than the Fiala method, it is the better approach to measurement based DPC assessment. However, the digital implementation of the Fiala method in simulation tools might represent a useful complement for counterchecking during the pre-development phase of new climatization technologies.

The comparison of the two cool-down scenarios shows, that the Park model's prediction accuracy is only high as long as no local cold discomfort occurs. In a well designed climate control, too intense local cooling and hence local cold discomfort must be avoided. Thus, a comprehensive cool-down performance assessment method must allow for quantifying local cold discomfort due to local cooling intensity. The comparison of local comfort prediction with subjects' mean thermal vote in section 4.3.3 shows that neither the Nilsson model nor the Zhang model can reliably be used for this purpose. Therefore, a new methodology to assess TTT_i is developed. The underlying theory and the supporting investigations are described in the following chapter.

Chapter 5

A New Methodology to Assess Local Thermal Tolerance Thresholds

This chapter presents a new methodology to determine the maximum cooling intensity that can be applied to a certain body part during vehicle cool-down, as proposed in chapter 3 and parts of which I published in [64]. In two human subject studies, these Local Thermal Tolerance Threshold (TTT_i) are quantified for three body parts in relation to the local climate impact measurements of the DressMAN system.

Based on literature on thermophysiology and thermal perception a theory of *Local Cold Discomfort under simultaneous Overall Warm Discomfort* is developed. From this theory corresponding research hypotheses are deduced and experimental designs to test them are introduced. The LTC models of Nilsson and Zhang are applied to the measured conditions of the experiments to compare their predictions with human subjects' actual responses. As these models do not reflect the evaluation of the human subjects with sufficient accuracy, the data obtained from the experiments is used to conduct regression analyses to develop new prediction models. From these models local cooling thresholds for neck, buttocks and back are derived.

5.1 Neck Cooling (Methodology Development)

For methodology development I chose the neck area since it meets the appropriate criteria, which I derived in part from literature and in part identified during pre-tests:

- Sensitivity: In order to determine tolerance thresholds in relation to cooling intensity, these thresholds need to be violated during subject studies. The distribution of cold receptors over the human body shows the highest density in the neck area [49], which suggests a high sensitivity and enables such violations at given technical resources with higher probability.
- Measurability: While developing the methodology, local skin temperature measurements are necessary for testing the hypotheses. A comparison of measuring methods for surface temperatures in preliminary tests showed that only IR thermography is sufficiently responsive and accurate for the occurring skin temperature dynamics with locally applied convective cooling. To measure skin temperature using an IR camera, an unclothed body area must be investigated, and the neck is often exposed in the summer.

- Relevance: DPC addresses those body areas, whose conditioning is expected to be most effective in cooling the entire human body. At low activity rates, the head has the highest metabolic heat production of the whole body [30] and it would be effective to apply convective cooling there. Thus, such DPC measures are expected for future vehicle climatization systems and the neck can be assumed to be always affected by convective head cooling. Since the neck is more sensitive than the face or the scalp, its tolerance threshold will hence be the limiting factor for head cooling as well.

5.1.1 Theory

In summer, when cool-down performance is relevant, a thermophysiological state of slightly above neutrality or already warm discomfort can be assumed for the moment a person enters the vehicle. The passively heated passenger compartment increases overall warm discomfort until climatization is activated. With the start of local cooling, relief from that discomfort takes place, as the rising of the overall body temperature is slowed down or even reversed. According to [25], local thermal sensation is related to local skin temperature and its temporal derivative and according to [65], local thermal comfort is related to local thermal sensation and the overall thermal state of the human body. The local cooling can hence be expected to evoke relief from the overall warm discomfort and thus thermal pleasure. However, depending on the intensity of local cooling, a shift of perception quality from pleasant to unpleasant can be assumed.

Local Cooling Intensity For a definition of local cooling intensity, I employ the principle of local thermal load, introduced in the description of the Park method in section 2.4.2. Adapting Fanger's method and combining all relevant climate impact effects [17], local thermal load $\dot{q}_{TL,i}$ comprises conductive ($\dot{q}_{TL,K,i}$), radiative ($\dot{q}_{TL,R,i}$), convective ($\dot{q}_{TL,C,i}$) and evaporative ($\dot{q}_{TL,E,i}$) local thermal load:

$$\dot{q}_{TL,i} = \dot{q}_{TL,K,i} + \dot{q}_{TL,R,i} + \dot{q}_{TL,C,i} + \dot{q}_{TL,E,i} \tag{5.1}$$

Only radiative, convective and conductive thermal load can be obtained from the DressMAN measurements. The evaporative thermal impact, however, is only considered stochastically for the entire human body, but not in terms of local thermal load, due to the lack of an appropriate sensor technology for measuring evaporative thermal load. Since the effect cannot be measured, the problem is here addressed as follows:

During vehicle cool-down, local cooling occurs mainly in the form of local air conditioning and seat conditioning. In both cases cooling intensity is a matter of air temperature or air velocity. The cooling intensity is hence built up from convection *and* evaporation. Yet, these two effects relate to each other. According to the ASHRAE Handbook: "Generally, parameters related to dry or evaporative heat flows are not independent because they both rely, in part, on the same physical processes."[3]. The Handbook presents the following

relationship between the evaporative heat transfer coefficient (h_e) and the convective heat transfer coefficient (h_c):

$$\text{Lewis Ratio:} \qquad LR = \frac{h_e}{h_c} \tag{5.2}$$

and continues "[...]at typical indoor conditions, LR equals approximately $16.5\frac{K}{kPa}$" [3]. Since LR is considered to be constant for the conditions investigated, equation 5.2 reveals a linear dependency of evaporation from convection. In short, an increase of convective heat loss always causes a proportional increase in evaporative heat loss. For local air conditioning, air temperature and air velocity may change significantly over time, while radiative heat load remains permanently high. Consequently, a decrease in measured equivalent temperature in locally conditioned air is dominated by convective heat loss. And since evaporation is proportional, $T_{eq,direct}$ is a measure of the immediate local cooling impact, caused by convection *and* evaporation. Specifically, in the very special case of *local air conditioning in overall hot environments, with no radiative cooling involved*, $T_{eq,direct}$ allows quantification of local thermal impact from convection, radiation and evaporation and can therefore represent local cooling intensity for air adjacent body areas.

For contact surface conditioning the definition of cooling intensity must be approached slightly different. In addition to conduction, the perforated surface of a conditioned seat also causes heat dissipation by convection and evaporation. The contact temperature measurement between *human subjects* and the seat, naturally includes all three effects. Hence, contact temperature can be considered cooling intensity, since it directly reflects the cooling effect on the occupants body surface.

The Percentage of Dissatisfied In thermal comfort research thermal discomfort can be quantified by the Percentage of Dissatisfied (PD) [17] [39]. PD expresses the percentage of people who perceive the conditions as unpleasant. With regard to local perception of DPC, it is the percentage of people who experience the local cooling as too intense, for which I here use the expression Percentage of Dissatisfied People by Local Cold Discomfort (PD_{cold}). Since it refers only to local discomfort, PD_{cold} can have values of 0% when no local cooling is applied at all.

As described in chapter 2.3.2, local thermal perception depends on local skin temperature ($T_{sk,}$) and its temporal derivative $\left(\frac{dT_{sk}}{dt}\right)$ [25]. Therefore, PD_{cold} can be expected to be a function of both quantities:

$$\text{Research Hypothesis } H_{R,neck,1}: \qquad PD_{cold} = f\left(T_{sk}, \frac{dT_{sk}}{dt}\right) \tag{5.3}$$

Nevertheless, skin temperature is not an appropriate input variable for an assessment method. During the assessment procedure, tolerance thresholds need to be determined from the climate measurement system used. Therefore subjects' thermal perception must

be related to climate variables. However, since both, skin temperature and its temporal derivative vary with cooling intensity and cooling duration, thresholds can be assumed to have a dynamic character. There must be *a moment in time* when passengers' perceptions of local cooling shift from pleasant to unpleasant, depending on body part and cooling intensity. Accordingly, Percentage of Dissatisfied people by local cold discomfort (PD_{cold}) cannot be predicted by cooling intensity alone, but must somehow relate to duration of cooling as well. Since this temporal dependency is actually due to the skin temperature evolvement at the conditioned body area, the heat transport effects in the human skin are examined next.

Local Heat Balance The area-specific heat dissipation from the skin to the environment is in equilibrium with the local heat generation, as illustrated in figure 5.1. Positive heat flux from blood perfusion (arterial inflow, venous outflow) ($\dot{q}_{bl}$), local metabolic heat production ($\dot{q}_m$), conductive heat flux from inner tissues ($\dot{q}_c$) and sensible heat release from skin temperature change $\left(\dot{q}\left(\frac{dT_{sk}}{dt}\right)\right)$ are opposed to heat dissipation to the environment ($\dot{q}_{env}$) (adapted from [11] and [19]).

$$\dot{q}_{env} = \dot{q}_m + \dot{q}_{bl} + \dot{q}_c + \dot{q}\left(\frac{dT_{sk}}{dt}\right) \tag{5.4}$$

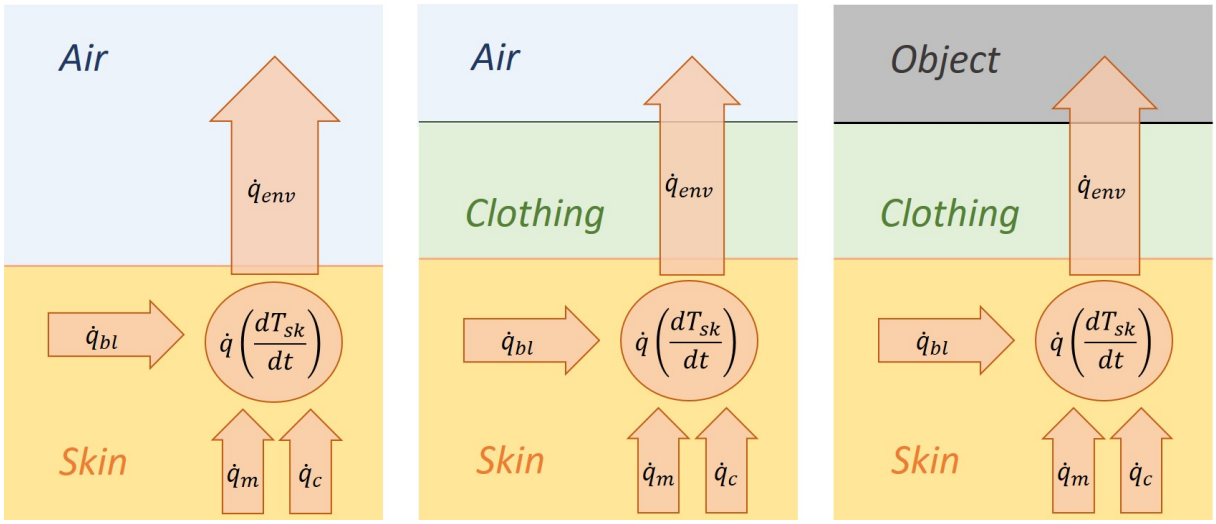

Figure 5.1: Illustration of local heat balance in the human skin for unclothed air adjacent body areas (left), clothed air adjacent body areas (middle) and clothed contacting body areas (right).

With respect to the heat transfer mechanisms and local heat balance, heat flux from the skin to the environment is driven by a gradient between the local skin temperature T_{sk} and the local environment temperature. The latter is just another expression for cooling intensity, represented by $T_{eq,direct}$. Thus, local heat flux can be expressed as a function of T_{sk} and $T_{eq,direct}$ (see equation 5.5).

$$\dot{q}_{env} = f\left(T_{sk}, T_{eq,direct}\right) \tag{5.5}$$

While in steady state conditions no temperature change occurs in the tissue, in transient conditions the internal thermal energy of the skin is either released or built up. Assuming constant blood perfusion and metabolic heat generation, the skin temperature change rate at a certain moment in time, must therefore depend somehow on the current skin temperature and the current heat dissipation to the environment:

$$\frac{dT_{sk}}{dt} = f\left(\dot{q}_{env}, T_{sk}\right) \tag{5.6}$$

Substituting $\dot{q}_{env}$ in equation 5.6 with the right side of equation 5.5, we obtain:

$$\frac{dT_{sk}}{dt} = f\left(f\left(T_{sk}, T_{eq,direct}\right), T_{sk}\right) \tag{5.7}$$

Since T_{sk} occurs twice, equation 5.7 can be put as follows:

$$\text{Research Hypothesis } H_{R,neck,2}: \qquad \frac{dT_{sk}}{dt} = f\left(T_{sk}, T_{eq,direct}\right) \tag{5.8}$$

Absolute skin temperature, again, is simply a result of its change over time:

$$T_{sk}(t + \Delta t) = T_{sk}(t) + \frac{dT_{sk}}{dt}(t) \cdot \Delta t \tag{5.9}$$

Combining the assumptions of equations 5.3, 5.8 and 5.9, $\mathrm{PD_{cold}}$ can be derived dynamically from the cooling intensity development over time, if the initial body surface temperature is known:

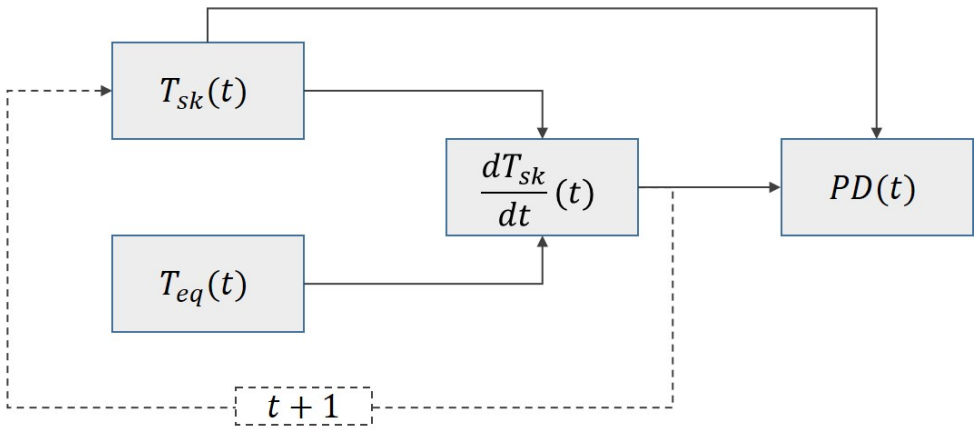

Figure 5.2: Hypothetical model for the derivation of time dependent body surface temperature, its temporal derivative and $\mathrm{PD_{cold}}$ from time-variable cooling intensity.

5.1.2 Methods

This section gives a description of the methods, used to investigate the relevant variables of the neck cooling perception. According to section 5.1.1 four quantities are required to enable hypothesis testing:

- Dependent Variable: $\mathrm{PD}_{\mathrm{cold}}$
- Mediator Variables: T_{sk}; $\frac{dT_{sk}}{dt}$
- Independent Variable: $T_{eq,direct}$

Experimental Design The tests were conducted in two adjacent climate chambers at the Fraunhofer Institute for Building Physics IBP in Holzkirchen, Germany, in October and November 2018. One chamber served as an acclimatization room, for preconditioning human subjects to thermal neutrality and to ensure equal thermophysiological starting conditions. In the other chamber the subjects were exposed to hot surrounding conditions in terms of operative temperature and relative humidity, intending to evoke overall warm discomfort. After spending sufficient time for experiencing such discomfort, cooled air was blown at the anterior neck area. Subjects were asked to rate overall and local thermal comfort, while at the same time local skin temperature and directed equivalent temperature were measured.

Figure 5.3 illustrates the test setup. Overall conditions are produced by heating and humidifying the air and tempering the inner surfaces of the climate chamber. The local cooling is provided by an external refrigeration unit and supplied to the subjects' neck via a supply pipe.

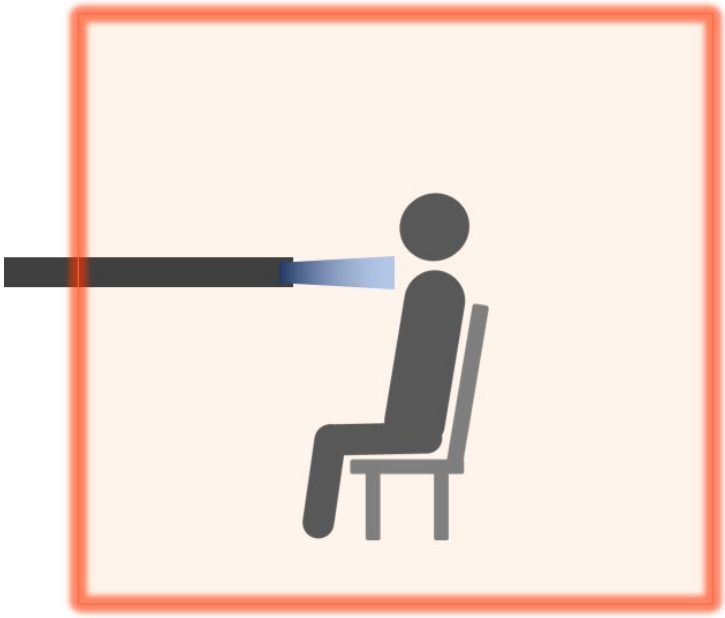

Figure 5.3: Illustration of the test setup for investigating the perception of local cooling at the neck area.

Overall Conditions

The general environmental conditions, which represent thermal conditions similar to those of a passively heated vehicle in summer, had two objectives:

- Evoking overall warm discomfort: As described earlier, overall summer conditions in a vehicle are characterized by high solar loads and therefore high surface and air temperatures.
- Inducing a high probability of sweating: Convective cooling devices cause a permanent removal of humidity sattured air and therefore a constantly high vapour pressure gradient between the skin surface and its immidate surrounding. If sweating occurs, the according latent heat loss causes a higher skin temperature change rate and therefore a cooler perception. Hence, for cooling intensity tolerance, sweating is the more critical case.

Creating such conditions would result in operative temperatures above 60°C, which is not justifiable for human subject studies with regard to health issues. Apart from that, the climate chambers used are technically not able to realize such high temperatures. In order to cause heat strain and sweating nevertheless, the test chamber was conditioned to an operative temperature of 40°C and a relative humidity of 60% in all four test scenarios.

Cooling Intensity Levels

For local cooling, air was sucked in through a water-air heat exchanger, which was coupled to an external chiller. The cold air was supplied through a nozzle in front of a chair. The supply air velocity was held constant for all tests to avoid variations of the area cooled at the subjects neck. Cooling intensity was varied only by adjusting the air temperature. The intensity levels were defined according to directed equivalent temperature measured at neck distance from the nozzle ($0.2m$).

A variation of the cooling intensity during a single test was technically difficult to implement and would have increased the probability of systematic errors. However, for reliable statements and statistical modeling, a sufficient number of test variable combinations must be ensured. Since T_{sk} and $\frac{dT_{sk}}{dt}$ were expected to vary over time and from person to person, a sufficient number of combinations could be assumed even for constant cooling intensity during a single test. The varaibles must take values that also occur (and may occur in future DPC systems) under real conditions in a vehicle. Since tolerance thresholds needed to be violated, a range of intensities had to be chosen suggesting also a broad range of $\mathrm{PD}_{\mathrm{cold}}$.

During pre-tests with two subjects, the time period for heat strain conditioning and the intensity levels for local cooling were determined. The lowest cooling intensity ($T_{eq,direct} = 12$°C) was chosen from Nilsson's comfort zones and should be perceived at least as "cold but comfortable". In hot overall conditions the human body is in an urgent need to cool down, which is why the tolerance for local cooling intensity is expected to be higher than in thermal neutrality. That is, lower local equivalent temperatures should be accepted than the Nilsson model allows. For the actual experiment four different cooling intensity levels were chosen. At each intensity level the overall climate conditions were the same. To get a variety of skin temperature change rates the maximum cooling intensity was applied from the beginning. Table 5.1 gives a comparison of supply air temperature and

local directed equivalent temperature at the supply air velocity of $3.0\frac{m}{s}$ at the nozzle, which resulted in $2.0\frac{m}{s}$ at neck distance, for each intensity level.

Table 5.1: Comparison of supply air temperature ($T_{a,sup}$) and local directed equivalent temperature ($T_{eq,direct}$) for an air velocity of $2.0\frac{m}{s}$ at neck distance.

	$T_{a,sup}$ at the nozzle	$T_{eq,direct}$ at neck distance
Intensity 1	16°C	12°C
Intensity 2	14°C	10°C
Intensity 3	11.5°C	8°C
Intensity 4	9°C	6°C

Experimental Procedure Figure 5.4 illustrates the chronological procedure of each test. The subjects spent one hour before the test in neutral conditions. They arrived in the thermal neutrality chamber and stood there for another 10 minutes to ensure an equal thermal state at the start of each test. Afterwards subjects spent another 10 minutes in the hot environment, followed by a 15 minute period of local cooling, while remaining in the hot environment.

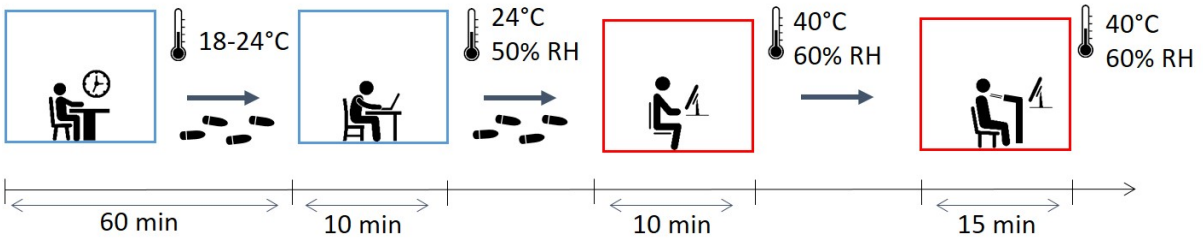

Figure 5.4: Experimental procedure of the neck cooling study.

The same procedure was conducted for all four intensity levels of local cooling, as defined in table 5.1. To avoid a bias from circadian rythm the sequence of cooling intensities was randomized for each subject.

Measurements

Directed Equivalent Temperature was measured separately from the subject tests under the same test conditions and in neck distance. For measuring $T_{eq,direct}$, *DressMAN 3.0* sensors were used.

Local Skin Temperature was measured by infrared camera recording, using an *optris PI 400* camera. The actual value for T_{sk} was captured every 30 seconds by visually identifying at each time step the same representative area at the neck to average the temperature.

Skin Temperature Derivative $\frac{dT_{sk}}{dt}$ was calculated from the corresponding differences of T_{sk} measurements between the time steps.

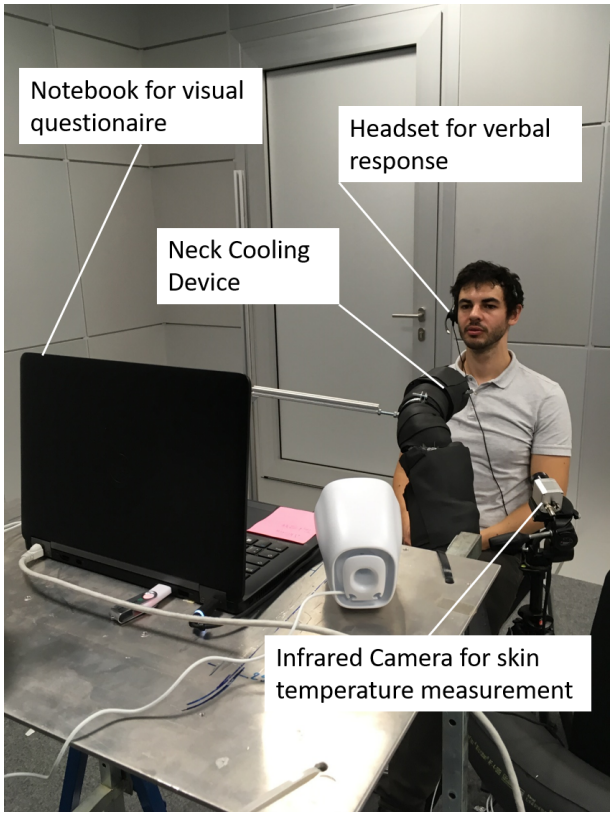

Figure 5.5: Test setup of the neck cooling study with a human subject being visually questioned via screen survey and wearing a headset for verbal response. The cooling device in front of him blows chilled air to his neck and an IR camera records the local skin temperature.

Subjects and Questionnaire A total of 18 German subjects, 9 male and 9 female, participated in the experiment at all four intensity levels. The subjects had a normal range of BMI and were between 21 and 43 years old. As in the vehicle cool-down study, the clothing ensemble was chosen according to light summer cloth, with a clo value of 0.6. Thermal perception was captured in 30 second steps, beginning with the start of the local cooling. Since thermal tolerance thresholds are a matter of both sensation and comfort, a mixed sensation and comfort rating scale was used for the thermal perception questionnaire (see table 5.2). The shift from "just right" to "too intense" was considered as violation of a person's local thermal tolerance threshold.

Table 5.2: Rating scale, used in the neck cooling experiment.

Value	LTC
1	not intense enough
2	just right
3	too intense

5.1.3 Results

This section gives a descriptive analysis of the investigated quantities of the neck cooling study by analyzing the evolvement of the relevant variables over the cooling duration time. Figure 5.6 shows the mean local skin temperature progression at the anterior neck, averaged over all test subjects (left) and the corresponding percentage of dissatisfied people in relation to local cooling intensity (right). After the heat strain phase of 10 minutes, the local skin temperature is with about 36.5°C identical in all four test scenarios. With the start of the local cooling it seems to follow an exponential trajectory with different gradients for each cooling intensity level and approaches different constant values accordingly.

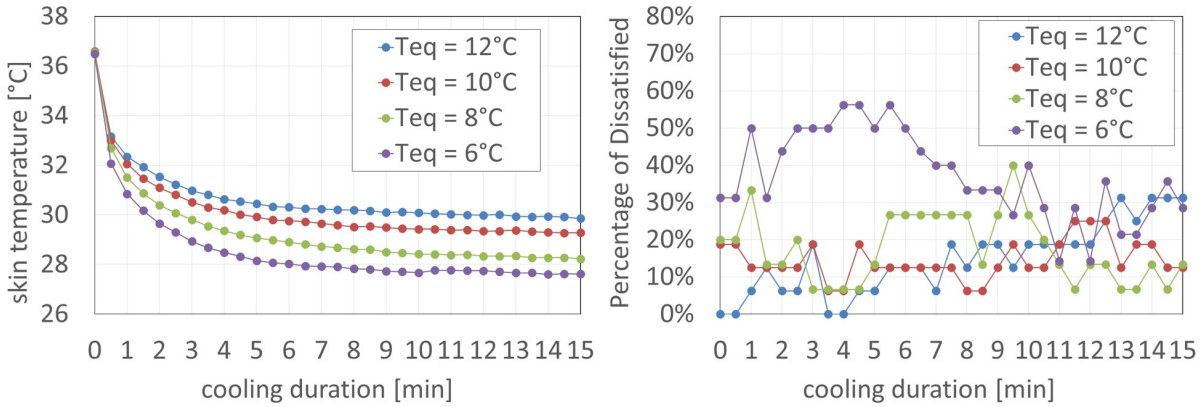

Figure 5.6: Left: Mean local skin temperature course over cooling duration time for all four cooling intensities, represented by $T_{eq,direct}$. Right: PD_{cold} over cooling duration time for all four cooling intensities, represented by $T_{eq,direct}$.

The progression of PD_{cold} reveals a variation of thermal perception over time, even though cooling intensity has not changed. This variation indicates a dependency of thermal perception from thermophysiological conditions, which do change over time. For the relation of absolute skin temperature and its temporal derivative vary permanently over time, a dependency of thermal perception from both variables seems plausible.

5.1.4 Thermal Perception Model Comparison

Like in the vehicel cool-down study, the thermophysiological model of Fiala and the thermal perception models of Nilsson and Zhang can be applied to the climate conditions measurements. Their predictions are compared to the results described to evaluate the models' suitability in TTT_i assessment.

Methods The Nilsson model provides no individual comfort zone for the neck area, but for head (scalp and face) and chest. Hence, these have been compared to subjects' votes. The lowest boundary of the corrseponding "cold but comfortable" zone (value 2) is at $T_{eq} = 10.9$°C for the head area. To compare the MTV scale predictions with the

rating scale used in the experiments (table 5.2 in section 5.1.2), I interpreted the Nilsson predictions as follows:

$$LTC = \begin{cases} 1 & \text{for} \quad LTC_{Nilsson} > 2 \\ 2 & \text{for} \quad LTC_{Nilsson} = 2 \\ 3 & \text{for} \quad LTC_{Nilsson} < 2 \end{cases}$$

For the Fiala/Zhang combination the measured climate conditions were used in THESEUS FE® as follows:

variable	overall body	neck area
T_a	40°C	$T_{eq,direct}$
$\bar{T}_r$	40°C	$T_{eq,direct}$
v_a	$0.05\frac{m}{s}$	$0.05\frac{m}{s}$
h_{cal}	$10\frac{W}{m^2K}$	$10\frac{W}{m^2K}$

To compare the simulation results with the subjects' votes, I interpreted the local thermal sensation and local thermal comfort output of the Zhang model as follows:

$$LTC = \begin{cases} 1 & \text{for} \quad LTS_{Zhang} \geq 0 \\ 2 & \text{for} \quad LTS_{Zhang} < 0 \quad \text{and} \quad LTC_{Zhang} \geq 0 \\ 3 & \text{for} \quad LTS_{Zhang} < 0 \quad \text{and} \quad LTC_{Zhang} < 0 \end{cases}$$

Results According to the Nilsson model the lowest cooling intensity ($T_{eq} = 12°C$) should be perceived as "just right", whereas already intensity 2 ($T_{eq} = 10°C$) would be interpreted as "too intense". Considering the PD_{cold} trajectories of figure 5.6 this is not the case.

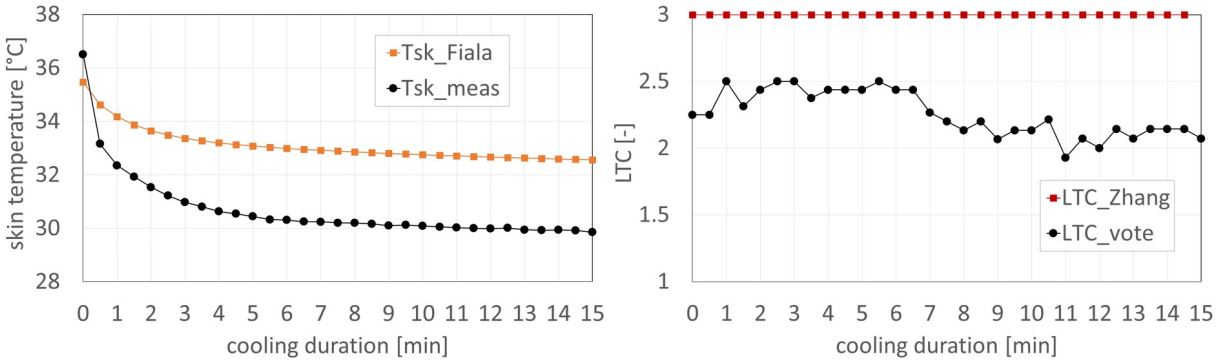

Figure 5.7: Comparison of the neck cooling study results with the Fiala/Zhang simulation. Left side: Course over cooling duration time of measured mean local skin temperature at human subjects (Tsk_meas) and simulated local skin temperature by the Fiala thermophysiological model (Tsk_Fiala). Right side: Course over cooling duration time of subjects' mean local thermal perception vote (LTC_vote) and simulated local thermal perception by the Zhang model (LTC_Zhang), according to the experimental thermal perception scale with (1) not intense enough, (2) just right and (3) too intense.

The comfort zones' boundaries of the Nilsson model are defined at 20% dissatisfied. However, intensities 1 to 3 result in an empirical PD_{cold} of 15% to 17%, averaged over the entire cooling duration time. Only at an intensity of $Teq = 6°C$ PD_{cold} suddenly exceeds 35%.

Figure 5.7 shows the results of the Fiala/Zhang predictions in comparison with subjects' mean vote at the lowest cooling intensity of $T_{eq,direct} = 12°C$. Apparently, the simulations of Fiala's thermophysiological model do not represent the actually resulting skin temperatures observed in the experiment. Even though the simulated $\frac{dT_{sk}}{dt}$ is lower and T_{sk} higher than the actual observed values, the Zhang model predicts "too intense" for the complete cooling duration, while subjects' mean vote is much closer to "just right". This underestimation of the Fiala model and overestimation of the Zhang model applies to the entire test series.

5.1.5 Model Development

The Fiala/Zhang combination is the only approach, which claims for validity in transient local discomfort quantification, yet its predictions differ significantly from the test results, when employed to climate measurements using the described methods. I therefore used the acquired data to develop a prediction model, especially designed for predicting PD_{cold} in relation to measured $T_{eq,direct}$ under high overall heat load. According to the theory of section 5.1.1, this can be achieved using a two step approach of firstly predicting local skin temperature progression from local climate impact and secondly predicting local thermal discomfort from local skin temperature progression.

Modeling Skin Temperature Progression As proposed in equation 5.8, the local skin temperature development is assumed to be predictable from local skin temperature and thermal impact at the moment. Therefore, I analyzed temporal gradients of mean skin temperature ($\frac{dT_{sk}}{dt}$) in respect to cooling intensity ($T_{eq,direct}$) and absolute skin temperature (T_{sk}) at the time. Figure 5.8 shows the temporal gradients of skin temperature over absolute skin temperature for different cooling intensities. An elimination of negative values and logarithmic scaling reveals a clear separation for each cooling intensity.

The plot suggests an exponential course of derivatives over absolute skin temperature. Since many natural phenomena follow the real exponential function with *Euler's number* as the basis, I also chose it for regression here (see equation 5.10).

$$\frac{dT_{sk}}{dt} = e^{T_{sk}} \tag{5.10}$$

To fit the basic model into the measured course of $\frac{dT_{sk}}{dt}$ over T_{sk} with regard to $T_{eq,direct}$, the slope is varied by the coefficient a, the horizontal position by coefficient b and the vertical position by coefficent c, as illustrated in figure 5.9 and defined in equation 5.11. I chose the coefficents with regard to physical plausibility and adjusted them to each cooling intensity separately.

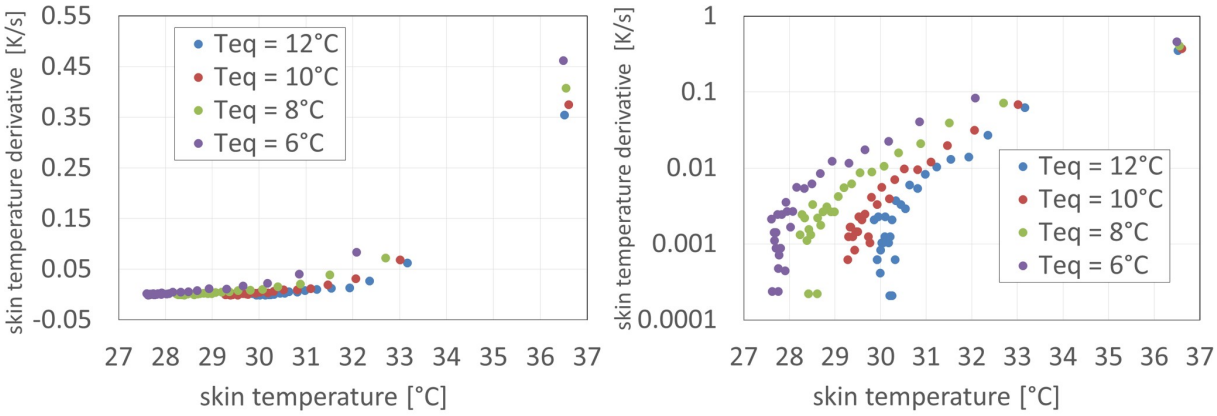

Figure 5.8: Mean skin temperature derivatives over absolute mean skin temperature for each cooling intensity, standard scaled (left) and logarithmic scaled (right).

$$\frac{dT_{sk}}{dt} = e^{(a*(T_{sk}-b))} - c \tag{5.11}$$

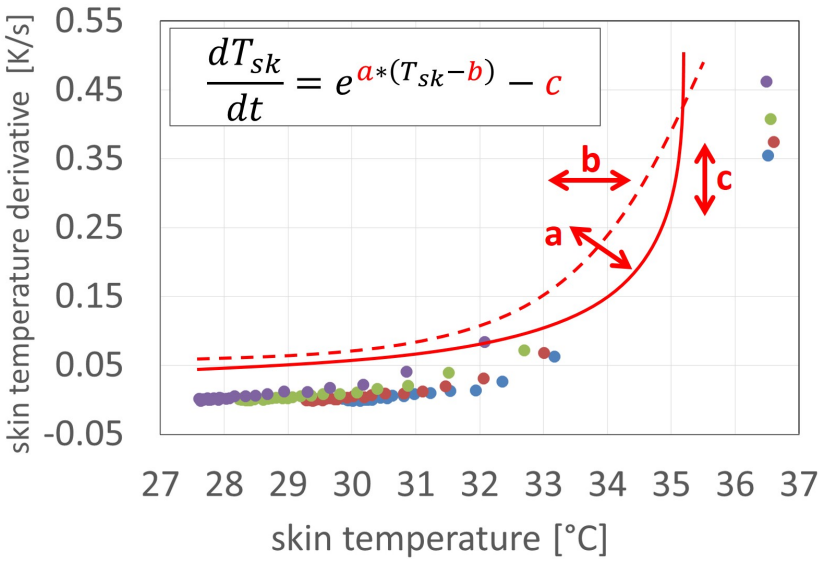

Figure 5.9: Illustration of the function fitting procedure for skin temperature derivatives in relation to skin temperature and cooling intensity.

Relating the coefficients to $T_{eq,direct}$ reveals a linear relation for the coefficients a and b while coefficent c can be integrated as constant value. Coefficient b appears to vary only minimal and might be represented by a constant value as well. However, a sensitivity analysis showed a significant influence on prediction accuracy when defining it as a constant. Considering these coefficents, $\frac{dT_{sk}}{dt}$ can be calculated using equation 5.12.

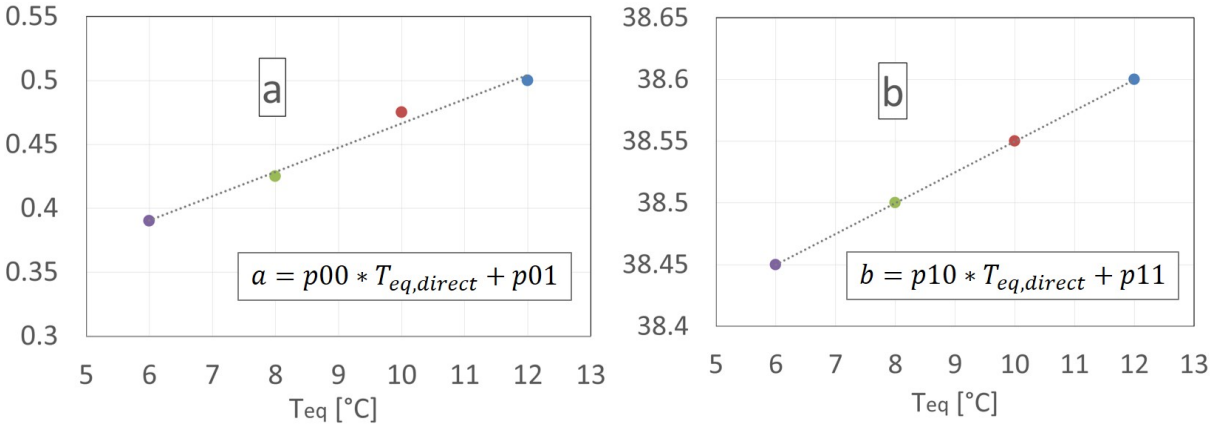

Figure 5.10: Regression functions for the coefficients a and b in relation to $T_{eq,direct}$.

$$\frac{dT_{sk}}{dt} = e^{((p00*T_{eq}+p01)*(T_{sk}-(p10*T_{eq}+p11)))} - p20 \tag{5.12}$$

p00	p01	p10	p11	p20
0.019	0.2765	0.025	38.3	0.014

Modeling the Percentage of Dissatisfied Figure 5.11 shows the relation between PD_{cold} and T_{sk}. It revelas that there is no data for skin temperatures between 33°C and 36.5°C, simply because change rates were too high for the 30 second thermal perception voting in this skin temperature range. Since derivatives at the beginning of the local cooling are disproportionately high but time intervals of the measurements are constant, skin temperature has already decreased to a relatively low level at the following measurements, where derivatives themselves are low. As can be seen from figures 5.8 and 5.11 this causes a large gap between the first data set (at high skin temperature) and the second data set (at significantly lower skin temperature). For a valid bivariate regression analysis, more sets of T_{sk} and $\frac{dT_{sk}}{dt}$ relations would be necessary.

However, for DPC tolerance thresholds these datasets may not be relevant anyway. In his book *"Thermal Sensation and Thermoreceptors in Man"* [25], Herbert Hensel reviews results of different studies, regarding thermal sensation. He concludes that according to [24] and [33], derivatives above $0.05\frac{K}{s}$ do not increase thermal sensation additionally. An investigation on thermal receptors impulse activity [26], allows conclusions to be drawn about the significance of dynamic sensation: Figure 5.12 shows the impulse frequency of a cold receptor from the human hand to different temperature profiles over time. Local cooling of approximately $1\frac{K}{s}$, which is higher than any of the applied cooling intensities in the present study, results in only a small superelevation compared to the static impulse frequency.

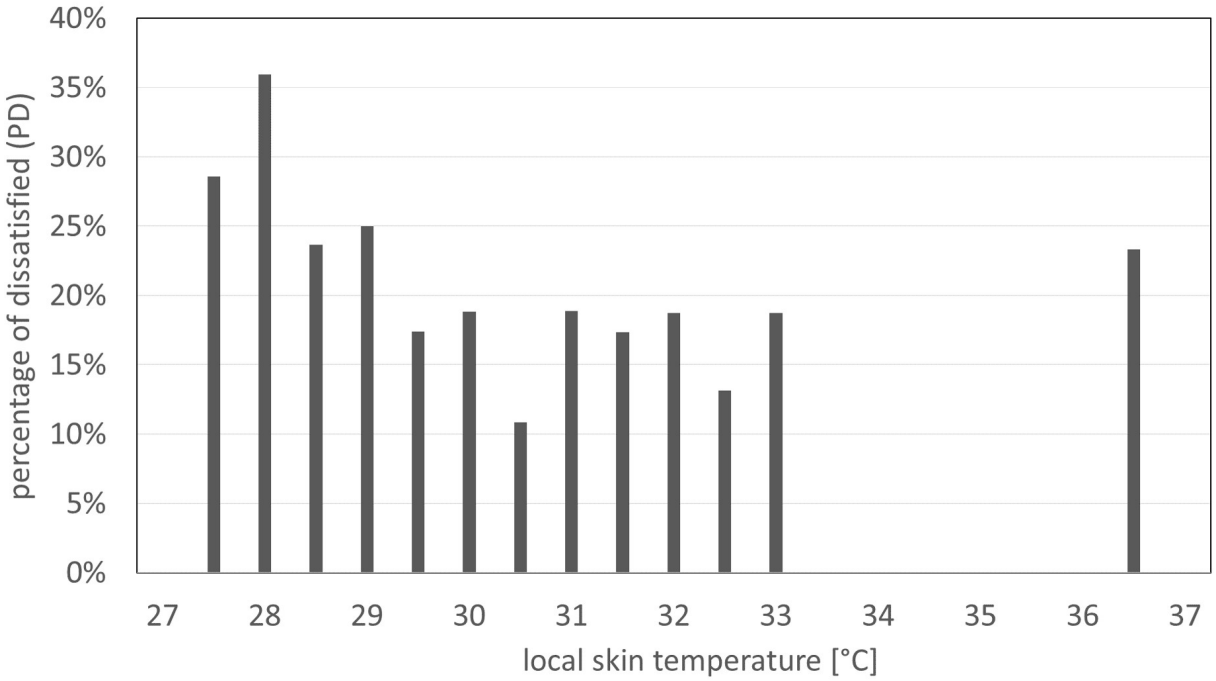

Figure 5.11: PD_{cold} over skin temperature clusters of $0.5K$.

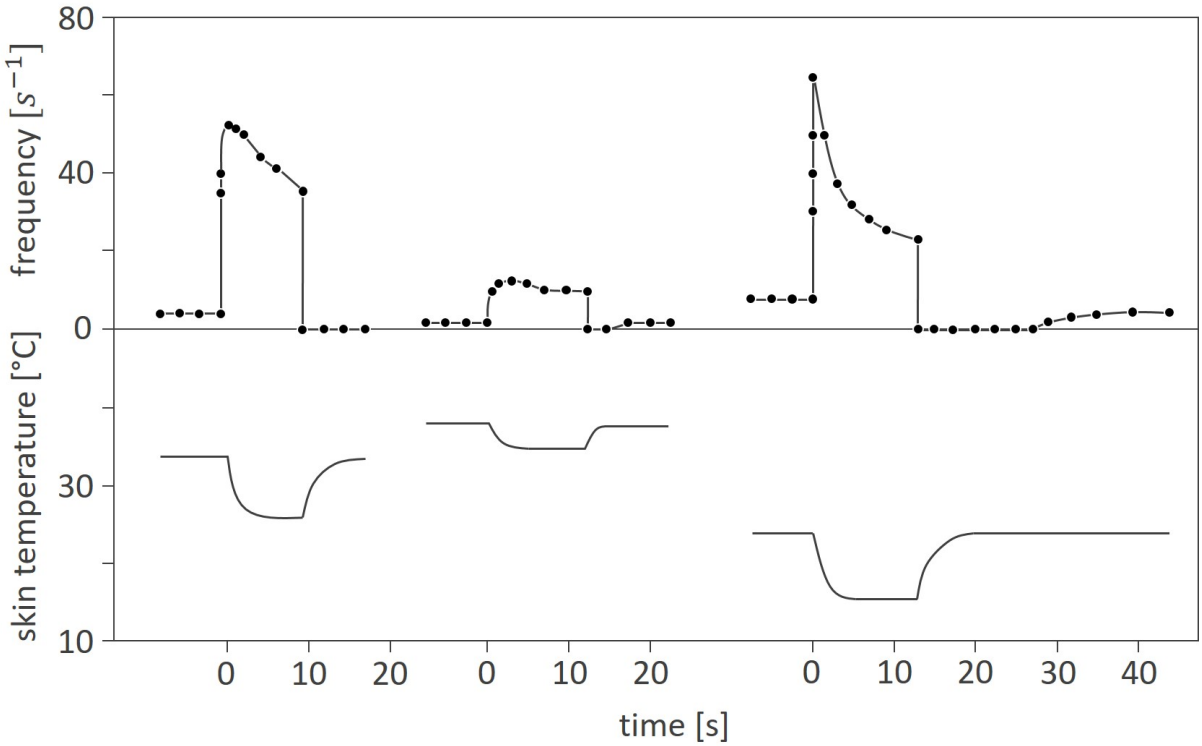

Figure 5.12: Impulse frequency of a cold fiber from the human hand in relation to skin temperature evolvement over time (redrawn from [25]).

At low derivatives, though, thermal sensation is dominated by absolute skin temperature. Cooling intensity in a real vehicle cool-down increases only slowly and high derivatives are not expected to occur. When considering only derivatives below $0.02\frac{K}{s}$ an univariate relation between $\mathrm{PD}_{\mathrm{cold}}$ and T_{sk} can be drawn (see figure 5.13). From the data distribution, a linear or exponential relationship may be assumed. However, since $\mathrm{PD}_{\mathrm{cold}}$ is limited to a range between 0% and 100%, this would not be a plausible relation. In inference statistics, a reasonable approach to such limited regression modeling, is the logistic function (or *"S" shape* function). Considering this, I found the percentage of dissatisfied to be a logistic function of skin temperature, for gradients below $0.02\frac{K}{s}$.

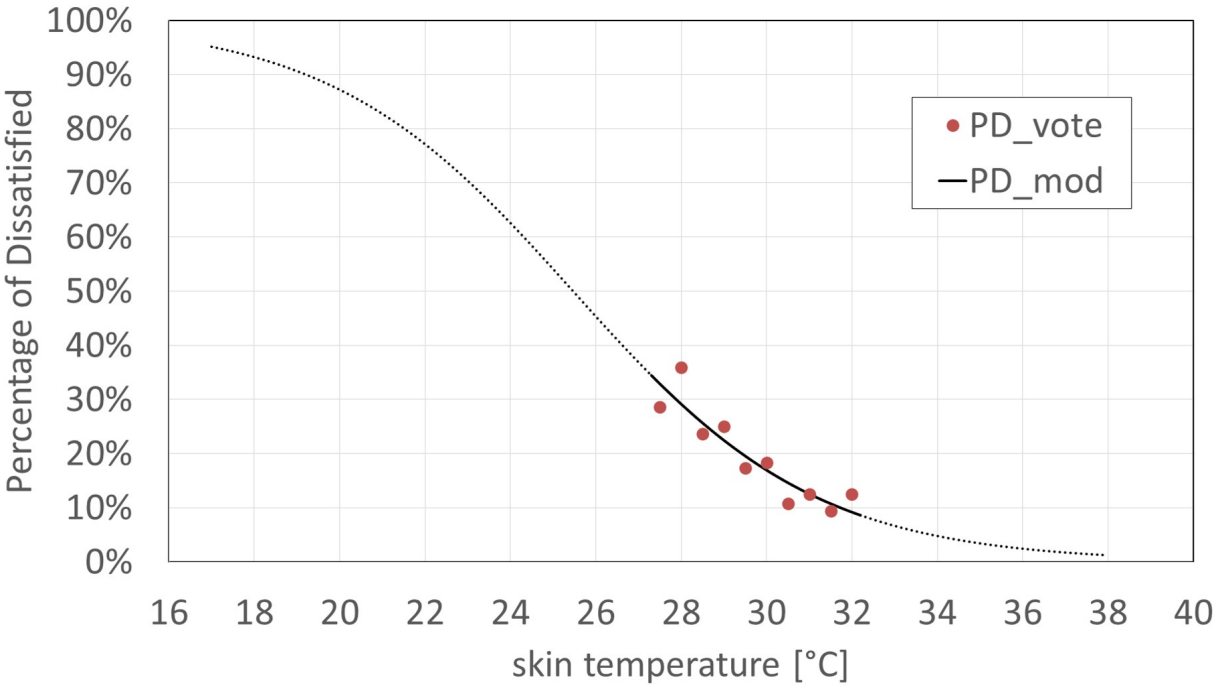

Figure 5.13: PD_{cold} over T_{sk} for low $\frac{dT_{sk}}{dt}$ (below $0.02K/s$) and logistic regression function. The red dots represent the percentage of dissatisfied subjects and the solid black curve shows the corresponding regression function. The dotted line is an extrapolation of the "S" shape function to illustrate the logistic regression.

$$PD_{cold,neck} = \frac{1}{1 + a_n * e^{(b_n * T_{sk,neck})}} \qquad R^2 = 0.84 \qquad (5.13)$$

a_n	b_n
$1.32 * 10^{(-4)}$	0.351

5.1.6 Model Evaluation

To evaluate the models for $\frac{dT_{sk}}{dt}$ and PD_{cold} I merged them to a dynamic prediction model of PD_{cold} from $T_{eq,direct}$.

Goodness of Fit I quantified the prediction quality of the dynamic model, simulating the same boundary conditions as used in the subject study and computing Mean Bias Error (MBE) and Root Mean Square Deviation (RMSD). I conducted this for the prediction of skin temperature progression and the percentage of dissatisfied over time, for each cooling intensity level. An example for intensity level 2 ($T_{eq,direct} = 10°C$) is shown in figure 5.14. Table 5.3 gives the corresponding MBE and RMSD for each cooling intensity. Since thermal perception is influenced by skin temperature derivatives at the beginning (which is not considered by the prediction model) the residuals analysis for PD_{cold} is conducted only with values from 5 minutes cooling duration.

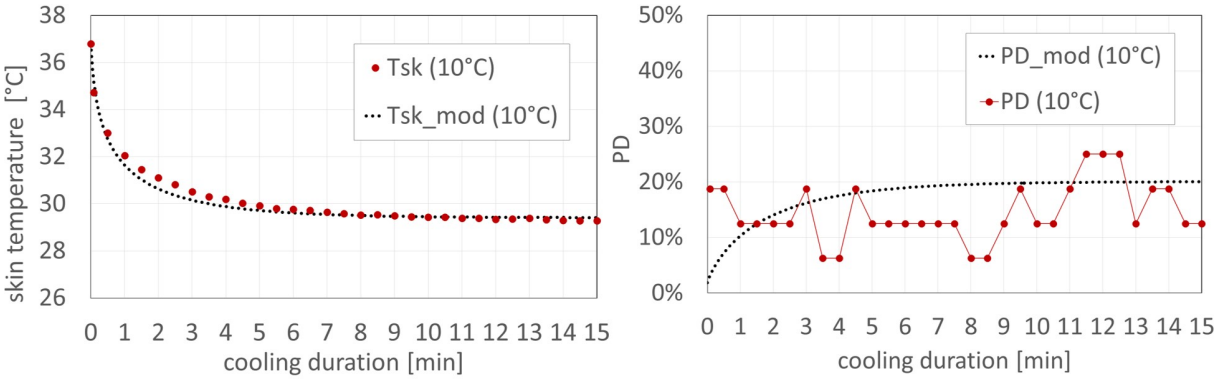

Figure 5.14: Comparison of the developed models' predictions with measured skin temperature and subjects' PD_{cold} for the example of a cooling intensity of $T_{eq,direct} = 10°C$ of the neck cooling study. Left: Mean skin temperature progression over cooling duration time. Right: Percentage of Dissatisfied over cooling duration time.

Table 5.3: MBE and RMSD for the perdiction of skin temperature progression and PD_{cold} for neck cooling.

Cooling Intensity ($T_{eq,direct}$)	MBE for T_{sk}	RMSD for T_{sk}	MBE for PD_{cold}	RMSD for PD_{cold}
12°C	−0.02°C	0.22°C	+3.0%	8.0%
10°C	+0.10°C	0.24°C	−4.8%	7.0%
8°C	−0.01°C	0.27°C	−6.0%	11.2%
6°C	+0.14°C	0.24°C	+1.9%	11.9%

The RMSD values of up to 12% seem high. However, as can be seen from figures 5.6 and 5.14, PD_{cold} disperses widely over time. The high RMSD is thus due to the despersion and not due to an absolute deviation, which is indicated by the MBEs of table 5.3. Nevertheless, the high dispersion leads to an uncertainty in thermal perception prediction that must be taken into account in practical applications.

Plausibilty The models were developed from a relatively small range of local cooling intensities. By applying the models to constant equivalent temperatures that are higher and lower than in the experiments, I studied the behaviour of the predictions for other cooling intensities. In figure 5.15 the resulting T_{sk} and $\mathrm{PD}_{\mathrm{cold}}$ after a cooling duration of 15 minutes are depicted. The green highlighted area represents the actually used experimental boundary conditions. The yellow area is the assumed plausibility area, which is derived especially from the predicted skin temperatures. The mild rise of resulting skin temperatures above a cooling intensity of $T_{eq,direct} = 12°\mathrm{C}$ seem plausible in respect of thermoregulation mechanisms and the observed skin temperatures without any cooling in hot environments. The steep decline below $T_{eq,direct} = 0°\mathrm{C}$ comprises a high uncertainty. Moreover, such cooling intensities are very unlikely to occur in a real vehicle DPC system.

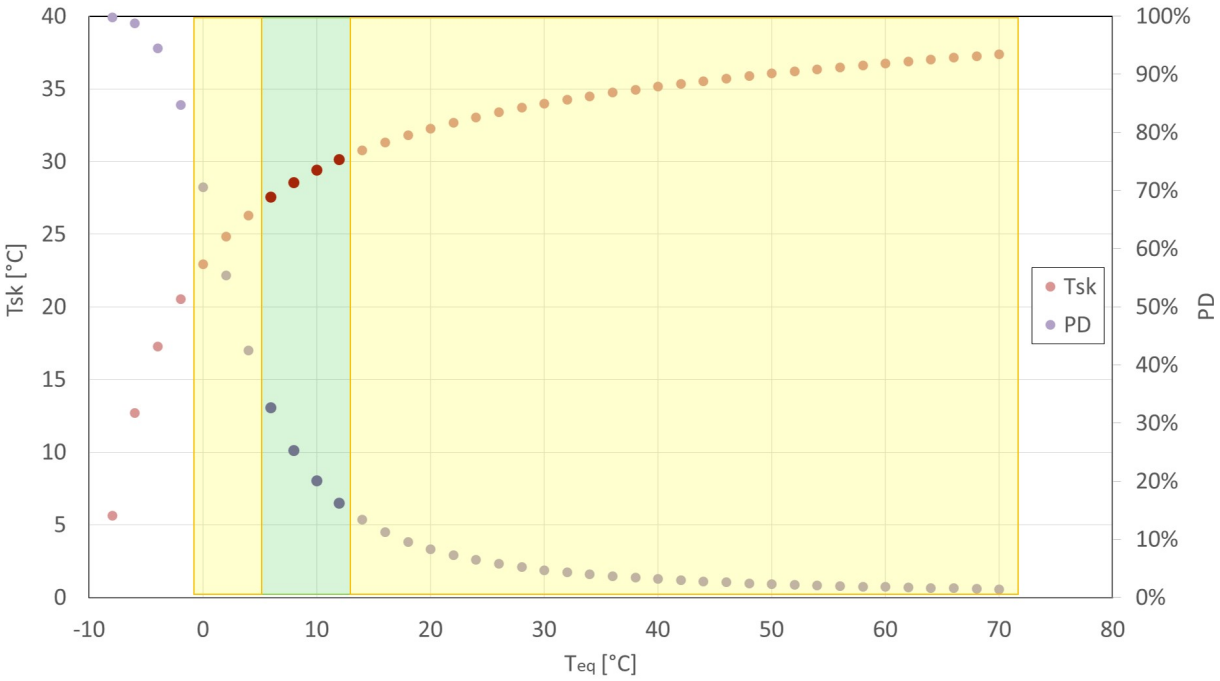

Figure 5.15: Plausibility limits of the prediction models for local skin temperature at the neck and the according $\mathrm{PD}_{\mathrm{cold}}$.

Test Scenario Simulation To study the models' behaviour under variable boundary conditions, as they occur during vehicle cool-down, I implemented them in a test simulation. The progression of local cooling intensity, represented by $T_{eq,direct}$ is designed as an extreme case with very quick increase of local cooling intensity. The corresponding skin temperature derivatives, though, do hardly exceed $0.02\frac{K}{s}$, which confirms the assumption that only low derivatives occur in a vehicle cool-down. The models' predictions of both skin temperature progression and $\mathrm{PD}_{\mathrm{cold}}$ throughout the simulation seems plausible. However, at the beginning of the simulated scenario, a drop in skin temperature can be observed, which is not plausible at conditions of 40°C. This phenomenon occurs when applying starting conditions below approximately 50°C and can be explained by the constitution of the $\frac{dT_{sk}}{dt}$ model. The model was developed only from data of local cooling between 6°C and 12°C equivalent temperature, which leads to uncertainties for higher and

lower cooling intensities and results in a levelling of the skin temperature at the beginning of the simulation. However, the model is robust enough to sufficiently converge during the first minute and skin temperatures adapt and stabalize.

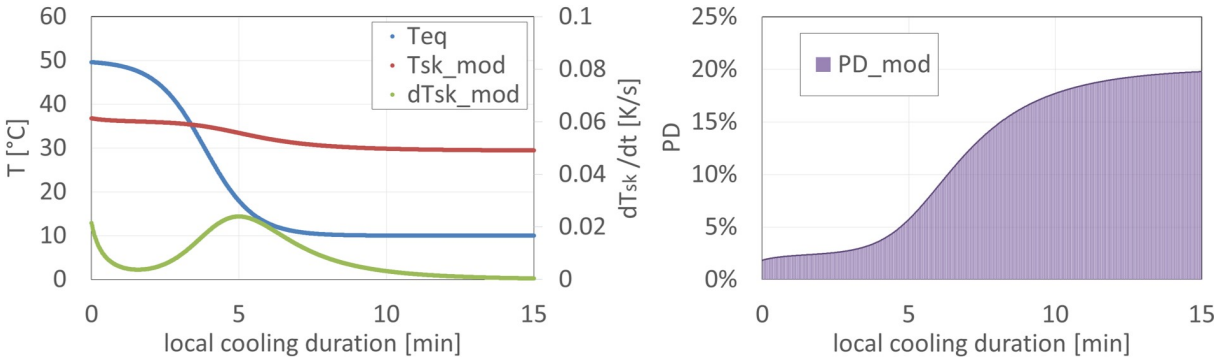

Figure 5.16: Simulation of a test scenario with variation of local cooling intensity at the neck over time.

5.2 Seat Cooling

One of the most promising DPC measures, which is already state of the art in vehicle climatization, is seat conditioning. Currently seat ventilation and seat cooling are optional extras and thus not part of the performance design of the climatization system. However, since seat conditioning is an effective measure for overall passenger conditioning, its future integration into the climate control system is very likely. To consider seat conditioning in the performance assessment procedure, the concept of TTT_i must thus be applied to seat conditioning as well. Since the basic argumentations and justifications are similar to the neck cooling study, statements are limited to descriptions. However, differences with regard to contact thermal impact and methodological improvements, based on learnings from the previous study, are explained in detail.

5.2.1 Theory

Different from the neck cooling, at body areas in contact with the seat, skin temperature cannot feasibly be measured. However, since contacting surfaces are expected to transfer heat immediately between each other a quasi-stationary heat exchange can be assumed. I hence expected the effect of seat cooling to be directly reflected in measured contact temperature, which is provided by the DressMAN system for contacting body segments. Thus, local thermal perception can be related directly to contact temperature T_c and no simulation of skin temperature evolvement is necessary:

$$\text{Research Hypothesis } H_{R,seat}: \qquad PD_{cold} = f(T_c) \tag{5.14}$$

5.2.2 Methods

This section gives a description of the methods used to investigate the relevant variables for TTT_{seat} (cushion) and TTT_{back} (backrest). There are two quantities to be examined for enabling hypothesis testing:

- Dependent Variable: PD_{cold}
- Independent Variables: T_c

Currently available conditioned vehicle seats do not yet have very strong conditioning power. To be able to violate tolerance thresholds and also control boundary conditions, a laboratory human subject study with a custom-developed seat cooling system was carried out.

Experimental Design The tests were conducted in two adjacent climate chambers at the Fraunhofer Institute for Building Physics IBP in Holzkirchen, Germany, in April 2019. One chamber served as an acclimatization room for preconditioning human subjects

to thermal neutrality and ensuring equal thermophysiological starting conditions. In the other chamber subjects were exposed to extreme surrounding conditions in terms of operative temperature and relative humidity with the intention of evoking heat strain. After spending sufficient time for experiencing overall warm discomfort, subjects were asked to sit down on a conditioned seat and rate overall and local thermal comfort. During the whole procedure contact temperature and heat flux between the seat and the subjects was measured.

Figure 5.17 illustrates the test setup. Overall conditions were realized by heating and humidifying the air and tempering the inner surfaces of the climate chamber. Seat and back cooling was realized by an especially designed test seat supplied by an external chiller and local blower.

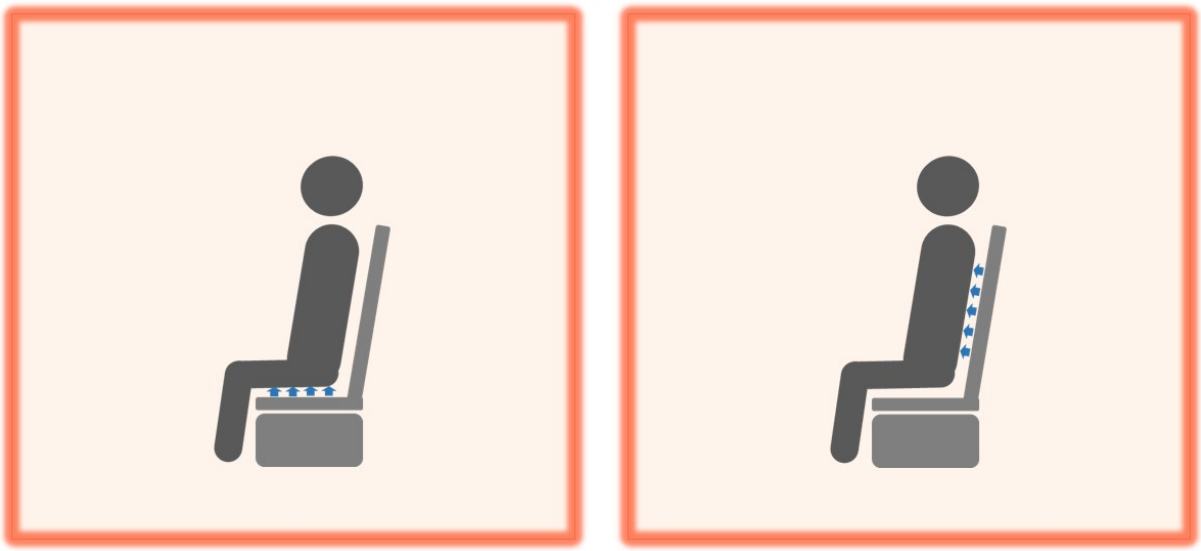

Figure 5.17: Illustration of the test setup for determining TTT_i for the seat (left) and the back (right)

Overall Conditions Like in the neck cooling study, two aims were pursued by the overall surrounding conditions: Induce overall thermal discomfort and trigger sweating. In the neck cooling study this was achieved by an operative temperature of 40°C and a relative humidity of 60%. During the neck cooling tests humidity control turned out to be unstable on such high levels of 60%. To ensure the two aims with a lower humidity of 40%, operative temperature was incresed to 45°C in all test scenarios.

Cooling Intensity Levels The cooling is realized by a combination of fluid chilled coils and cooled air, both provided at a perforated surface and supplied from an external chiller (see figure 5.20). The cooling intensity levels were set by varying supply fluid temperature and measuring surface temperature under steady state conditions ($T_{s,ss}$). Figure 5.18 shows the corresponding cooling intensities. All intensities were realized similar for seat and back, except the "Ref" intensity, which was only air ventialtion without cooling at the seat and no conditioning at all at the back, resulting in significantly different surface temperatures. The cooling intensity *m20cp* was only applied at the back as additional test scenario, since tolerance thresholds could not be violated at the lower intensities.

Intensity	Resulting surface temperature under steady state conditions (Seat)	Resulting surface temperature under steady state conditions (Back)
Ref	37.1°C	43.7°C
p20	32.4°C	31.9°C
0	28.5°C	27.8°C
m20	24.6°C	24.9°C
m20cp	-	17.9°C

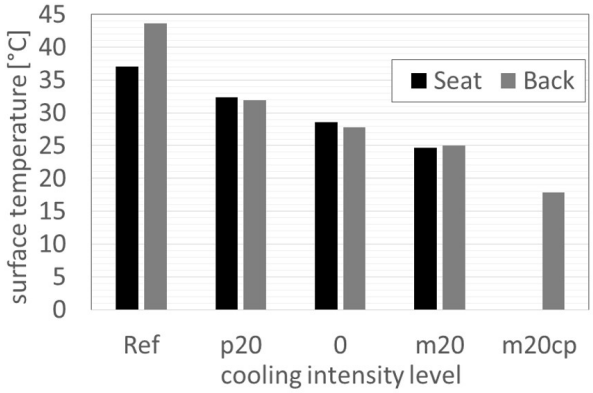

Figure 5.18: Designations of the cooling intensity levels and the resulting surface temperatures under steady state conditions $T_{s,ss}$.

Experimental Procedure Figure 5.19 illustrates the chronological procedure in each test. Subjects spent one hour before the test in neutral conditions. At the end of that period, they were questioned about their thermal state. Afterwards subjects spent 14 minutes in the hot environment, followed by a 15 minute period of local cooling, while remaining in the hot environment.

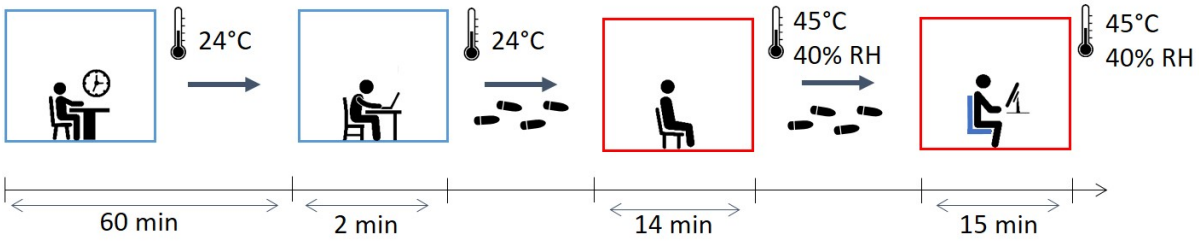

Figure 5.19: Experimental procedure of the seat cooling study.

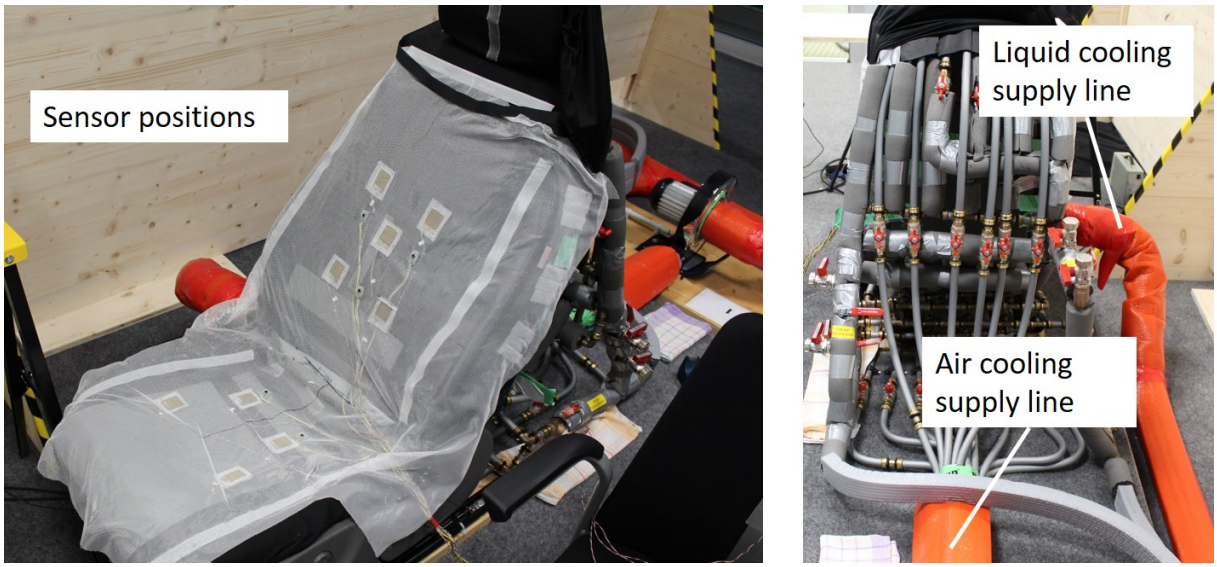

Figure 5.20: Test setup of the seat cooling study.

The same procedure was conducted for both seat cooling and back cooling at all intensity levels, as defined in figure 5.18. To avoid a bias from circadian rythm the sequence of cooling intensities was randomized for each subject.

Measurements In figure 5.20 pictures of the test setup show the prepared car seat with distribution of sensor positions. Contact temperature and heat flux were measured using *FluxTeq PHFS01* sensors.

Subjects and Questionaire A total of 17 German subjects, 8 male and 9 female, participated in the experiment at all intensity levels. The subjects had a normal range of BMI and were between 19 and 57 years old. The clothing ensemble was similar to the neck cooling study, with a clo value of 0.6. Thermal perception was captured in 30 second steps, beginning with the start of the local cooling. The subjects were questioned visually via screen survey, supported by read out questions over headphones. Their response was given via mouse click on the screen. Figure 5.21 shows an example of a subject being questioned.

Figure 5.21: Human subject completing the questionnaire in the seat cooling study.

During the neck cooling study, some subjects had difficulties to decide between the votes "just right" and "too intense". Therefore a preference rating scale was chosen (see table 5.5), giving the subjects the opportunity for a more differenciated evaluation. To monitor subjects' overall thermal state, the ASHRAE scale was used (see table 5.4).

Table 5.4: OTS scale used in the seat cooling study

OTS	value
hot	3
warm	2
slightly warm	1
neutral	0
slightly cool	-1
cool	-2
cold	-3

Table 5.5: local cooling preference scale used in the seat study

LTC	value
much warmer	3
warmer	2
slightly warmer	1
no change	0
slightly cooler	-1
cooler	-2
much cooler	-3

5.2.3 Results

This section gives a descriptive analysis of the investigated quantities of the seat cooling study. For all variables conclusions are drawn regarding their course over cooling duration time. Contact temperature measurements are analysed with respect to the different cooling intensites. The percentage of dissatisfied is analysed in comparison with the contact temperature course.

Contact Temperature Figure 5.22 shows the progression of the mean local contact temperature for seat and back, averaged over all subjects for each cooling intensity. Compared to the skin temperature progression at the neck cooling, contact temperatures show relatively low differences between the beginning and the end of the local cooling. However, the stronger the cooling intensity, the higher the gradients.

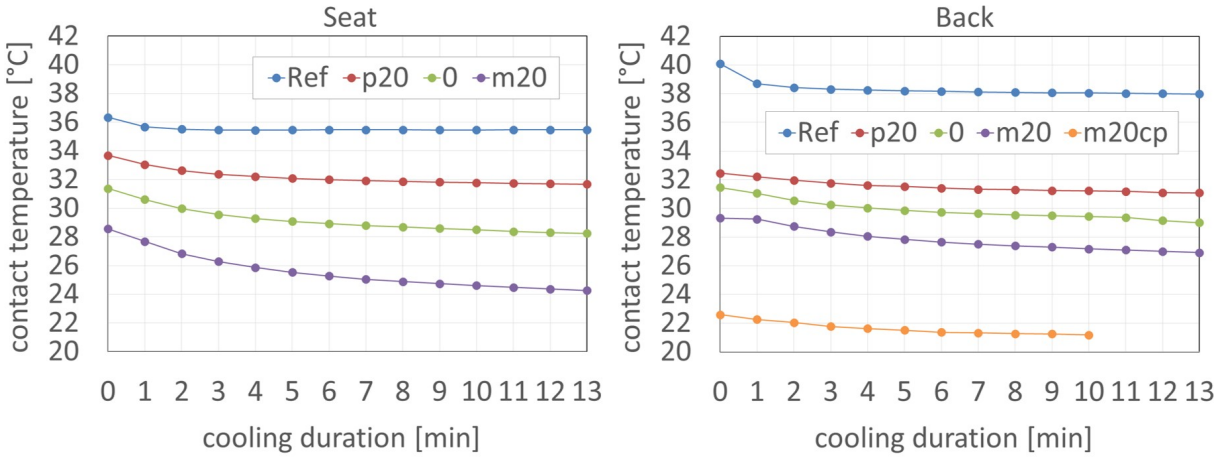

Figure 5.22: Contact temperature progression over cooling duration time, for seat (left) and back (right) at different cooling intensities.

For the seat cooling, a clear separation of T_c courses between different cooling intensities can be observed. At the back, this separation is less significant. A possible reason for this difference can be found in the behaviour of the human subjects. Although they were told to lean well on the backrest, a slight tendency to straightening during the cooling

phase could sometimes be observed. Since sensors were attached to the backrest, the measurements are influenced by the surrounding air, when the contact between person and backrest is light. However, such behaviour is considered as representative for the seating position in a real passenger car and the cooling intensity must be evaluated according to such realistic vehicular requirements.

Percentage of Dissatisfied Ratings from "slightly warmer" upwards (1 to 3) on the preference scale were interpreted as adjustment desire towards lower cooling intensity and hence a violated tolerance threshold. Thus, for each time step the percentage of votings above 0 was calculated and defined as the percentage of dissatisfied with the local cooling (PD_{cold}). Figure 5.23 shows the course of PD_{cold} over the cooling duration time for each intensity level.

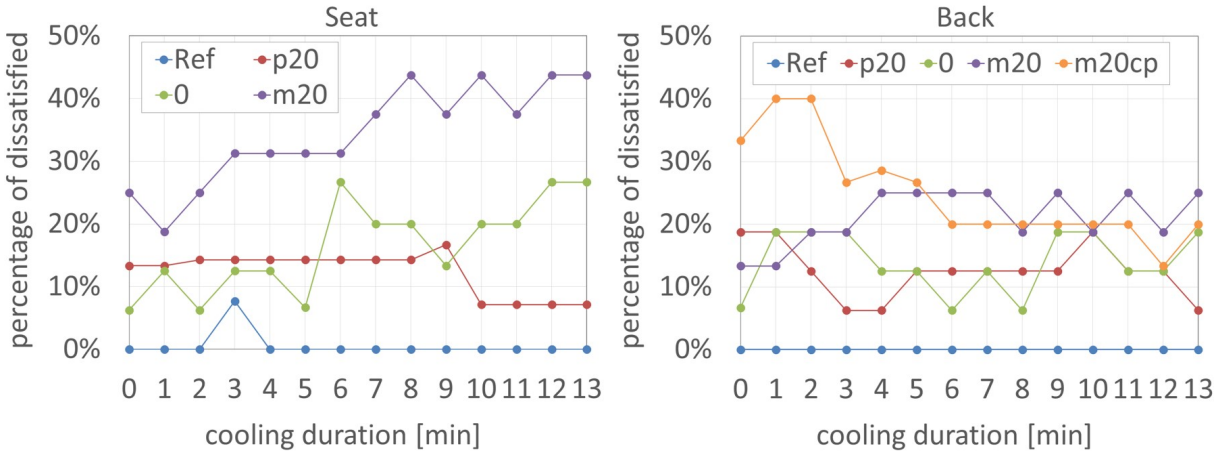

Figure 5.23: Progression of PD_{cold} over cooling duration time for seat (left) and back (right) at different cooling intensities.

The course of PD_{cold} rises over cooling duration time at high cooling intensities. The same is true for back cooling, however, with lower significance. At intensity *p20* PD_{cold} seems to result in approximately 10% over the entire cooling duration, for both body areas. The reference test, without active cooling, results in a constant PD_{cold} of zero, as would be expected. Generally can be concluded that PD_{cold} courses of seat cooling show a relatively clear separation from each other, while back cooling courses are rather close to one another, which fits with the contact temperature courses. High PD_{cold} occur at low T_c and vice versa, which suggests a relation between the two, as assumed.

5.2.4 Thermal Perception Model Comparison

The results of the seat study have also been compared to the predictions of the Zhang/Fiala approach and the Nilsson comfort zones.

Methods For the application of the thermal comfort models, the same procedure as described in section 5.1.4 for the neck model was applied. To investigate the validity of

the Nilsson model for contact, the Contact Equivalent Temperature (CET) was calculated from the measured contact temperature and heat flux, as defined in equation 4.7 of section 4.1.1 (see figure 5.24). The calculated $T_{eq,contact}$ have been applied to the local comfort zones for seat and back of the Nilsson model. The boundary between "cold but comfortable" and "too cold" is at 15.3°C for both, back and seat in the Nilsson model. The rating was interpreted according to the argumentation for PD_{cold} adapted to the preference scale of the experiment:

$$LTC = \begin{cases} 1 & \text{for} \quad LTC_{vote} < 0 \quad \text{(not intense enough)} \\ 2 & \text{for} \quad LTC_{vote} = 0 \quad \text{(just right)} \\ 3 & \text{for} \quad LTC_{vote} > 0 \quad \text{(too intense)} \end{cases}$$

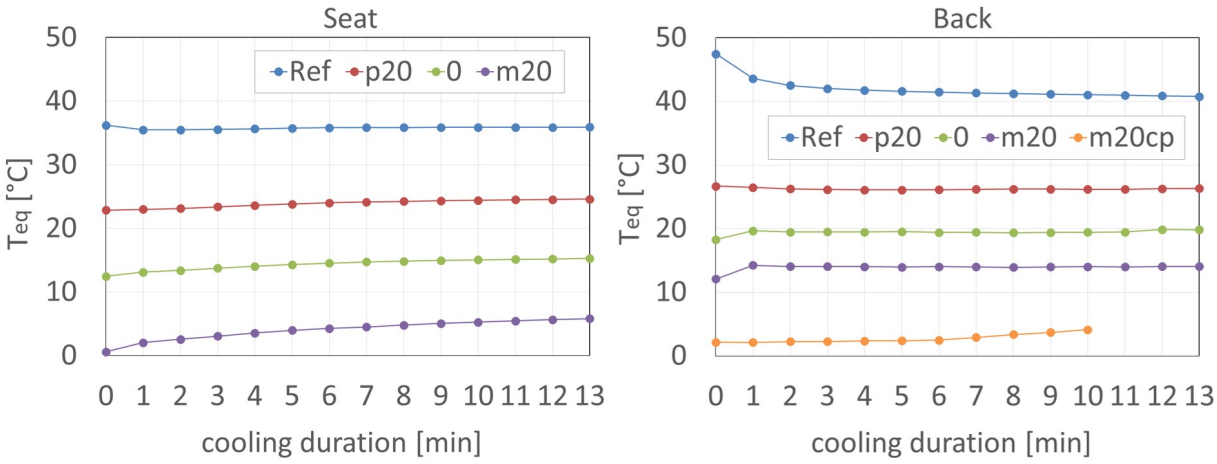

Figure 5.24: Contact equivalent temperature progression over cooling duration time, for seat (left) and back (right) at different cooling intensities.

Results Figures 5.25 and 5.26 show the results of the comparison for the cooling intensity *m20*. The predictions of the Fiala model differ widely from the actually measured mean contact temperatures.

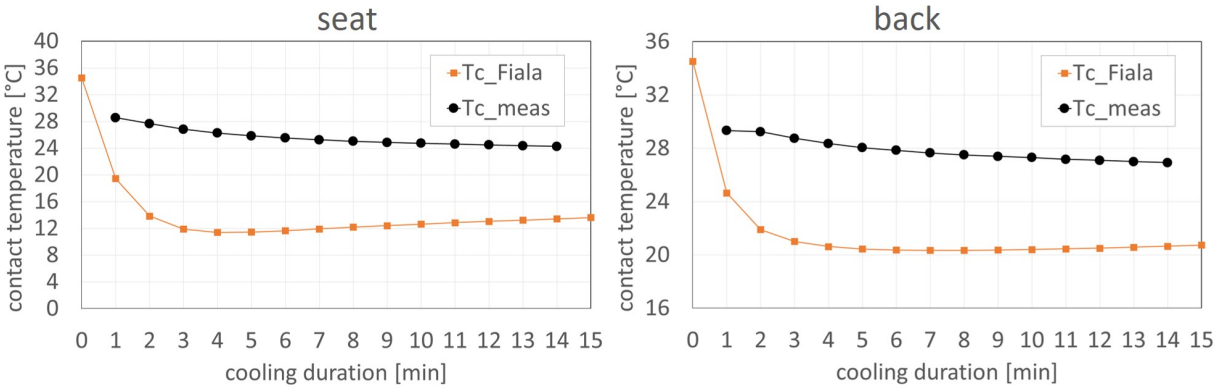

Figure 5.25: Comparison of the contact temperature measurements with the Fiala model predictions for for the cooling intensity *m20*.

Accordingly, the Zhang predictions fail significantly in their LTC predictions. The prediction accuracy of the Nilsson model can be evaluated similarly. It assesses the cooling intensity for both seat and back as "too intense" over the entire cooling duration, although subjects' actual mean vote is "not intense enough". In summary, both potential models for LTC prediction fail in the applied procedure of using them in combination with the DressMAN measurements and the intorduced adaptation models.

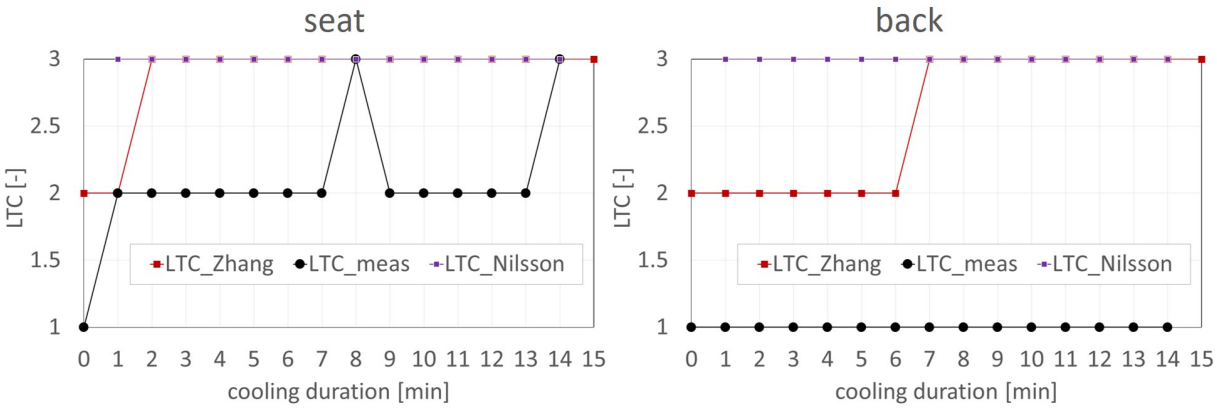

Figure 5.26: Comparison of the local thermal comfort evolvement with the Zhang/Fiala and Nilsson predictions, according to a thermal perception scale with (1) not intense enough, (2) just right and (3) too intense.

5.2.5 Model Development

Following the same principle as introduced for the neck cooling PD_{cold} shall be derived from the DressMAN system. Since the current method uses contact temperature measurements between an average sized man and the seat, PD_{cold} is modeled from T_c.

Modeling the Percentage of Dissatisfied For determining PD_{cold} at a certain local contact temperature, I clustered the T_c data in steps of 0.5 Kelvin. Since some contact temperatures occur more often than others, for a statistically representative result, I only considered samples of at least 10 values. Using this method I could find a proper logistic fitting function for the seat data. However, since dispersion is very broad for the back area, there was no reliable function slope for the corresponding regression. I therefore applied another modeling method averaging the T_c data over all subjects for each time step at each cooling intensity. With this averaged data, I was able to find reasonable coefficients for the regression functions in comparison of the two methods. Figures 5.27 and 5.28 show the calculated PD_{cold} from subjects' responses and the fitted logistic regression function. In the following the two different modeling approaches are described.

Clustering over defined contact temperature ranges

1. Defining data clusters for all occuring contact temperatures in the entire data set $T_{c,i}$ - $T_{c,j}$ in ranges of 0.5 K ($T_{c,(i-0.25K)}$ to $T_{c,(i+0.25K)}$)
2. Calculating the total number of votings ($v(T_{c,i})$) and the number of votings "too intense" ($v(T_{c,i}) > 0$) for each temperature range
3. Relating $v(T_{c,i}) > 0$ to $v(T_{c,i})$ to get $PD_{cold}(T_{c,i})$ in each cluster
4. Relating $PD_{cold}(T_{c,i})$ to the clusters $T_{c,i}$

Averaging over subjects at each cooling intensity

1. Calculating the mean contact temperature at each time step for each cooling intensity (see figure 5.22)
2. Calculating the percentage of dissatisfied at each time step for each cooling intensity (see figure 5.23)
3. Relating PD_{cold} to T_c at each time step for each cooling intensity

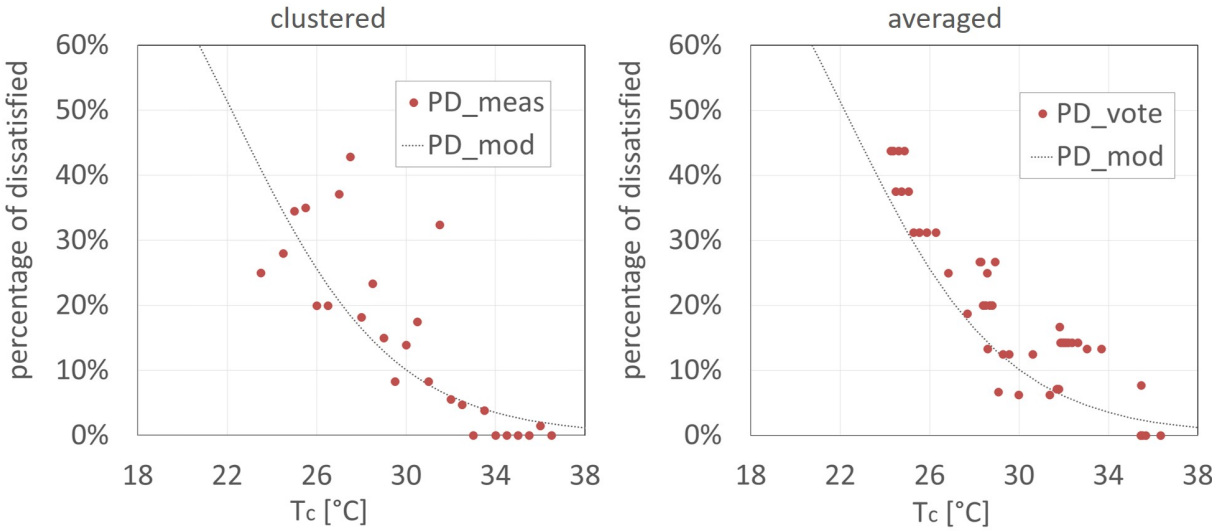

Figure 5.27: $PD_{cold,seat}$ over T_c and logistic prediction function, for clustered data (left) and averaged data (right).

$$PD_{cold,seat} = \frac{1}{1 + a_s * e^{(b_s * T_c)}} \qquad (5.15)$$

$$PD_{cold,back} = \frac{1}{1 + a_b * e^{(b_b * T_c)}} \qquad (5.16)$$

a_s	b_s
0.002	0.28

a_b	b_b
0.1	0.15

Figure 5.28 shows the broad dispersion of PD_{cold} for tha back data. A potential reason for this dispersion is the behviour of the human subjects as described above. Some subjects

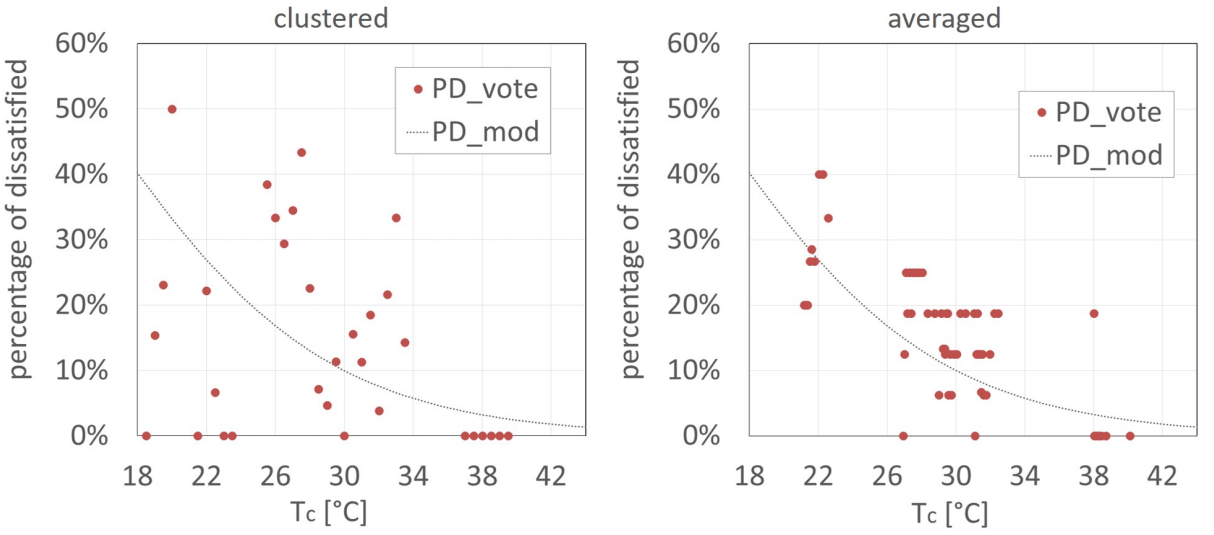

Figure 5.28: $PD_{cold,back}$ over T_c and logistic prediction function, for clustered data (left) and averaged data (right).

had lighter pressure on and less contact to the backrest than others. Since T_c was measured at the surface of the backrest, some T_c values are stronger influenced by the subjects' body temperature than others, while also the cooling impact on the subjects varies with regard to their sitting posture.

5.2.6 Model Evaluation

Goodness of Fit In contrast to the neck cooling model, the seat cooling models relate PD_{cold} directly to T_c. The corresponding GOF is thus represented by the Root Mean Square Error (RMSE) instead of the Root Mean Square Deviation (RMSD), as described in section 4.1.3. The resulting regression functions from a least squares regression analysis did not seem to represent an appropriate model for both clustered and averaged data. I therefore adjusted the coefficients by minimalizing RMSE for both data sets, which naturally results in an MBE unequal to zero. Table 5.6 presents the corresponding measures for both methods, *clustered* and *averaged*.

Table 5.6: MBE and RMSE for the regression of PD_{cold} over contact temperature.

data set	MBE for seat	RMSE for seat	MBE for back	RMSE for back
clustered	−1.8%	9.5%	−0.7%	18.1%
averaged	−3.6%	6.3%	−2.4%	7.1%

Plausibility To evaluate the prediction quality of the PD_{cold} models I simulated the same boundary conditions as used in the subject study and compared MBE and RMSD at each cooling intensity. Figure 5.29 shows the comparison of the calcualted PD_{cold} from subjects' responses and the models' predictions for the example of the cooling intensity 'm20'. Table 5.7 presents the accuracy measures for all cooling intensities.

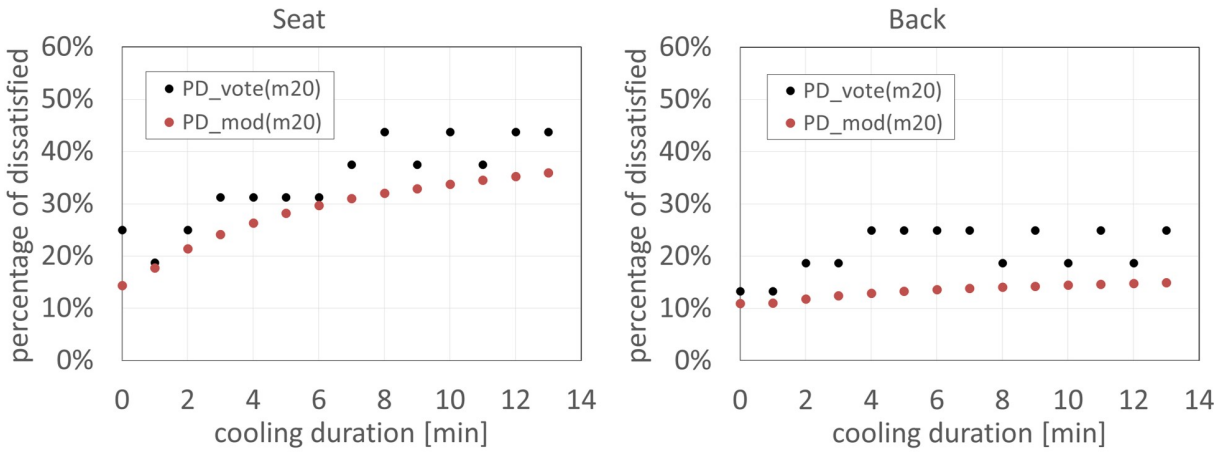

Figure 5.29: Progression of subjects' PD_{cold} and the models' prediction over cooling duration time for the cooling intensity *m20*, for seat (left) and back (right).

Table 5.7: MBE and RMSD for the perdiction of PD_{cold} from T_c for seat cooling.

Cooling Intensity	MBE for $PD_{cold,seat}$	RMSD for $PD_{cold,seat}$	MBE for $PD_{cold,back}$	RMSD for $PD_{cold,back}$
Ref	+1.8%	2.7%	+3.1%	3.1%
p20	−6.5%	7.5%	−2.5%	5.0%
0	−3.7%	6.7%	−3.7%	6.1%
m20	−6.0%	6.8%	−7.7%	8.5%
m20cp	-	-	+1.2%	2.7%

As can be seen from table 5.7 the deviations of the models' predictions from the subjects' responses is relatively high. However, the high RMSDs are mainly due to the high fluctuations of subjects' assessment over time.

5.3 Defining Local Cooling Thresholds

To use the results of the local cooling studies in climatization effectiveness assessment, Local Thermal Tolerance Thresholds (TTT_i) need to be defined. That is, a certain percentage of dissatisfied with local cooling intensity is to be accepted in favour of effectively compensating overall heat load. However, there is no scientifically substantiated basis for decision-making. Fanger found the lowest percentage of dissatisfied with overall conditions to be 5% [18], which was questioned by Mayer, who considers 15% as the lowest achievable percentage of dissatisfied [38]. However, this minimum is caused by people's different perception of the overall thermal environment. Some people experience a certain temperature a bit too warm, while others perceive the same temperature as a bit too cool, although it is neutral for the majority. In the case of tolerance thresholds the approach is a little different. As can be seen from the PD_{cold} models in section 5.2.5, there in fact occur PD_{cold} of 0%. This is due to the definition of PD_{cold}. Only dissatisfaction with local cooling is considered, not dissatisfaction due to local warmth. Hence, when there is no

local cooling at all, there can be no satisfaction with it. The subject is thus very similar to Nilssons definition of his comfort zones (see section 2.4.3). For the boundaries of these zones, he had to decide for which percentage of people the zones shall be comfortable. He defined it at 80%, however, in his argumentation there is no scientific justification for that [39]. Nevertheless, high local PD_{cold} allow lower local equivalent temperatures and hence utilizing more cooling capacity for the entire body. With regard to the S-shape of the regression function for PD_{cold}, the range of equivalent temperatures for very low PD_{cold} is relatively high. The lower the local temperature the steeper the prediction function for PD_{cold}. That means, the ambition to have only 5% dissatisfied people with local cooling is accompanied by a considerable compromise in overall cooling effectiveness and hence higher overall warm discomfort. Thus, TTT_i should be defined at a rather high PD_{cold}. As will be explained in the Conclusion chapter, I consider the TTT_i a complement to the established evaluation method of ISO 14505-2 incorporating the Nilsson model for steady-state conditions. To achieve consistency in the assessment methodology, I define TTT_i here also at $PD_{cold} = 20\%$.

5.3.1 Tolerance Thresholds for the Neck

To define a specific local cooling threshold for the neck, I studied the behaviour of the derived prediction models in simulations of realisitc cool-down conditions. Simulating various cooling intensity courses over time, there are different moments in time, when TTT_{neck} is violated. The according time step is labled here $t_{TTT,neck}$ which is reached as soon as PD_{cold} rises above the defined 20%. Since the skin temperature and PD_{cold} model combination is complex and derived from a narrow range of cooling intensities, I compared the determination of $t_{TTT,neck}$ by the complex model with a much simpler approach:

In real vehicle cool-down situations, local cooling intensity increases only slowly and hence a quasi-stationary condition between local cooling and local skin temperature can establish. Figure 5.30 shows the percentage of dissatisfied, averaged over cooling duration. The red bars represent PD_{cold} over the entire cooling duration. Since at the beginning of local cooling, there are high skin temperature derivatives and according local sensation envolved, I also included the average of PD_{cold} between 5 and 15 minutes of local cooling duration in the figure (blue bars). However, the tendency is the same. When defining TTT_i at $PD_{cold} = 20\%$, local cooling below $T_{eq,direct} = 8°C$ is to be avoided. With this definition $t_{TTT,neck}$ can be determined by monitoring $T_{eq,direct}$ directly.

I tested both the complex model and the simple method, simulating a broad range of local cooling scenarios and comparing the obtained $t_{TTT,neck}$ (see figure 5.31). The mean deviation between the two approaches is 62 seconds or 7% of the simulated cooling duration of 15 minutes. This seem to be a low difference and therefore favours the simple approach for application. However, the complex approach ultimately allows for slightly longer operation of high cooling intensity, which may have a significant benefit for the overall passenger conditioning and thus thermal comfort. For current, rather slowly responding air conditioning it might be advisable to apply the simple approach, since it is less prone to errors and is expected to be more reliable in boundary conditions not covered by the investigations of this dissertation.

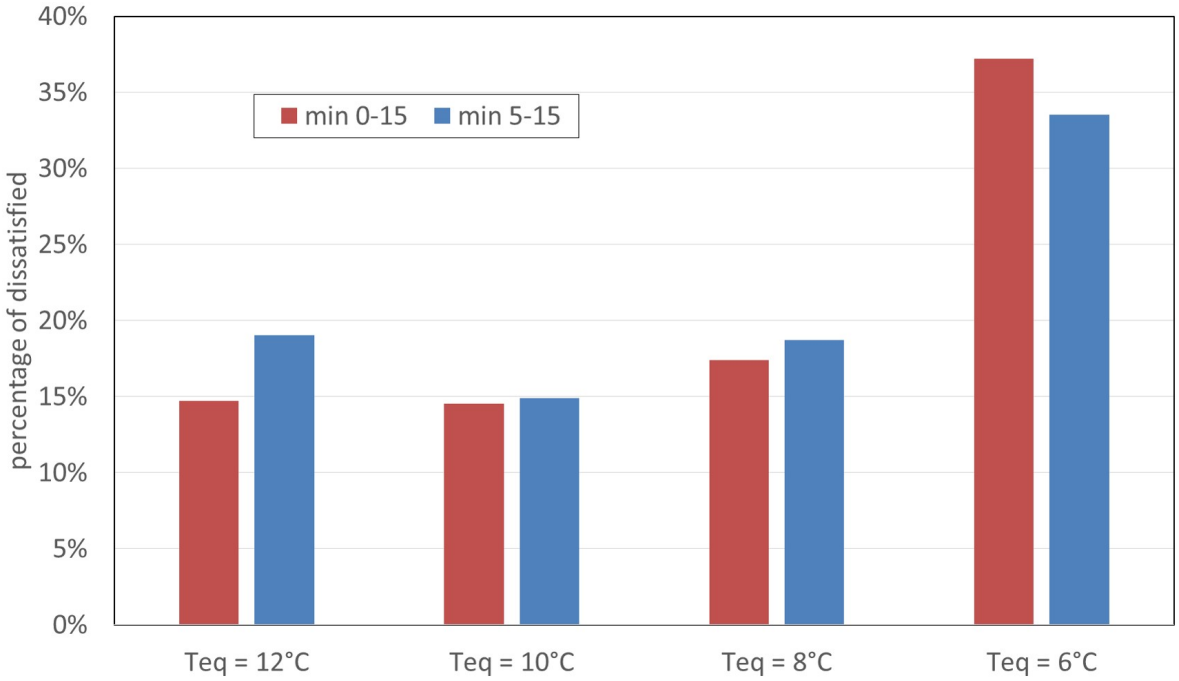

Figure 5.30: Mean PD_{cold} of the neck area for each tested cooling intensity (represented by $T_{eq,direct}$) averaged over the entire cooling duration (blue) and averaged over minute 5 to 10 (red).

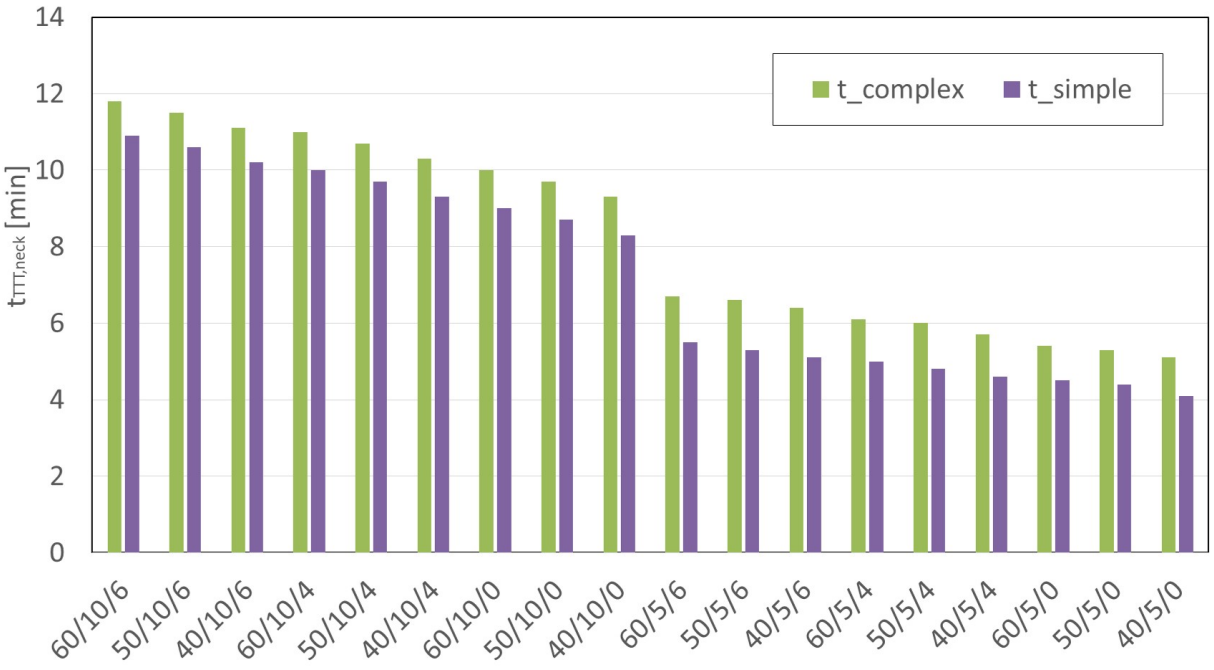

Figure 5.31: Comparison of $t_{TTT,neck}$ for the simple and the complex method, simulating different local cooling scenarios.

The cooling tolerance threshold with regard to local equivalent temperature can thus be defined as follows:

$$TTT_{neck} : T_{eq,direct} = 8°C \tag{5.17}$$

Since the local air flow at neck distance fluctuated slightly, the measured $T_{eq,direct}$ varied by approximately 0.4 Kelvin at each cooling intensity; thus specifying TTT_i to another digit is not useful.

5.3.2 Tolerance Thresholds for Seat and Back

For seat cooling, tolerance thresholds can be defined using the PD_{cold} models directly. By transforming the regression functions in equations 5.15 and 5.16 for calculating T_c and defining thresholds at $PD_{cold} = 20\%$, we get:

$$T_c(PD_{cold}) = LN\left(\frac{PD_{cold}^{-1} - 1}{a}\right) \cdot \frac{1}{b}$$

The averaged and clustered T_c data includes relatively high high dispersion in parts, as described above. TTT_i are therefore also specified without decimal place for the contact body areas.

$$TTT_{seat} : T_c = 27°C \tag{5.18}$$

$$TTT_{back} : T_c = 25°C \tag{5.19}$$

However, future generations of the DressMAN system are expected to incorporate a sensor for objective cooling intensity evaluation and thresholds are to be determined from those measurements. I suggest to employ the concept of Contact Equivalent Temperature (CET), introduced in this dissertation for objective measurement of thermal impact from contact surfaces. Since the relation between $T_{eq,contact}$ and T_c is quasi-stationary, PD_{cold} can also be directly related to $T_{eq,contact}$. I calculated $T_{eq,contact}$ from T_c and $\dot{q}_{env,c}$ using equation 4.7 in section 4.1.1. Figure 5.32 shows the corresponding graphs for seat and back and the averaged PD_{cold}. The logistic regression functions are shown in equation 5.20 and 5.21. Table 5.8 gives the indicators for their prediction quality.

$$PD_{cold,seat} = \frac{1}{1 + a_s \cdot e^{(b_s \cdot T_{eq})}} \tag{5.20}$$

$$PD_{cold,back} = \frac{1}{1 + a_b \cdot e^{(b_b \cdot T_{eq})}} \tag{5.21}$$

a_s	b_s
1.05	0.102

a_b	b_b
1.8	0.07

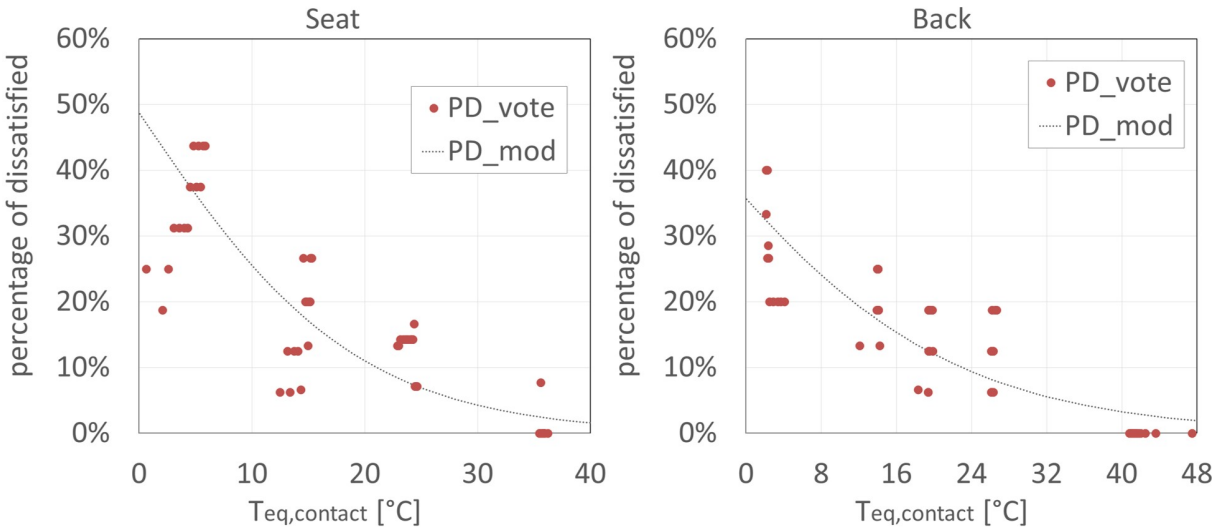

Figure 5.32: PD_{cold} over T_{eq} and logistic regression function for seat (left) and back (right).

Table 5.8: MBE and RMSE for the regression of PD_{cold} from $T_{eq,contact}$.

data set	MBE for seat	RMSE for seat	MBE for back	RMSE for back
clustered	−2.0%	13.4%	−2.7%	19.3%
averaged	+0.6%	7.9%	−0.3%	5.8%

When using these regression functions for PD_{cold} prediction and considering 20% as the acceptable percentage of dissatisfied, the following tolerance thresholds can be defined with regard to CET:

$$TTT_{seat} : T_{eq,contact} = 13°C \qquad (5.22) \qquad TTT_{back} : T_{eq,contact} = 11°C \qquad (5.23)$$

Chapter 6

Conclusion and Future Work

This chapter presents suggestions for practical applications of the findings of this dissertation. It critically reflects on such application with regard to the scientific methods employed and makes recommendations for further research.

6.1 Practical Application

To employ the results of this dissertation in evaluating vehicular climatization, a distinction is made between (1) Vehicular Climatization Effectiveness Assessment and (2) Early-stage DPC Evaluation.

6.1.1 Vehicular Climatization Effectiveness Assessment

To assess climatization systems already implemented in vehicles, two features need to be distinguished, as introduced in section 2.1: Climate Control Quality (CCQ) and Climatization Performance (CP). CCQ denotes the ability to maintain passengers at thermal neutrality during steady state conditions, regardless of exterior climate conditions and short term fluctuations. CCQ can be assessed using the Nilsson model [39] or ISO 14505-2 [9]. CP denotes the ability to generate thermal neutrality for passengers from extreme thermal discomfort conditions (during cool-down or heat-up). CP can be assessed for central HVAC using the method of DIN 1946-3. The findings of this dissertation allow to adapt the CP assessment procedure of DIN 1946-3 to equivalent temperature measurements and combine it with the CCQ evaluation methods of ISO 14505-2 to one universal approach for assessing vehicular climatization effectiveness, applicable to both DPC *and* central HVAC.

Adapting the approach of Park et al. [44] I suggest to generalize the target air temperature in DIN 1946-3 to *Thermal Neutrality*. The results of the vehicle cool-down study showed that the prediction accuracy of all investigated thermal perception models is high near thermal neutrality and hence any of the models could be used with the DressMAN system. Since the Nilsson model is already used for CCQ evaluation, target values for overall conditions in summer and winter should also be defined according to Nilsson's comfort zone for the whole body. Thus, I suggest largely adopting the DIN 1946-3 procedure and replacing the target value *Air Temperature (T_a)* with *Equivalent Temperature for the whole body ($T_{eq,whole}$)*. As an additional requirement, I propose the unconditional compliance with local tolerance thresholds. Table 6.1 provides the corresponding definitions of boundary conditions and requirements adapted from [8].

Table 6.1: Adaptation of the boundary conditions and target values for cool-down and heat-up tests of DIN 1946-3 (adapted from [8]).

Condition	cooling mode	heating mode
passive conditioning target	$T_{cabin} = T_{env}$ + 60 min solar radiation	$T_{cabin} = T_{env}$
driving speed	$32\frac{km}{h}$ (20 mph)	$32\frac{km}{h}$ (20 mph)
outside air temperature	$40°C$	$-20°C$
solar irradiation	$1'000\frac{W}{m^2}$	-
air humidity	40%	-
equivalent temperature of the whole body after 30 min of active DPC	$T_{eq,whole} < 26°C$	$T_{eq,whole} > 21°C$
Local Thermal Tolerance Thresholds	$PD < 20\%$	$PD < 20\%$

When using the static tolerance thresholds defined in section 5.3 in the form of local equivalent temperatures ($T_{eq,direct}$ and $T_{eq,contact}$), the Nilsson diagram can be extended with cooling thresholds and thus used for the entire evaluation procedure of both CP and CCQ. Figure 6.1 illustrates the principle by marking the thresholds in the thermal comfort diagram.

The solid light blue line marks the thresholds I obtained from my experiments and the dotted light blue line suggests any unknown local tolerance thresholds for other body areas not yet investigated. The thresholds for the neck area are applied to the scalp and chest, since the neck was chosen as the most critical area in the head region. However, to obtain potentially lower tolerable temperatures and thus higher cooling capacity, further experiments are necessary. The diagram in figure 6.1 can be read as follows: During vehicle cool-down, local cooling intensity must not fall below the local equivalent temperatures for thermal tolerance thresholds, marked by the light blue line. As soon as steady-state conditions are reached, local equivalent temperatures should not occur outside the zones "cold but comfortable", "neutral" and "warm but comfortable".

The responsiveness of the climatization system is also relevant for passengers' overall satisfaction but not necessarily reflected in the *Time to Equivalent Temperature*. Since only the Park model can reliably quantify the deviations from thermal neutrality after a certain conditioning duration, it can be integrated in the procedure to assess CP during the entire cool-down or heat-up, e.g. after 1 minute, 5 minutes, 10 minutes and 20 minutes.

Since all the suggested models use equivalent temperature as input variable, the DressMAN measurements (model input) can be used to assess the effectiveness of the climatization as a whole. In this respect, using a common assessment quantity (model output) appears appropriate as well. Equivalent temperature can be considered "perceived temperature" and is therefore a more tangible quantity than Thermal Load. I therefore recommend mathematically converting Park's thermal perception model to a function of $T_{eq,whole}$ instead of $\dot{q}_{TL,dr}$.

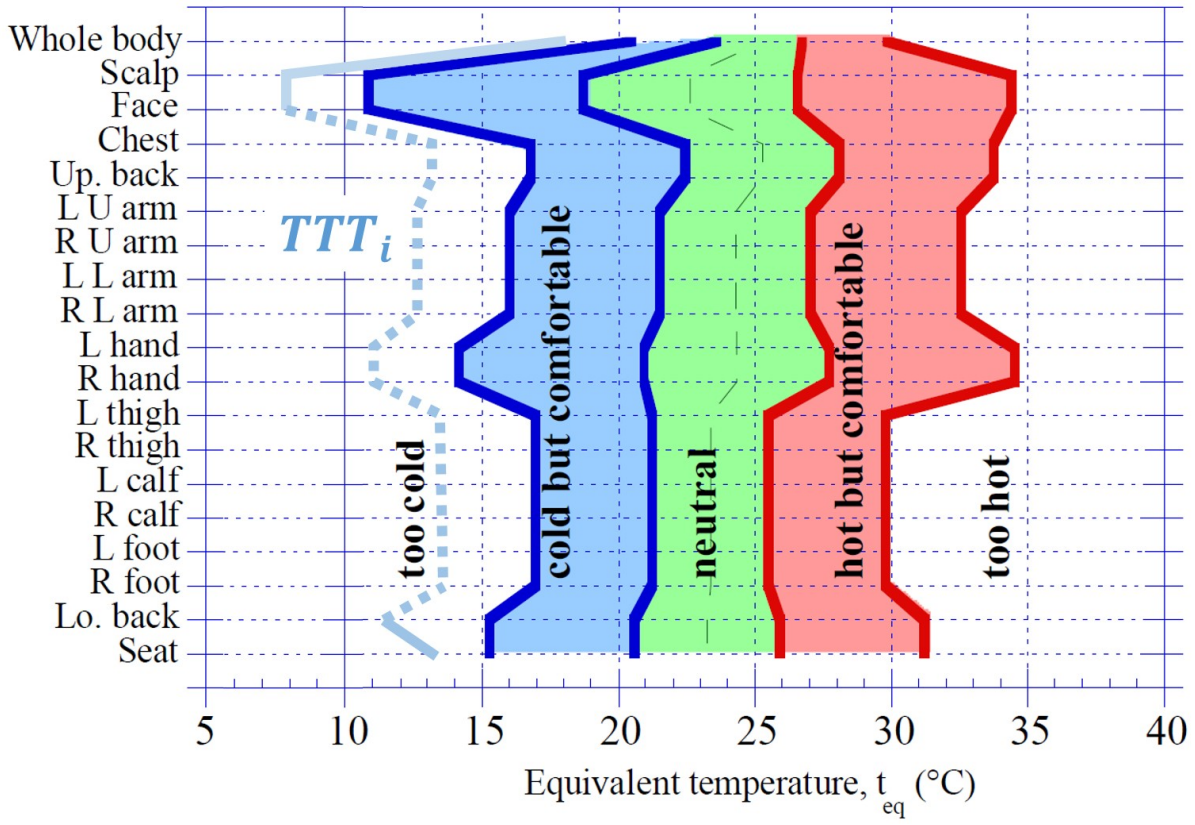

Figure 6.1: Extension of Nilsson's comfort zones with thresholds for local cooling during vehicle cool-down (adapted from [39]).

6.1.2 Early-stage DPC Evaluation

Apart from assessing climatization systems already implemented in vehicles, I suggest also employing thermal perception models in early stage designs of new climatization technologies and concepts. For this purpose a complementary approach of simulation-based and measurement-based evaluations is useful. Effects on passengers of newly designed DPC measures can be quantified by modeling and adapting these measures in thermal simulation environments incorporating the thermophysiological model of Fiala [19] and the thermal perception models of both Fiala [19] and Zhang [65]. The effects of individual measures can thus be estimated virtually and, if necessary, alternatives can be compared, providing a basis for early decision-making in the development of effective climatization measures.

To evaluate first prototypes, local equivalent temperatures can be measured for tolerance thresholds to be considered already in an early stage. In the next stage of first mockups of the entire climatization concept, the DressMAN system can be employed to measure climate impact, and the Park model [44, 41] combined with the TTT_i can be employed for interactively evaluating adjustments of local measures.

6.2 Critical Reflection

This section critically examines the knowledge gained from the research carried out and points out limitations with regard to their practical application.

6.2.1 Reflecting on the Evaluation of Multiple Thermal Perception Models

In chapter 4 the prediction accuracy of different thermal perception models employed with the DressMAN system were studied. Since these thermal perception models were originally designed for other purposes, the results and conclusions drawn may not necessarily refer to the accuracy of the models per se, but their accuracy in a very specific application in combination with the DressMAN system, the introduced adaptation models and the method of scale norming. There are a number of other ways to apply these thermal perception models using different climate measurements and adaptation models. The statements made in this dissertation regarding prediction accuracy should therefore only be understood in the context of the outlined theory in section 4.1.

After completing the vehicle cool-down study, a problem with the equivalent temperature sensors used was discovered, which apparently led to a systematic error in the measurements. As introduced in section 2.4.2, directed equivalent temperature is calculated from a measured dry heat flux of a heated surface. However, the quantity measured by the sensor is a thermoelectric voltage from which the heat flow is derived using an interpretation model. A new manufacturing method for the sensors caused a design flaw which led to a misinterpretation of the thermoelectric voltage, underestimating the heat flux at high radiation intensities. The $T_{eq,direct}$ is hence too low at such high radiation intensities, especially when the sensor is exposed to direct solar irradiation. In the vehicle cool-down study, this was the case for the sensor positions at arms and upper legs, leading to potential errors of $4.0K$ at the left arm and $2.5K$ at the right arm and the upper legs. These errors may influence the evaluations of the LTC models of Zhang and Nilsson for these body areas, which, however, were not decisive for the conclusions drawn. The $T_{eq,direct}$ errors also lead to a deviation in the integrated $T_{eq,whole}$, influencing the overall thermal perception predictions of all models investigated. The maximum error on $T_{eq,whole}$ that may be involved is $0.9K$, resulting in a prediction error in Fanger's PMV of 4.5% and in Park's OTS of 3%. The error for the Nilsson predictions can not be quantified the same way, since it uses a categorial evaluation. However, the direction of the $T_{eq,whole}$ deviation only supports the conclusions drawn with regard to its prediction accuracy. The error may result in a slight underestimation of the Fiala and Zhang prediction accuracy. Since this underestimation is considered low and these methods are in any case not suitable for DPC assessment due to feasibility requirements, the error is not relevant here. Regarding the comparison of the Park predictions for the LOW and the STRONG scenario, the error is not significant, although it tends to support the statements made regarding the research gap. In summary, the $T_{eq,direct}$ error does not appear to influence the conclusions drawn from the measurements in the vehicle cool-down study. However, a definitive conclusion can only be drawn by repeating the measurements under exactly the same conditions.

As reported in section 4.2, due to a technical problem, the relative humidity measurements were not recorded during the experiment and a substitute data set from a similar DPC study was used for RH. Since the Park model is sensitive to humidity the model's predictions might differ if the real humidity data were used. The LOW scenario was very similar to the scenario used for acquiring the substitute data, so I would not expect significant differences. The STRONG scenario has a much higher air exchange rate with cooled and thus dried air, which could lead to lower humidity than shown in the substitute data set. However, a sensitivity analysis with minimal air humidity assumed during the entire cool-down still leads to a significant lower accuracy of the Park predictions in the STRONG scenario compared to the LOW scenario [41].

6.2.2 Reflecting on the Local Thermal Tolerance Thresholds

The investigations of local cooling perception were conducted under laboratory conditions. Such conditions offer the advantage of keeping confounders low and boundary conditions stable, but are accompanied by the risk of a biased perception on the part of the subjects due to the artificial environment. That is, passengers' perceptions may be different in a real vehicular environment. The local thermal tolerance thresholds TTT_i were developed using isolated conditioning of local body areas to prevent a potential influence on local thermal perception from other sources than the investigated measure. In reality DPC tolerance thresholds might be different, if several segments are conditioned simultaneously.

Laboratory experiments are expensive to conduct and appropriate human subjects are hard to obtain. Therefore, the models developed and the state of the art models introduced are based on a relatively small amount of data. In the studies this fact is taken into account by selecting the subjects according to very narrowly defined attributes to still get statistical representative results. However, this narrow definition also leads to a narrow validity for the models with regard to certain social and ethnic groups. The models might therefore not reliably represent the thermal perception of people outside the groups investigated.

Apart from that, the developed PD_{cold} models contain a degree of uncertainty, mainly due to two reasons: (1) The dispersion of PD_{cold} was high, especially for back cooling, which results in a lower reliability of the model's predictions. (2) The models hwere developed on the basis of a relatively narrow range of independent variables, especially in the case of neck cooling. The models should therefore only be used in the range of the conditions studied and thresholds should be defined rather conservatively.

The high variance of PD_{cold} also speaks for a high subjectivity in local thermal perception. The evolvement of T_{sk} and T_c under local cooling is similarly very different from person to person. Hence, Local Thermal Comfort (LTC) is harder to generalize than Overall Thermal Perception (OTP) and the models should be used carefully in individually sensitive applications, such as climate control algorithms.

6.3 Further Investigations

The here developed models for local cooling thresholds prediction in cool-down situations, contribute to the state of the art of thermal environment evaluation methods and vehicular climatization effectiveness assessment. However, during my investigations I encountered a number of open research questions, which will be discussed in the following.

6.3.1 Tolerance Thresholds of other Body Areas

For comprehensively applying climatization effectiveness assessment according to the suggestions made in section 6.1, further human subject studies are necessary to obtain tolerance thresholds for all body areas. Apart from local cooling under overall warm discomfort, such thresholds are to be investigated also during winter conditions for local heating. Considering the above discussed uncertainties, the TTT_i models must also be validated conducting further human subject studies, especially in field studies under realistic conditions and circumstances.

6.3.2 Thermal Impact from Contact Surfaces

The current approach of the DressMAN system, measuring contact temperature between a human occupant and the vehicle seat, is neither feasible nor objective and need to replaced by an appropriate method. My suggestion for a contact equivalent temperature $T_{eq,contact}$ in section 4.1 is in conformity with the general definition of equivalent temperature in ISO 14505-2 and can be utilized in the Park method, the Nilsson method and the TTT_i assessment and therfore in the entire assessment procedure of vehicular climatization effectiveness. I recommend to put effort in the development of an appropriate sensor, taking into account the inhomogeneity of thermal impact over the contact surface (sufficient sensor size) and the influence of contact pressure. As soon as an appropriate sensor is available I recommend to calibrate the PD_{cold} models (equations 5.20 and 5.21) and the corresponding $T_{eq,contact}$ related tolerance thresholds (equations 5.22 and 5.23) in section 5.3.2 according to the objective measurements.
Apart from the CP assessment thermal impact from contact surfaces is also relevant for CCQ assessment. The Nilsson model [39] is not enirely implemented in ISO 14505-2 [9]. Since the comfort zones for seat and back were derived from boundary conditions different from vehicle seats, they do not reflect local thermal comfort for these body areas reliably in the context of vehicular climatization and were hence not integrated. Therefore, investigations of LTC in relation to $T_{eq,contact}$ measurements in steady state conditions can complement the comfort zones in the standard.

6.3.3 Evaporative Impact

Evaporation of humidity at the body surface has significant influence on local thermal perception and thus on cooling intensity tolerance. For DPC assessment the approach

of cooling intensity definition introduced in section 5.1.1 is considered sufficent, as it assumes a constantly high sweat rate and therefore covers the more critical case of TTT_i. In terms of climate control strategy and climatization personalization, however, the actual humidity at any moment in time is relevant for cooling intensity regulation. This could be realized by integrating a humidity sensor in the vehicle seat and develop measurement related evaporative thermal sensation models. The data can also be used for developing evaporative thermal load models for incorporation in the Park model, which might also increase reliability of OTS predictions.

6.3.4 PD Optimization

The suggestions for practical application in section 6.1 refer to the combination of the PD_{cold} output of the local discomfort models with the OTS output of the Park model. Using thermal comfort evaluations of human subjects during vehicle cool-down, the Park model can be extended by an overall discomfort model providing PD with regard to the overall thermal conditions. PD models for both local and overall effects can be optimized against each other, which would allow local thresholds to be dynamically defined in terms of maximum overall conditioning performance for the currently dominant percentage of dissatisfied. Such dynamic variation of TTT_i would not be restricted to 20% dissatisfied. If, for example, the PD due to overall heat load is at 40%, local cooling power can be increased to just below 40% and thus improve overall cooling performance and overall satisfaction.

6.3.5 Equidirectional Local Thermal Discomfort

TTT_i measures local cold discomfort under overall warm discomfort, which can be put as *counter-directional* Local Thermal Discomfort. If, for example, direct solar irradiation evokes local discomfort during cool-down (and thus during overall warm discomfort), such local discomfort is equidirectional, as it is also directed towards warmth. Such equidirectional local thermal discomfort is not considered by the Park model, since it refers to overall thermal load. The influence of such local discomfort on the passengers' satisfaction with the thermal environment in the vehicle might be relevant in the overall assessment (especially regarding passive climatization measures) and should be investigated in addition to TTT_i.

6.3.6 Local Thermal Perception Sensitivity

As can be seen from the comparison of thermal perception predictions of the STRONG scenario in section 4.3.1, all applied models fail to predict the steep fall of thermal sensation due to only cooling the head. Since the head produces the high metabolic heat even at low activity rates and is well perfurated, it dissipates more heat at identical cooling intensity than other body areas (thermophysiological climate impact). The Fanger and Nilsson model are farthest from the subjects perceptions, as they assume thermophysiological impact evenly supplied over the entire body ($T_{sk,mean} = 34°C$). The Park

model uses a weighting factor, assigning a stronger thermophysiological impact to the head at identical equivalent temperature, which enables a prediction closer to the actual valuations. Fiala's thermophysiological model considers body tissues and physiological processes in detail, which affects both Fiala's and Zhang's thermal perception predictions. But despite these considerations of local thermophysiological sensitivity, subjects sensation evolves significantly different from the model's predictions. This deviation might be explained by another physiological aspect closer related to thermal sensation. In section 2.3.2 thermal receptors and the relation of their activity rates to thermal sensation were introduced. According to [49] and [47] thermal receptors in the hypothalamus (part of the brain) are responsible for the sensation of overall warmth and according to [5] and [65] the hypothalamus temperature (or measured tympanic temperature) correlates with overall warm discomfort. Considering the location of the hypothalamus, it seems plausible that head cooling effects a strong cold sensation for the entire body. However, there might also be no physiological explanation for locally different thermal perception, other than impact area or local metabolism, which are already considered. Such *Local Thermal Perception Sensitivities* need deeper investigations for comprehensive thermal environment assessment methods.

6.3.7 Thermo-Acoustic Comfort

Vehicular climatization, especially the cooling mode, relies mainly on air conditioning. This is also true for DPC, which incorporates local air conditioning measures. Air conditioning in vehicles requires forcing air through narrow pipes and outlets, causing loud unpleasant noises. The more air is used, the louder it gets. Since more air usually means more effective cooling, thermal comfort and acoustic comfort are contrary to each other during cool-down. To provide the best compromise for overall comfort the extend of discomfort must be evaluated for both aspects and be dynamically optimized against each other. To do this thermal comfort models and acoustic comfort models must be calibrated in their relative magnitude during a comprehensive human subject study.

6.3.8 DPC Personalization

An important fact I encountered in thermal comfort literature and my own human subject studies is the wide dispersion in thermal perception among people, especially regarding local perception. There appears to be a wide range of preferences regarding decentralized close-to-body climatization, which may be due to race, gender, age, cultural background or other factors. I consider the use of statistical mean or percentage of dissatisfied reasonable only in the *assessment* of vehicular climatization effectiveness. In designing climate control strategies, however, such individual preferences need to be considered for a sufficient user satisfaction. In current vehicle HVAC systems individualized climate control is realized by central setpoint temperature adjustment. However, as soon as DPC measures are included in climate control strategies of vehicles, simultaneous adjustment of several local conditioning measures would be necessary while driving, which is not feasible for users. Thus, individual preferences with regard to local conditioning intensity should

be considered for each person separately by adaptable feedback control, incorporating learning algorithms in order to successively adapt to the person's preferences. For such adaptive DPC feedback control, human subject studies regarding the design of climate control must be conducted and adaptive base line models for conditioning preference need to be developed.

6.3.9 Decentralized Frequency-Optimized Impulse Climatization

The interaction between the three dimensions of thermal comfort allows a conclusion to be drawn about an unconventional climate control strategy for DPC measures. A certain local cooling intensity causes a temperature gradient between the body surface and the environment and thus triggers a cooling of the conditioned body area. Due to this cooling, the temperature gradient and with it the heat flux and thus the effectiveness of the local conditioning measure gradually decreases. At the same time, the PD for this body area increases and causes local cold discomfort for an increasing number of people. Both the problem of decreasing cooling capacity and that of local discomfort can be avoided with alternating impulse cooling. To achieve this, the cooling intensity on different parts of the body is alternately increased or reduced. This allows the local skin temperature to recover, thus avoiding local discomfort while effectively using the available cooling capacity elsewhere. The recurring local relief from overall warm discomfort also creates Thermal Pleasure. Such Decentralized Frequency-Optimized Impulse Climatization (DeFrOI) therefore has great potential from a physical, thermophysiological and Thermal Perception point of view and should be studied in detail.

Chapter 7

Summary

This dissertation addresses the need for a new methodology to assess the effectiveness of vehicular climatization due to a shift from central Heating Ventilation and Air-Conditioning (HVAC) to Direct Passenger Conditioning (DPC) systems.

The state of the art method for assessing climatization performance [8] is designed for conventional central HVAC systems and relies on air temperature measurements during an artificially generated vehicle cool-down scenario in a climate wind tunnel and assesses a system's performance by *Time to Temperature*. DPC systems incorporate local air conditioning, radiative technologies and contact surface conditioning, which are not designed to affect the compartment's air temperature but to condition passengers directly. Thus, although the state of the art procedure per se is considered good practice, DPC requires a different evaluation quantity with regard to thermal comfort.

Thermal comfort can be understood as a cognitive interpretation of physiological responses to surrounding climate conditions, and evaluation quantities must consider three dimensions, respectively: (1) climate conditions, (2) thermophysiology and (3) thermal perception. Climate conditions with regard to DPC comprise *local* conductive, radiative, convective and evaporative thermal impact on passengers' bodies. Thermophysiology denotes responses to these climate conditions in terms of body heat distribution, tissue temperatures, thermoregulatory effects and activity rates of thermal receptors, which again relate to thermal perceptions [25, 49, 47]. These perceptions depend on thermophysiological states and conditions and can be divided into thermal sensation and thermal comfort [35, 65, 45]. Thermal sensation is a rather objective assessment of the thermal environment in terms of "warm" and "cold". Thermal comfort is an interpretation of this perception with regard to the current thermophysiological state and is expressed in more emotional and subjective terms, such as "I am freezing". Local Thermal Perception (LTP) must therefore be distinguished from Overall Thermal Perception (OTP), both of which can occur in different combinations, depending on a person's thermal state and the current climate conditions. In the case of vehicle cool-down by means of DPC, local cooling relieves from overall thermal discomfort and causes *Thermal Pleasure*, which may shift to local cold discomfort as the local cooling intensity increases.

To assess thermal environments, current thermal comfort research provides evaluation methods, whose principles were introduced in line with the three dimensions of thermal comfort. Physical quantities to describe climate impact on passengers have been identified as contacting and non-contacting surface temperatures, solar irradiation, air temperature, air velocity and partial water vapour pressure. These can be measured directly or by using Combined Climate Indicators (CCI) (see [10, 15, 53]), which encompass the combined impact of several physical quantities on the human body. Physiological responses to

climate conditions can either be simulated in detailed thermophysiological models (see [6, 32]) or only rudimentarily in terms of rough interpretations as Thermophysiological Impact, here namely *Thermal Load*, which is a hypothetical area-specific heat flux at the human body, assuming constant thermophysiological conditions (skin temperature, sweat rate) in varying climate conditions (see [18, 42, 44, 43]). Thermal perception models are usually built upon stochastic relations, correlating thermal perceptions of human subjects with measured physiological or climate variables.

State of the art evaluation methods were analyzed in section 2.4 with regard to their potential to provide appropriate models for assessing vehicular climatization effectiveness. For this analysis, methodological requirements were defined: (1) local climate impact measurement, (2) assessment of Overall Thermal Sensation (OTS) and (3) quantification of Local Thermal Comfort (LTC) in transient and non-uniform climate conditions. As well as feasibility criteria: (1) transparency and (2) simplicity of the evaluation methods. As a result of this analysis the Park method [44, 41] was considered the most promising approach, since it was developed in transient conditions of vehicular DPC cool-down, incorporates thermal impact from contact surfaces and comprises a sensor system for local thermal impact measurements, the DressMAN system ([37, 20]). However, a research gap was uncovered, regarding *measurement-based evaluation of local thermal comfort in transient and non-uniform climate conditions.*

To compare the prediction quality of different methods of thermal environment evaluation, a new concept was developed to evaluate multiple thermal perception models using one common climate measurement system. Adaptation models were developed, allowing different thermal perception models to be applied to the DressMAN system. The concept of dry thermal load ($q_{TL,dr}$) was adopted from the Park method and combined with Fanger's thermal comfort equation to obtain overall thermal load from local equivalent temperature measurements. To employ the Nilsson model [39] for both air-adjacent and contacting body areas, a concept for Contact Equivalent Temperature (CET) was proposed and mathematically defined. Zhang's thermal perception model [65] was merged with a simulation implementation of Fiala's thermophysiological model [50], which in turn was subjected to thermal boundary conditions from equivalent temperature measurements. In a comprehensive vehicle cool-down study, the thermal perception predictions of five different models (Fanger [17, 18], Park [44, 41], Nilsson [39, 9], Fiala [19] and Zhang [65]) were standardized to a norm scale and compared to human subjects' responses, which confirmed the highest prediction accuracy with the Park model. The investigations of another vehicle cool-down scenario with strong thermal asymmetries showed that the Park model's prediction accuracy suffered significantly, as local cold discomfort occurred, which confirmed the relevance of the research gap.

This research gap was addressed with introducing a new methodology to assess Local Thermal Tolerance Thresholds (TTT_i). For this, a literature-based theory on *Local Cold Discomfort under simultaneous Overall Warm Discomfort* was developed and corresponding research hypotheses were investigated in a series of human subject studies. Test persons were subjected to overall hot surrounding conditions with local cooling of a certain body area. The cooling intensity was varied during the experiments and subjects were asked to rate their thermal perception. The subjects' evaluations were compared with the predictions of the LTC models of Nilsson and Zhang, which originally have been designed

for other purposes. Since these models' predictions did not fit the subjects' responses, the acquired data was used to develop new assessment models for local cold discomfort in relation to measured cooling intensity. Thermal perceptions were related to measured skin temperature (for neck cooling) and contact temperature (for seat cooling), which in turn were related to local equivalent temperatures, representing cooling intensity. The resulting regression models allow dynamic quantification of cooling tolerance thresholds for the neck, buttocks and back.

For industrial application of the scientific findings a universal approach for assessing the effectiveness of vehicular climatization was proposed. Climatization effectiveness was differentiated into *Climate Control Quality* and *Climatization Performance*. Climate control quality is the ability to keep passengers at thermal neutrality during steady state conditions, regardless of exterior climate conditions and short term fluctuations. This quality can be assessed using the Nilsson model [39] or ISO 14505-2 [9]. Climatization performance is the ability to generate thermal neutrality for passengers from extreme thermal discomfort conditions (during cool-down or heat-up). By changing the evaluation condition from *Time to Temperature* to *Time to Equivalent Temperature* and requiring additional compliance with TTT_i, the state of the art procedure of DIN 1946-3 [8] for climatization performance was generalized to both central HVAC and decentralized DPC systems. In considering the proposal for Contact Equivalent Temperature (CET) in this dissertation and the relation between Dry Thermal Load ($\dot{q}_{TL,dr}$) and Equivalent Temperature (T_{eq}), the evaluation of both climate control quality and climatization performance can now be conducted in relation to decentralized local equivalent temperature measurements. Ultimately, a holistic assessment for vehicular climatization effectiveness is facilitated using the measurement principles and evaluation methods introduced in this dissertation.

Bibliography

[1] EQUIV: Development of Standard Test Methods for Evaluation of Thermal Climate in Vehicles: EU-project SMT 4 – CT95-2017 (Final report). EU-project SMT 4 – CT95-2017 (Final report), 1999.

[2] A. Alahmer, Ahmed Mayyas, Abed A. Mayyas, M. A. Omar, and Dongri Shan. Vehicular Thermal Comfort Models; a Comprehensive Review. *Applied Thermal Engineering*, 31(6-7):995–1002, 2011.

[3] American Society of Heating, Refrigerating and Air-Conditioning Engineers, editor. *ASHRAE Handbook - Fundamentals (SI)*. 2009.

[4] American Society of Heating, Refrigerating and Air-Conditioning Engineers. ASHRAE 55: Thermal Environmental Conditions for Human Occupancy, 2017.

[5] T. H. Benzinger and E. Mayer. Definition der thermischen Behaglichkeit. *IBP Mitteilung*, (115), 1986.

[6] Yuanda Cheng, Jianlei Niu, and Naiping Gao. Thermal Comfort Models: A Review and Numerical Investigation. *Building and Environment*, 47:13–22, 2012.

[7] Paul Danca, Andreea Vartires, and Angel Dogeanu. An Overview of Current Methods for Thermal Comfort Assessment in Vehicle Cabin. *Energy Procedia*, 85:162–169, 2016.

[8] DIN Deutsches Institut für Normung e.V. DIN 1946-3: Ventilation Systems; Part 3: Airconditioning of Passenger Cars and Commercial Vehicles, 03.2009.

[9] DIN Deutsches Institut für Normung e.V. DIN EN ISO 14505-2: Ergonomics of the Thermal Environment - Evaluation of Thermal Environments in Vehicles; Part 2: Determination of Equivalent Temperature, 14.12.2006.

[10] DIN Deutsches Institut für Normung e.V. EN ISO 7726: Ergonomics of the Thermal Environment - Instruments for Measuring Physical Quantities (ISO 7726:1998); German Version EN ISO 7726:2001, April 2002.

[11] DIN Deutsches Institut für Normung e.V. DIN EN ISO 7933: Ergonomics of the Thermal Environment - Analytical Determination and Interpretation of Heat Stress using Calculation of the Predicted Heat Strain, December 2004.

[12] DIN Deutsches Institut für Normung e.V. DIN EN ISO 10551: Ergonomics of the Physical Environment - Subjective Judgement Scales for Assessing Physical Environments (ISO 10551:2019); German Version EN ISO 10551:2019, February 2020.

[13] DIN Deutsches Institut für Normung e.V. DIN EN ISO 7730: Ergonomics of the Thermal Environment - Analytical Determination and Interpretation of Thermal Comfort using Calculation of the PMV, Mai 2006.

[14] DIN Deutsches Institut für Normung e.V. DIN EN ISO 9920: Ergonomics of the Thermal Environment - Estimation of Thermal Insulation and Water Vapour Resistance of a Clothing Ensemble (ISO 9920:2007, Corrected Version 2008-11-01); German Version EN ISO 9920:2009, October, 2009.

[15] Kristian Fabbri. A Brief History of Thermal Comfort: From Effective Temperature to Adaptive Thermal Comfort. In Kristian Fabbri, editor, *Indoor Thermal Comfort Perception*, volume 37, pages 7–23. Springer International Publishing, Cham, 2015.

[16] Kristian Fabbri. *Indoor Thermal Comfort Perception*. Springer International Publishing, Cham, 2015.

[17] Povl Ole Fanger. Calculation of Thermal Comfort: Introduction of a Basic Comfort Equation. *ASHRAE Transactions*, 73, Part 2, 1967.

[18] Povl Ole Fanger. *Thermal Comfort. Analysis and Applications in Environmental Engineering*. Danish Technical Press, 1970.

[19] Dusan Fiala. *Dynamic Simulation of Human Heat Transfer and Thermal Comfort*. Dissertation, De Monfort University, Leicester, 1998.

[20] Fraunhofer-Institute for Building Physics. Produktblatt DressMAN: Objektive Komfortmessung mit dem DressMAN 3.2, 2020.

[21] A. P. Gagge and Y. Nishi Stolwijk. An Effective Temperature Scale Based on a Simple Model of Human Physiological Regulatory Response. *ASHRAE Transactions*, 77:247–262, 1971.

[22] Holger Großmann. *Pkw-Klimatisierung*. Springer Berlin Heidelberg, Berlin, Heidelberg, 2013.

[23] J. D. Hardy. Thermal Comfort: Skin Temperature and Physiological Thermoregulation. In *Physiological and Behavioural Temperature Regulation*, pages 856–873.

[24] Herbert Hensel. Physiologie der Thermoreception. In *Ergebnisse der Physiologie, Biologischen Chemie und Experimentellen Pharmakologie*, pages 166–368.

[25] Herbert Hensel. *Thermal Sensations and Thermoreceptors in Man*, volume publication no. 1056 of *American Lecture Series*. Thomas Books, Springfield, Illinois, 1982.

[26] Herbert Hensel and K. K. A. Boman. Afferent Impulses in Cutaneous Sensory Nerves in Human Subjects. *Journal of Neurophysiology*, 23:564–578, 1960.

[27] Heinz Herwig and Andreas Moschallski. *Wärmeübertragung*. Springer Fachmedien Wiesbaden, Wiesbaden, 2019.

[28] Diana Hintea, John Kemp, James Brusey, Elena Gaura, and Neil Beloe. Applicability of Thermal Comfort Models to Car Cabin Environments. *Conference on Proceedings of the 11th International Informatics in Control, Automation and Robotics*, 2014.

[29] Ingvar Holmér. Thermal Manikin History and Applications. *European journal of applied physiology*, 92(6):614–618, 2004.

[30] Riikka Holopainen. *A Human Thermal Model for Improved Thermal Comfort*, volume 23 of *VTT science*. VTT, Espoo, 2012.

[31] Rob J. Hyndman and Anne B. Koehler. Another Look at Measures of Forecast Accuracy. *International Journal of Forecasting*, 22(4):679–688, 2005.

[32] Katarina Katić, Rongling Li, and Wim Zeiler. Thermophysiological Models and their Applications: A Review. *Building and Environment*, 106:286–300, 2016.

[33] Dan R. Kenshalo, Charles E. Holmes, and Paul B. Wood. Warm and Cool Thresholds as a Function of Rate of Stimulus Temperature Change. *Attention, Perception, & Psychophysics*, 3:81–84, March 1968.

[34] Martin Konz, Nicholas Lemke, Sven Försterling, and Marjam Eghtessad. Spezifische Anforderungen an das Heiz-Klimasystem elektromotorisch angetriebener Fahrzeuge. *FAT-Schriftenreihe*, 233, 2011.

[35] Satoru Kuno. Comfort and Pleasantness. *Proceedings of the Pan Pacific Symposium on Building and Urban Environmental Conditioning*, pages 383–392, March 1995.

[36] Mathworks Inc. Matlab Documentation, 2020.

[37] E. Mayer and R. Schwab. Presentation of a Dummy Representing Suit for Simulation of huMAN heatloss (DRESSMAN). *European journal of applied physiology*, 92(6):626–629, 2004.

[38] Erhard Mayer. A new Correlation between Predicted Mean Votes (PMV) and Predicted Percentages of Dissatisfied (PPD). In *Proceedings of the International Conference on Healthy Buildings*, 1997.

[39] Hæakan O. Nilsson. *Comfort Climate Evaluation with Thermal Manikin Methods and Computer Simulation Models*. Dissertation, Royal Institute of Technology, Stockholm, 2004.

[40] Hæakan O. Nilsson and Ingvar Holmér. Definitions and Measurements of Equivalent Temperature: EQUIV Report No 1. EQUIV Report No 1, 1999.

[41] Sumee Park. Properties of an Overall Thermal Sensation Model based on DressMAN Measurements for Vehicle Cool-Down: Personal Correspondence, 14.04.2020.

[42] Sumee Park, Runa T. Hellwig, Gunnar Grün, and Andreas Holm. Local and Overall Thermal Comfort in an Aircraft Cabin and their Interrelations. *Building and Environment*, 46(5):1056–1064, 2011.

[43] Sumee Park, Sebastian Stratbücker, Vladislav Nasyrov, Arnav Pathak, and Rudolf Schwab. E-Komfort: Innovative Klimatisierungs- und Thermische Komfortkonzepte zur Optimierung der Reichweite von Elektrofahrzeugen. 23.12.2014.

[44] Sumee Park, Sebastian Stratbücker, Michael Visser, and Gunnar Grün. Thermal Comfort Measurement Methodology during a Heat-up or Cool-down Phase of a Vehicle Equipped with Microclimate Heating and Cooling Elements. 17.04.2019.

[45] Thomas Parkinson, Richard de Dear, and Christhina Candido. Perception of Transient Thermal Environments: Pleasure and Alliesthesia. *Proceedings of Windsor Conference*, 7, 2012.

[46] Thomas Parkinson, Richard de Dear, and Christhina Candido. Thermal Pleasure in Built Environments: Alliesthesia in Different Thermoregulatory Zones. *Building Research & Information*, 44(1):20–33, 2016.

[47] Ken Parsons. *Human Thermal Environments: The Effects of Hot, Moderate, and Cold Environments on Human Health, Comfort, and Performance*. CRC Press, 6000 Broken Sound Parkway NW, Suite 300, Boca Raton, FL 33487-2742, 3 edition, 2014.

[48] Stefan Paulke. Consideration of Heat Flux Measurements as Input Variable for Local Heat Exchange at Contacting Body Areas of the Fiala FE Passive System: Telephone, September 2019.

[49] Pontus B. Persson. Energie- und Wärmehaushalt, Thermoregulation. In Robert F. Schmidt, Florian Lang, and Manfred Heckmann, editors, *Physiologie des Menschen*, Springer-Lehrbuch, pages 834–853. Springer-Verlag Berlin Heidelberg, Berlin, Heidelberg, 2011.

[50] P+Z Engineering GmbH. THESEUS-FE: Theory Manual. March 2017.

[51] Carolin Schmidt, Daniel Wölki, Henning Metzmacher, and Christoph van Treeck. Equivalent Contact Temperature (ECT) for Personal Comfort Assessment as Extension for ISO 14505-2. *Proceedings of Windsor Conference*, 12:451–466, 2018.

[52] Fabian Schüppel. *Optimierung des Heiz- und Klimakonzepts zur Reduktion der Wärme- und Kälteleistung im Fahrzeug*. Cuvillier Verlag, Göttingen, 1st ed. edition, 2015.

[53] Rudolf Schwab and Gunnar Grün. Ableitung eines messbaren Klimasummenmaßes für den Vergleich des Fahrzeugklimas konventioneller und elektrischer Fahrzeuge. *FAT-Schriftenreihe*, (257), 2013.

[54] Marcel Schweiker, Xaver Fuchs, Susanne Becker, Masanori Shukuya, Mateja Dovjak, Maren Hawighorst, and Jakub Kolarik. Challenging the Assumptions for Thermal Sensation Scales. *Building Research & Information*, 45(5):572–589, 2017.

[55] Society of Automotive Engineers. Surface Vehicle Recommended Practice: Taxonomy and Definitions for Terms Related to Driving Automation Systems for On-Road Motor Vehicles, 2018.

[56] J.A.J. Stolwijk. A Mathematical Model of Physiological Temperature Regulation in Man. 1971.

[57] Paul E.B. Stuke. *Vertical Interior Cooling System for Passenger Cars: Trials and Evaluation of Feasibility, Thermal Comfort and Energy Efficiency*. Dissertation, Technische Universität München, Munich, 18.10.2016.

[58] Thermetrics. Product Sheet: Automotive HVAC Manikin, 2019.

[59] Armin Töpfer. *Erfolgreich Forschen*. Springer Berlin Heidelberg, Berlin, Heidelberg, 2012.

[60] Dieter Urban and Jochen Mayerl. *Angewandte Regressionsanalyse: Theorie, Technik und Praxis*. Springer Fachmedien Wiesbaden, Wiesbaden, 2018.

[61] Mingyu Wang, Edward Wolfe, Debashis Ghosh, Jeffrey Bozeman, Kuo-huey Chen, Taeyoung Han, Hui Zhang, and Edward Arens. Localized Cooling for Human Comfort. *SAE International Journal of Passenger Cars - Mechanical Systems*, 7(2):755–768, 2014.

[62] Alexander Warthmann, Daniel Wölki, Henning Metzmacher, and Christoph van Treeck. Personal Climatization Systems - A Review on Existing and Upcoming Concepts. *Applied Sciences*, 9(1):35, 2019.

[63] Udo Wehner and Jan Ackermann. Neue Ansätze zur Klimatisierung von Elektrofahrzeugen. *ATZ - Automobiltechnische Zeitschrift*, 113(7-8):586–591, 2011.

[64] Wolfgang Wöhrle and Sumee Park. Local Cooling Intensity Thresholds during Vehicle Cool Down. In Technische Akademie Esslingen e.V., editor, *Fahrzeugklimatisierung*, 2019.

[65] Hui Zhang. *Human Thermal Sensation and Comfort in Transient and Non-Uniform Thermal Environments*. Dissertation, University of California, Berkeley, 09.01.2003.

[66] Hui Zhang, Edward Arens, Charlie Huizenga, and Taeyoung Han. Thermal Sensation and Comfort Models for Non-uniform and Transient Environments: Part I: Local Sensation of Individual Body Parts. *Building and Environment*, 45(2):380–388, 2010.

[67] Hui Zhang, Edward Arens, Charlie Huizenga, and Taeyoung Han. Thermal Sensation and Comfort Models for Non-uniform and Transient Environments: Part II: Local Comfort of Individual Body Parts. *Building and Environment*, 45(2):389–398, 2010.

[68] Hui Zhang, Edward Arens, Charlie Huizenga, and Taeyoung Han. Thermal Sensation and Comfort Models for Non-uniform and Transient Environments: Part III: Whole-body Sensation and Comfort. *Building and Environment*, 45(2):399–410, 2010.

[69] Yin Zhao, Hui Zhang, Edward A. Arens, and Qianchuan Zhao. Thermal Sensation and Comfort Models for Non-uniform and Transient Environments: Part IV: Adaptive Neutral Setpoints and Smoothed Whole-body Sensation Model. *Building and Environment*, 72:300–308, 2014.

List of Figures

1.1 Conceptual research approach of the dissertation 3

2.1 Characterization and interrelation of the three dimensions of thermal comfort. 7
2.2 Illustration of the static and dynamic properties of thermoreceptors in the human skin. 12
2.3 Principle of thermal environment evaluation models 16
2.4 Evaluation principle of the Fanger method. 20
2.5 Evaluation principle of the Park method. 23
2.6 Comfort Zones of the Nilsson model relating to $T_{eq,segment}$ and $T_{eq,whole}$ . . 24
2.7 Evaluation principle of the Nilsson method. 25
2.8 Evaluation principle of the Fiala method. 27
2.9 Illustration of Zhang's thermal perception model. 28
2.10 Evaluation principle of the Zhang method. 30
2.11 Comparison of properties of various thermal environment evaluation methods. 32

3.1 Visualization of the applied research design. 38

4.1 Illustration of the principle of Contact Equivalent Temperature (CET). . . 42
4.2 Illustration of the adaptation of the CET principle to human subject measurement. 42
4.3 Illustration of the concept for applying multiple thermal perception models to the DressMAN system. 45
4.4 Illustration of the test setup for vehicle cool-down with DPC. 52
4.5 Illustration of cooling asymmetries in the two vehicle cool-down scenarios. 53
4.6 Thermal asymmetries in the two vehicle cool-down scenarios. 53
4.7 Experimental procedure of the vehicle cool-down study. 54
4.8 Photographs of a person undergoing the experimental procedure of the vehicle cool-down study. 54
4.9 Pictures of the DressMAN 3.1 system in the experiment vehicle. 55
4.10 Course of segmental and overall equivalent temperature over cooling duration time, for both scenarios of the vehicle cool-down study. 56
4.11 Course of segmental thermal comfort over cooling duration time for both scenarios of the vehicle cool-down study. 57
4.12 OTP courses and their relative residuals over cooling duration time in the LOW scenario of the vehicle cool-down study. 58
4.13 Mean Bias Error (MBE) and Normalized Root Mean Square Deviation (NRMSD) of thermal perception predictions in the LOW scenario of the vehicle cool-down study. 58
4.14 OTS comparison of subjects' mean vote with the Park model predictions in both scenarios of the vehicle cool-down study. 59
4.15 OTP courses over cooling duration time and their corresponding NRMSD in the STRONG scenario of the vehicle cool-down study. 60

4.16 NRMSD of the Nilsson and Zhang LTC predictions in the vehicle cool-down study for each body segment. . . . 61
4.17 MBE of the Nilsson and Zhang LTC predictions in the vehicle cool-down study for each body segment. . . . 61
4.18 Progression of the Nilsson and Zhang LTC predictions and subjects' actual mean vote in the STRONG scenario of the vehicle cool-down study for the head area. . . . 61

5.1 Illustration of local heat balance in the human skin. . . . 66
5.2 Hypothetical model for the derivation of time dependent body surface temperature, its temporal derivative and PD_{cold} from time-variable cooling intensity. . . . 67
5.3 Illustration of the test setup for investigating the perception of local cooling at the neck area. . . . 68
5.4 Experimental procedure of the neck cooling study. . . . 70
5.5 Test setup of the neck cooling study with a human subject 71
5.6 Courses for mean local skin temperature and its temporal derivative over cooling duration time for all four cooling intensities of the neck cooling study 72
5.7 Comparison of the neck cooling study results with the Fiala/Zhang simulation 73
5.8 Mean skin temperature derivatives over absolute mean skin temperature for each cooling intensity of the neck cooling study 75
5.9 Illustration of the function fitting procedure for skin temperature derivatives in relation to skin temperature and cooling intensity in the neck cooling study. . . . 75
5.10 Meta regression functions for the coefficients of the regression equation for skin temperature derivatives prediction. . . . 76
5.11 PD_{cold} over skin temperature clusters of $0.5K$. . . . 77
5.12 Impulse frequency of a cold fiber from the human hand in relation to skin temperature evolvement over time. . . . 77
5.13 PD_{neck} over T_{sk} for low $\frac{dT_{sk}}{dt}$ and logistic regression function. . . . 78
5.14 Comparison of the developed models' predictions with measured skin temperature and subjects' PD_{cold} of the neck cooling study. . . . 79
5.15 Plausibility limits of the prediction models for local skin temperature at the neck and the according PD_{cold}. . . . 80
5.16 Simulation of a test scenario with variation of local cooling intensity at the neck over time. . . . 81
5.17 Illustration of the test setup for determining TTT_i for the seat and the back. 83
5.18 Designations of the cooling intensity levels and the resulting surface temperatures under steady state conditions $T_{s,ss}$. . . . 84
5.19 Experimental procedure of the seat cooling study. . . . 84
5.20 Test setup of the seat cooling study 84
5.21 Human subject completing the questionnaire in the seat cooling study. . . 85
5.22 Contact temperature progression over cooling duration time in the seat cooling study. . . . 86
5.23 Progression of PD_{cold} over cooling duration time in the seat cooling study. 87

5.24 Contact equivalent temperature progression over cooling duration time in the seat cooling study. 88
5.25 Comparison of the contact temperature measurements with the Fiala model predictions in the seat cooling study 88
5.26 Comparison of the local thermal comfort evolvement with the Zhang/Fiala and Nilsson predictions in the seat cooling study 89
5.27 $PD_{cold,seat}$ over T_c and logistic prediction function. 90
5.28 $PD_{cold,back}$ over T_c and logistic prediction function 91
5.29 Comparison of subjects' PD_{cold} and thermal perception models' predictions in the seat cooling study 92
5.30 Mean PD_{cold} of the neck area for each tested cooling intensity averaged over cooling duration. 94
5.31 Comparison of $t_{TTT,neck}$ for the simple and the complex method, simulating different local cooling scenarios. 94
5.32 PD_{cold} over T_{eq} and logistic regression function for seat and back. 96

6.1 Extension of Nilsson's "Summer" comfort zones with thresholds for local cooling during vehicle cool-down 99

A.1 Equivalent temperature sensors position on the DressMAN 3.1 system (Front). 118
A.2 Equivalent temperature sensors position on the DressMAN 3.1 system (Side). 119
A.3 Equivalent temperature sensors position on the DressMAN 3.1 system (Top/Bottom). 119

B.1 T_c measurements over $T_{eq,contact}$ with linear regression function for data of the seat cooling study 120
B.2 T_c measurements over $T_{eq,contact}$ with linear function validated with data of the vehicle cool-down study 121
B.3 PD_{seat} over calculated T_c and logistic regression function. 122
B.4 PD_{back} over calculated T_c and logistic regression function. 122
B.5 Simulation of a test scenario for seat cooling with variation of cooling intensity over time. 123

List of Tables

2.1 Boundary conditions and target values for cool-down and heat-up tests according to DIN 1946-3 [8]. 6
2.2 Thermal sensation scale in the Fanger PMV model [13]. 19
2.3 Mixed thermal sensation and comfort scale of the Nilsson model [39]. . . . 24
2.4 Thermal sensation scale of the Zhang model [65]. 29
2.5 Thermal comfort scale of the Zhang model [65]. 29

4.1 (Extended) ASHRAE scale. 47
4.2 (Limited) MTV scale. 47
4.3 Illustration of the norming principle for the different Thermal Perception Scales. 49
4.4 LTC norming concept. 49
4.5 Thermal sensation scale used in the vehicle cool-down study. 55
4.6 Thermal comfort scale used in the vehicle cool-down study. 55

5.1 Comparison of supply air temperature ($T_{a,sup}$) and local directed equivalent temperature ($T_{eq,direct}$) for an air velocity of $2.0\frac{m}{s}$ at neck distance. 70
5.2 Rating scale, used in the neck cooling experiment. 71
5.3 MBE and RMSD for the perdiction of skin temperature progression and PD_{cold} for neck cooling. 79
5.4 OTS scale used in the seat cooling study 86
5.5 local cooling preference scale used in the seat study 86
5.6 MBE and RMSE for the regression of PD_{cold} over contact temperature. . . 91
5.7 MBE and RMSD for the perdiction of PD_{cold} from T_c for seat cooling. . . . 92
5.8 MBE and RMSE for the regression of PD_{cold} from $T_{eq,contact}$. 96

6.1 Adaptation of the boundary conditions and target values for cool-down and heat-up tests of DIN 1946-3 (adapted from [8]). 98

B.1 MBE and RMSD for the prediction of local contact temperature from contact equivalent temperature. 121

Appendix A

Sensor Positions of the DressMAN System

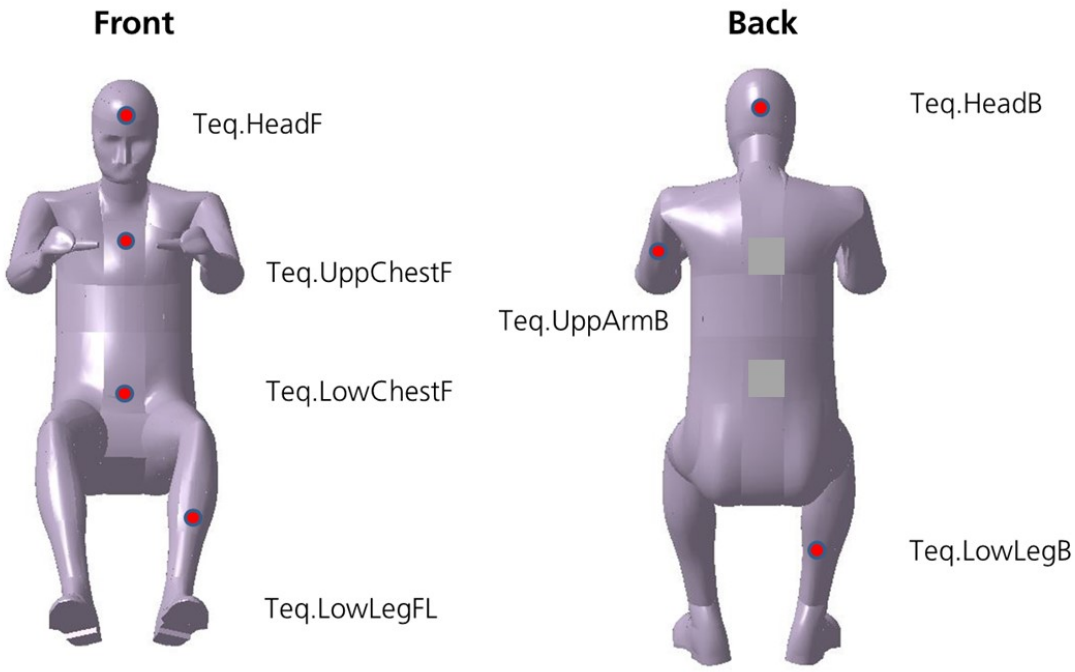

Figure A.1: Equivalent temperature sensors position on the DressMAN 3.1 system (Front).

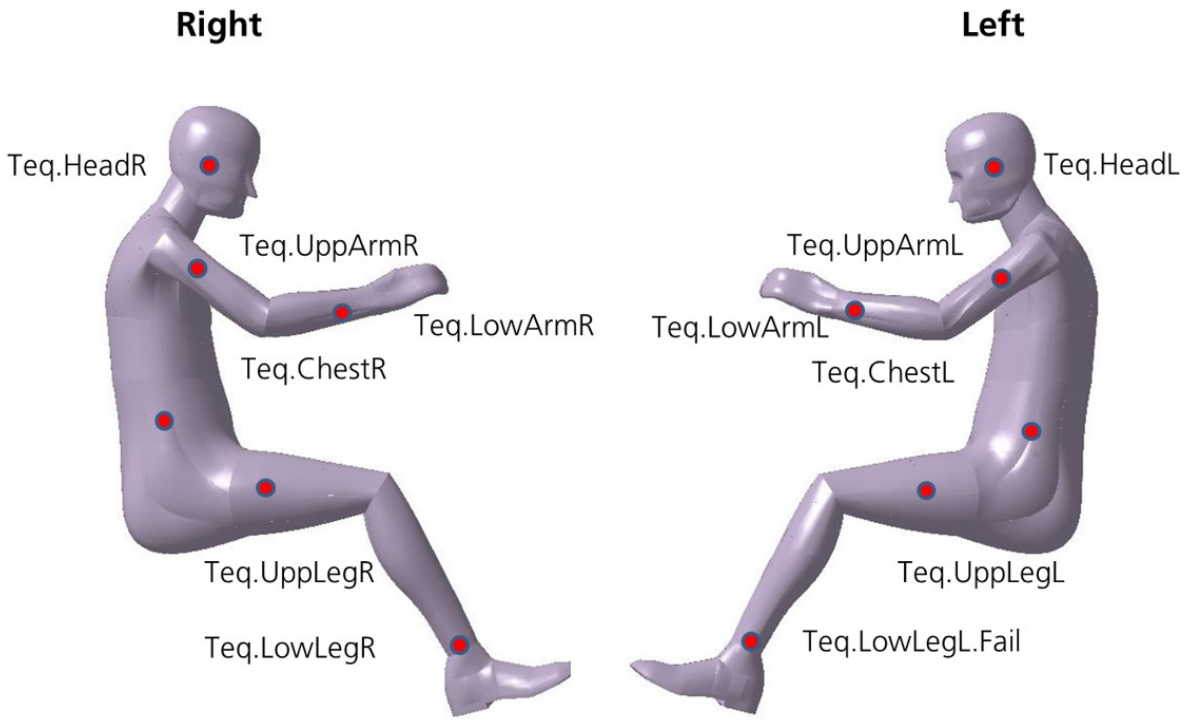

Figure A.2: Equivalent temperature sensors position on the DressMAN 3.1 system (Side).

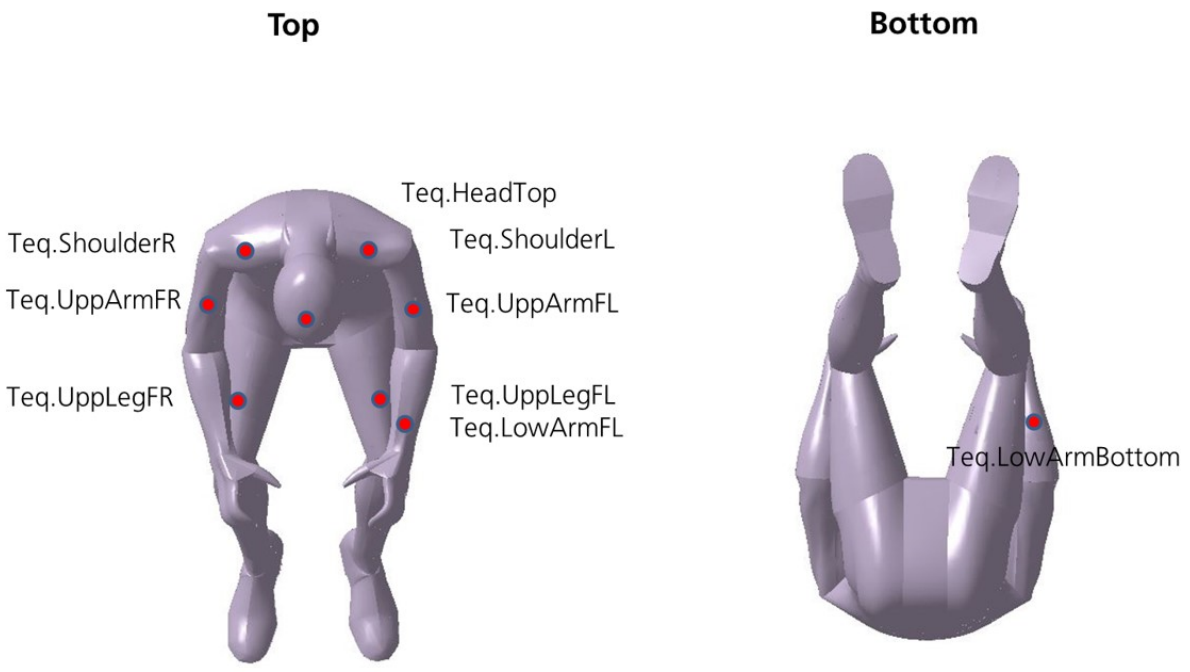

Figure A.3: Equivalent temperature sensors position on the DressMAN 3.1 system (Top/Bottom).

Appendix B

Further Model Evaluations

Linearity between T_c and $T_{eq,contact}$

The definition of $T_{eq,contact}$ introduced in equation 4.7 of section 4.1.1 assumes quasi-stationary conditions between contacting surfaces. Using measurements of T_c and $\dot{q}_{env,c}$ at each time step, a stochastic relation can be analyzed from the data. To model the according function, I used data of the seat cooling study in section 5.2.6. Figure B.1 shows the measured contact temperatures over the calculated CET and the according regression functions for seat and back. Since the seat was pre-conditioned when subjects sat down, the contact heat exchange at the beginning of the local cooling took place under transient conditions and approached steady state only during conditioning duration. To be able to model in accordance to quasi-stationary conditions, as they occur during real vehicle cool-down, I only took measurements at the end of the local cooling duration into account. These measurements are highlighted in blue circles in figure B.1, whereas the red dots represent the entire data. Equations B.1 and B.2 present the mathematical definition of the models.

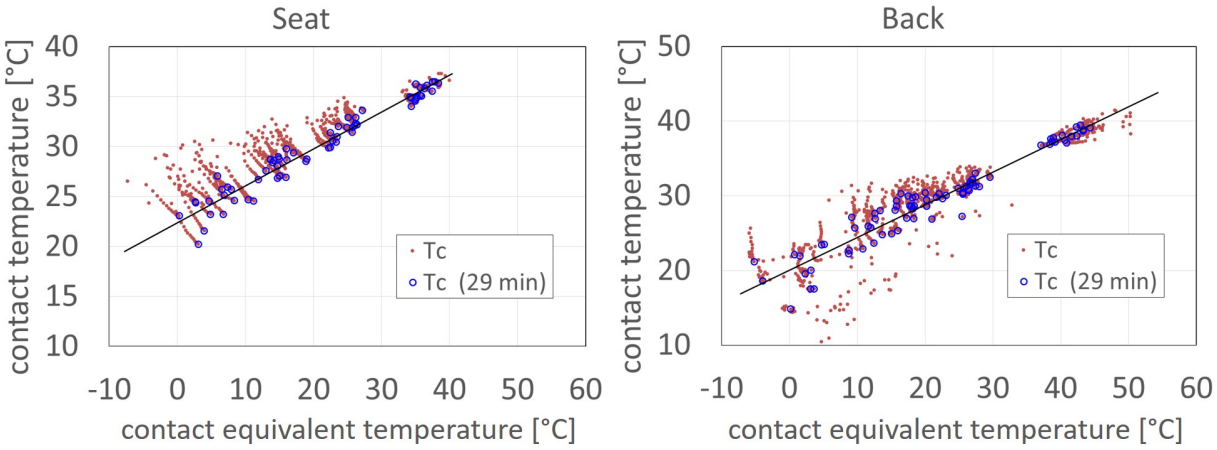

Figure B.1: T_c measurements over $T_{eq,contact}$ with linear regression function for seat (left) and back (right).

$$T_{c,seat} = 0.369 \cdot T_{eq,contact} + 22.38 \qquad R^2 = 0.95 \qquad \text{(B.1)}$$

$$T_{c,back} = 0.438 \cdot T_{eq,contact} + 20.04 \qquad R^2 = 0.93 \qquad \text{(B.2)}$$

I validated these models using data from the LOW scenario of the vehicle cool-down study, where local cooling takes place with slowly rising cooling intensity and therefore most likely under quasi-stationary conditions. In the vehicle cool-down study, seat cooling was off at the beginning and rose in intensity during the cool-down duration. Thus, steady-state conditions could establish. Figure B.2 shows both models and the corresponding measured contact temperatures.

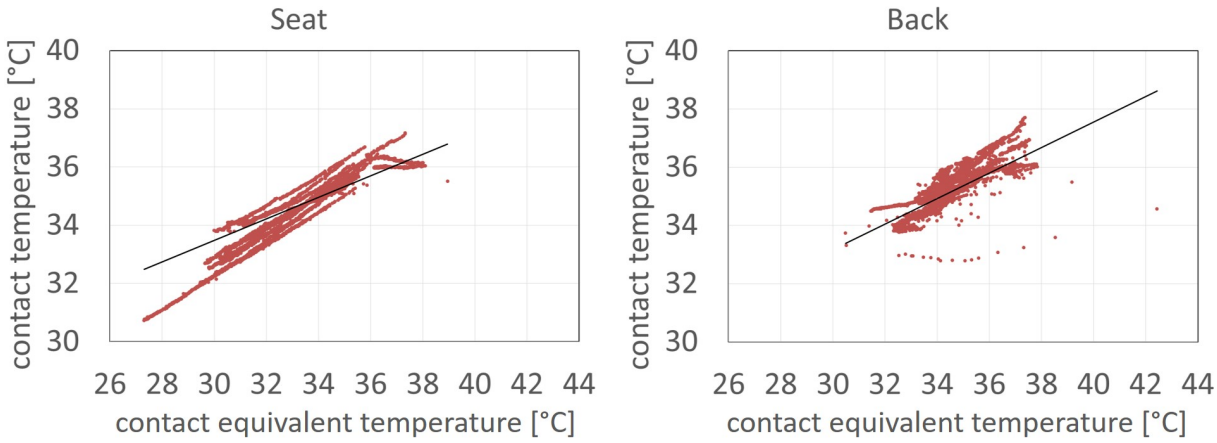

Figure B.2: T_c measurements over $T_{eq,contact}$ with linear function validated with data of the vehicle cool-down study for seat (left) and back (right).

Table B.1: MBE and RMSD for the prediction of local contact temperature from contact equivalent temperature.

MBE for seat	RMSD for seat	MBE for back	RMSD for back
+0.22 K	0.58 K	−0.14 K	0.42 K

Regression for $\mathrm{PD_{cold}}$ in Relation to Calculated T_c

The prediction models for $\mathrm{PD_{cold}}$ in section 5.2.5 were built upon *measured* contact temperatures at human subjects. By applying the introduced linear models of equations B.1 and B.2, contact temperatures can be calculated from contact equivalent temperatures, which can then be used for further model evaluation. Figures B.3 and B.4 show the percentage of dissatisfied (both clustered and averaged) in relation to *calculated* contact temperature and the according regression functions of section 5.2.5.

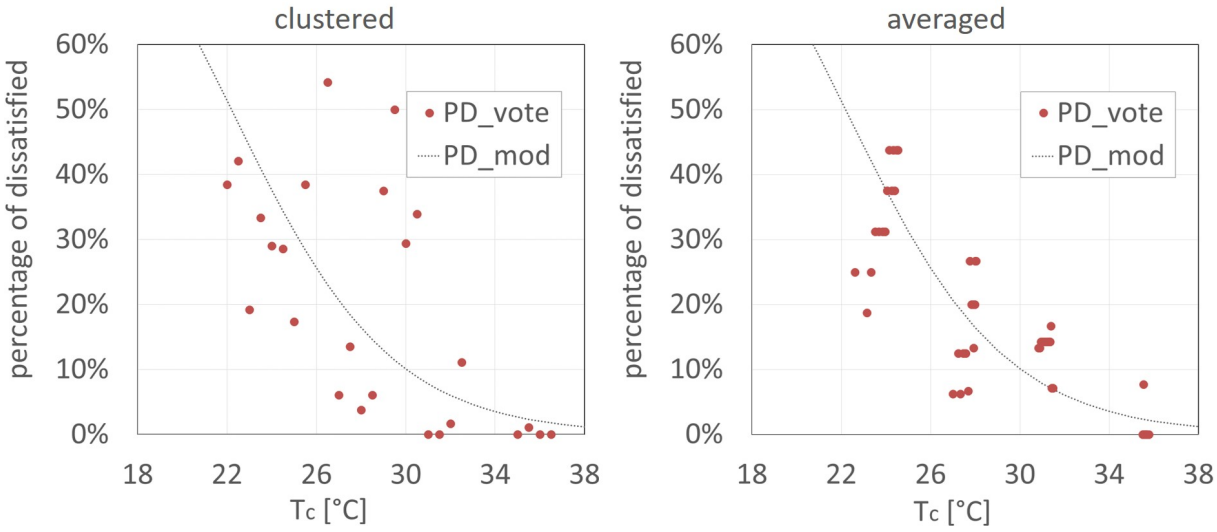

Figure B.3: PD_{seat} over calculated T_c and logistic regression function, for clustered data (left) and averaged data (right) in the seat study.

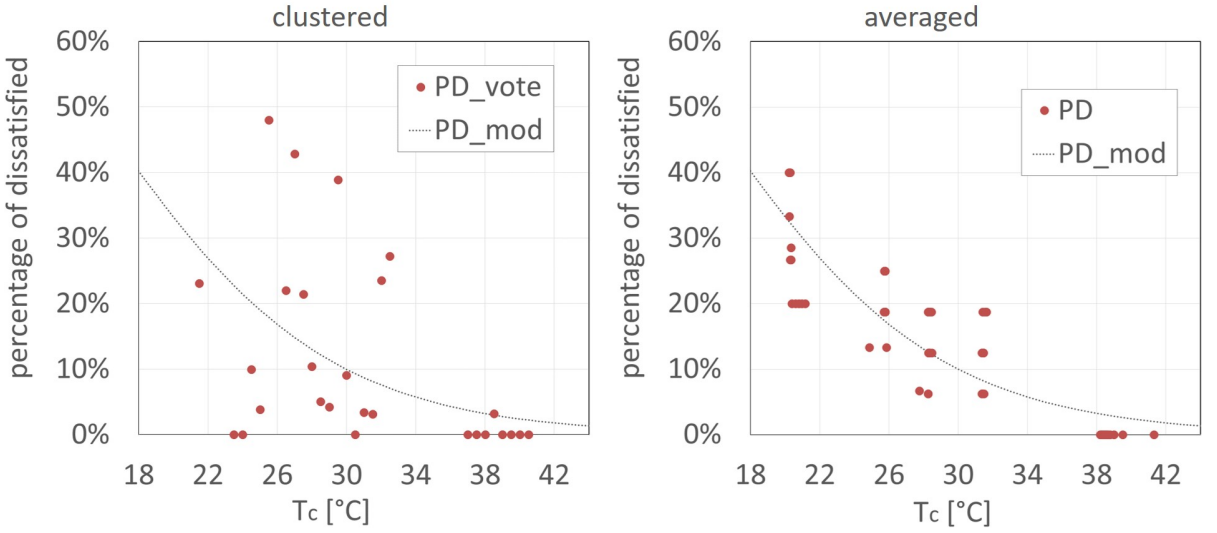

Figure B.4: PD_{back} over calculated T_c and logistic regression function, for clustered data (left) and averaged data (right) in the seat study.

Test Scenario Simulation Similar to the neck cooling study, I simulated a local cooling scenario for both, seat and back and implemented the models for contact temperature and PD_{cold}. Figure B.5 shows the designed $T_{eq,contact}$ and corresponding progression of T_c on the left side and the resulting PD_{cold} on the right side. The scenario reveals, that in realistic conditions, contact temperatures at the buttock and the back evolve very similar. The corresponding PD_{cold} however, can vary significantly according to the temporal progression and cooling intensity.

I varied the parameters of the $T_{eq,contact}$ progression in a series of simulations. Above 17°C PD_{cold} does not exceed 14% for both body segments and differences between them

are below 3%. Only when $T_{eq,contact}$ falls below 17°C, differences rise with each negative temperature step. At a cooling intensity of $T_{eq} = 0$°C, the differences of PD_{cold} between the two segments can reach over 15%.

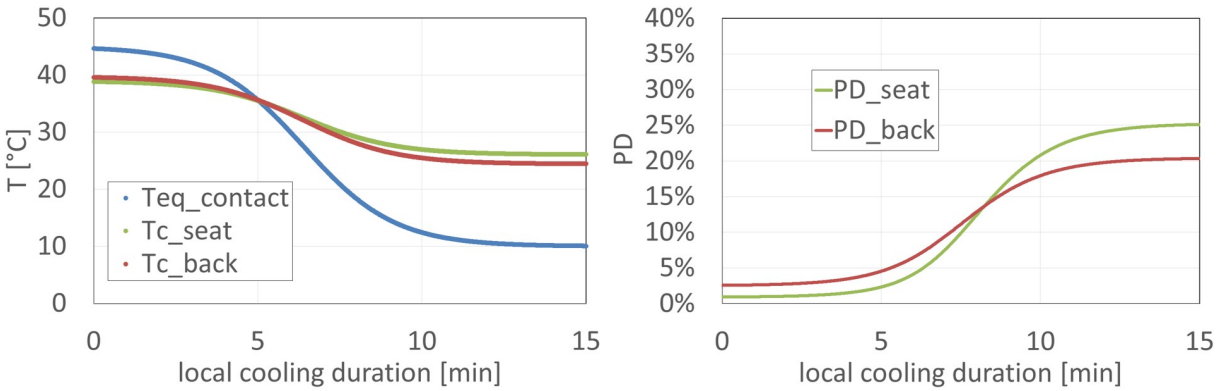

Figure B.5: Simulation of a test scenario for seat cooling with variation of cooling intensity over time.